

The adsorption and reduction of dioxygen on metal phthalocyanines

Citation for published version (APA):

Elzing, A. (1987). *The adsorption and reduction of dioxygen on metal phthalocyanines*. [Phd Thesis 1 (Research TU/e / Graduation TU/e), Chemical Engineering and Chemistry]. Technische Universiteit Eindhoven.
<https://doi.org/10.6100/IR274689>

DOI:

[10.6100/IR274689](https://doi.org/10.6100/IR274689)

Document status and date:

Published: 01/01/1987

Document Version:

Publisher's PDF, also known as Version of Record (includes final page, issue and volume numbers)

Please check the document version of this publication:

- A submitted manuscript is the version of the article upon submission and before peer-review. There can be important differences between the submitted version and the official published version of record. People interested in the research are advised to contact the author for the final version of the publication, or visit the DOI to the publisher's website.
- The final author version and the galley proof are versions of the publication after peer review.
- The final published version features the final layout of the paper including the volume, issue and page numbers.

[Link to publication](#)

General rights

Copyright and moral rights for the publications made accessible in the public portal are retained by the authors and/or other copyright owners and it is a condition of accessing publications that users recognise and abide by the legal requirements associated with these rights.

- Users may download and print one copy of any publication from the public portal for the purpose of private study or research.
- You may not further distribute the material or use it for any profit-making activity or commercial gain
- You may freely distribute the URL identifying the publication in the public portal.

If the publication is distributed under the terms of Article 25fa of the Dutch Copyright Act, indicated by the "Taverne" license above, please follow below link for the End User Agreement:

www.tue.nl/taverne

Take down policy

If you believe that this document breaches copyright please contact us at:

openaccess@tue.nl

providing details and we will investigate your claim.

**THE ADSORPTION AND REDUCTION OF DIOXYGEN
ON METAL PHTHALOCYANINES**

**Cover: ARTISTS IMPRESSION OF DIOXYGEN REDUCTION ON A
METAL PHTHALOCYANINE.**

THE ADSORPTION AND REDUCTION OF DIOXYGEN ON METAL PHTHALOCYANINES

PROEFSCHRIFT

ter verkrijging van de graad van doctor aan de
Technische Universiteit Eindhoven, op gezag
van de rector magnificus, Prof. dr. F.N. Hooge,
voor een commissie aangewezen door het College
van Decanen in het openbaar te verdedigen op
vrijdag 11 december 1987 te 14.00 uur

door

ALBERTUS ELZING

geboren te Sleen

**Dit proefschrift is goedgekeurd
door de promotoren:**

Prof. E. Barendrecht

Prof. dr. R. van Santen

Co-promotor: Dr. W. Visscher

Voor Lizette

Aan mijn ouders

The present investigations have been carried out with the support of the Netherlands Foundation for Chemical Research (S.O.N.) and with financial aid from the Netherlands Organization for the Advancement of Pure Research (Z.W.O.).

Contents

1. Introduction	1
1.1. References	3
2. Literature review on cathodic dioxygen reduction, catalyzed by transition metal chelates	5
2.1. Introduction	5
2.2. Dioxygen reduction	5
2.3. Light absorption spectroscopy	6
2.4. References	9
3. Dioxygen adsorption on metal chelates. Theoretical considerations	11
3.1. Introduction	11
3.2. Electronic structure of dioxygen and of a metal chelate	11
3.3. Electronic structure of dioxygen adducts. Qualitative models	13
3.4. Electronic structure of dioxygen adducts. Quantitative models	17
3.5. Dioxygen bridged metal complexes	28
3.6. References	29
4. Dioxygen adsorption on metal chelates. Experimental part	32
4.1. Introduction	32
4.2. The Rotating Ring Disc Electrode (RRDE)	32
4.3. Cyclic voltammetry	35
4.4. In situ light absorption spectroscopy	36
4.5. Polarography	39
4.6. References	39
5. The cathodic reduction of dioxygen at cobalt phthalocyanine: Influence of electrode preparation on electrocatalysis	41
5.1. Introduction	41
5.2. Theoretical aspects	41
5.3. Experimental	43
5.4. Results and discussion	45
5.5. Conclusions	51
5.6. References	52

6. The cathodic reduction of dioxygen at metal tetrasulfonato-phthalocyanines: influence of adsorption conditions on electrocatalysis	54
6.1. Introduction	54
6.2. Experimental section	55
6.3. Results and discussion	56
6.3.1. The adsorption process	56
6.3.2. Dioxygen reduction on CoTSPc	62
6.3.3. Dioxygen reduction on FeTSPc	65
6.3.4. FePc compared with FeTSPc	69
6.4. References	71
7. The mechanism of the dioxygen reduction at iron tetrasulfonato-phthalocyanine incorporated in polypyrrole	73
7.1. Introduction	73
7.2. Experimental	73
7.3. Results and discussion	74
7.3.1. Dioxygen reduction at polypyrrole applied on Cp	74
7.3.2. Dioxygen reduction at FeTSPc incorporated in polypyrrole	76
7.4. Concluding remarks	84
7.5. References	85
8. The electrocatalysis of dioxygen reduction in an acidic solution of iron tetrasulfonato-phthalocyanine	86
8.1. Introduction	86
8.2. Results and discussion	86
8.2.1. (Spectro-)electrochemical measurements in a dinitrogen-saturated solution of FeTSPc	86
8.2.2. (Spectro-)electrochemical measurements in a dioxygen-saturated solution of FeTSPc	94
8.3. Concluding remarks	103
8.4. References	105
9. Polarography of dioxygen in solutions of metal tetrasulfonato-phthalocyanines	106
9.1. Introduction	106
9.2. Results and discussion	106
9.2.1. Dioxygen reduction on mercury	106
9.2.2. Dioxygen reduction on mercury in the presence of dissolved metal tetrasulfonato-phthalocyanines	109

9.3. Concluding remarks	112
9.4. References	112
10. Electroreflectance spectroscopic measurements	114
10.1. Introduction	114
10.2. Theoretical aspects	114
10.3. Results for alkaline solution	115
10.4. Results in acidic solution	118
10.5. Discussion	120
10.6. Concluding remarks	123
10.7. References	124
11. In situ light absorption spectroscopy of metal tetrasulfonato- phthalocyanine/polypyrrole layers	125
11.1. Introduction	125
11.2. Co ⁻ and FeTSPc solutions	125
11.3. Co ⁻ and FeTSPc in polypyrrole	128
11.3.1. General considerations	128
11.3.2. Spectra of CoTSPc, incorporated in polypyrrole	131
11.3.3. Spectra of FeTSPc, incorporated in polypyrrole	133
11.4. Concluding remarks	135
11.5. References	136
12. Concluding remarks	137
List of abbreviations and symbols	141
Summary	144
Samenvatting	147
Curriculum vitae	150
Dankwoord	151

1. Introduction

Molecular oxygen takes part in many reactions, and for most biological systems, it is an essential species to satisfy their energy demands. In spite of this, its activation to react is difficult. On the one hand, this has the advantage that no spontaneous reactions occur and that the existence of dioxygen, together with combustible compounds in the same environment, is possible. On the other hand, some reactions, which are thermodynamically favoured, are in practice so slow that they do not occur at all under normal (moderate) conditions. In biological systems, we see a great variety of biocatalysts (enzymes) which ultimately activate the dioxygen molecule at moderate (low) temperature [1].

The subject of this thesis: the electrochemical reduction of dioxygen, is also an example of a thermodynamically favourable, but in practice, slow reaction [2]. This reaction is important with respect to energy conversion. A fuel cell is a device for the conversion of the chemical energy of an apt fuel into electrical energy. At the cathode of this cell dioxygen accepts electrons and is reduced. At the other electrode, the anode, the fuel (for instance H_2) is oxidized [3]. Theoretically, it can be derived that the conversion efficiency of a fuel cell is higher than those of more conventional means of electricity production, where first heat is produced by combustion of the fuel and, thereafter, converted by steam turbines into electricity [4]. For this reason, a considerable effort is given in the last two decades to the study of the electrochemical reduction of dioxygen [5].

The rate of the reduction reaction of molecular oxygen depends on the electrode material, i.e. the electrode surface material. Platinum is commonly used in a fuel cell as electrocatalyst [6]. However, the high cost of this noble metal and its low availability resulted into a search for alternatives [7].

Metal phthalocyanines (MePc) are an alternative [8]. This class of compounds consists of a metal ion surrounded by four nitrogen atoms of the phthalocyanine ring structure (see figure 1.1. Also the structure of metal porphyrin (MeP), a biological more important compound than MePc, is given in the figure). Especially, the phthalocyanines with cobalt or iron (CoPc or FePc) as a central metal ion are active [9].

The work described in this thesis has been concentrated on the fundamental aspects of the dioxygen reduction, catalyzed by cobalt and iron tetra-sulfonato-phthalocyanine (Co- and FeTSPc), see figure 1.1. The substituent

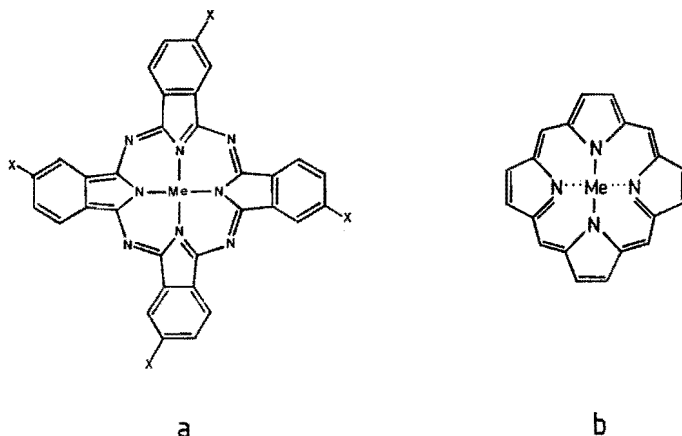


Fig. 1.1 Molecular structure of metal phthalocyanine (MePc) (a) with on the place of X a hydrogen atom; in the case of metal tetrasulfonato-phthalocyanine (MeTSPc) X is NaSO_3^- ; and metal porphyrin (MeP) (b).

"sulfonato" is introduced to make the complex soluble in water. Here, we studied the behaviour of the catalysts under very different conditions and in very different environments, such as dissolved in water, adsorbed on graphite or incorporated in a conducting polymer (polypyrrole), in order to investigate the influence of the environment on the electrochemistry of dioxygen. From this, some conclusions can be drawn about the reduction mechanism of dioxygen.

In chapter 2, a short literature overview of the basic electrochemical principles, which are important to understand the electrocatalysis of the dioxygen reduction, is given. In this chapter also some attention is paid to the results of light absorption spectroscopy for Co- and FeTSPc.

In chapter 3, a literature survey will be given about the models (classical and quantum mechanical) for the adsorption of dioxygen on the metal chelates.

In the next chapter, 4, the experimental methods used to obtain the results described in this thesis, are treated.

Different electrode preparation methods are discussed in chapter 5. First, a theoretical derivation for the effect of the number of active sites on the overall activity of the electrode is given. Secondly, several preparation methods, with regard to the number of active catalyst sites on the electrode surface, are studied. The factors and rules, determining whether the catalyst molecule forms an active site or not, are discussed.

There are two preparation methods, which result in an electrode surface where all the present catalyst molecules are active. Their electrochemical behaviour is studied in more detail in chapter 6 (adsorption on pyrolytic graphite) and in chapter 7 (incorporation in polypyrrole).

Electrochemical measurements, carried out in solutions of water soluble phthalocyanines, are reported in the chapters 8 and 9. Although in practical systems solutions of phthalocyanines in such high concentrations ($\sim 10^{-3}$ M) will be never used, some striking observations can be made about the dioxygen reduction reaction catalyzed by FeTSPc. In chapter 8, the reduction of dioxygen on electrode materials such as pyrolytic graphite (Cp) and glassy carbon (Cg) is investigated. This chapter is completed with in situ absorption spectroscopy, carried out to clarify the nature of the observed reactions. In chapter 9, the reduction of dioxygen catalyzed by phthalocyanines on mercury is reported. Also, a comparison is made between the dioxygen reduction on Cp and mercury.

The way of adsorption of the metal chelates on the basal plane of stress annealed pyrolytic graphite (BP of SA-Cp) is studied by using electroreflectance spectroscopy [10], and the results are described in chapter 10. The reason for this study was the proposal, made in chapter 6, about the way of adsorption of FeTSPc on Cp.

In chapter 11, the in situ absorption spectroscopy performed on the catalysts incorporated in polypyrrole, is described. These investigations were carried out to verify the explanation given in chapter 7 for the striking behaviour observed for FeTSPc incorporated in polypyrrole.

In the last chapter, 12, some conclusions about dioxygen reduction are given. Also, some outlines and ideas for future research are proposed.

1.1. References

1. G.L. Zubay, 'Biochemistry', Addison-Wesley Publishing Company, Inc., Reading (Massachusetts) (1983).
2. J.P. Hoare, 'Oxygen' in Encyclopedia of Electrochemistry of the Elements, Vol. II, edited by A.J. Bard, Marcel Dekker, Inc., New York (1974).
3. J.O'M. Bockris and S. Srinivasan, 'Fuel Cells; Their Electrochemistry', McGraw-Hill Book Company (1969).
4. K. Kordes, 'Brennstoffbatterien', Springer Verlag Wien-New York (1984).
5. J.P. Hoare, 'The Electrochemistry of Oxygen', Interscience, New York (1968).

6. G. Sandstede, 'Introduction-types of Fuel Cells' in 'From Electrocatalysis to Fuel Cells' edited by G. Sandstede, published for Battelle Seattle Research Center by the University of Washington Press, Seattle and London (1972).
7. F. van den Brink, E. Barendrecht and W. Visscher, Recl. Trav. Chim. Pays-Bas 99 (1980) 253.
8. R. Jasinski, J. Electrochem. Soc. 112 (1965) 526.
9. J.A.R. van Veen and C. Visser, Electrochim. Acta 24 (1979) 921.
10. J.P. Dalbera, C. Hinnen and A. Rousseau, J. de Phys. C5, 38 (1977) 185.

2. Literature review on cathodic dioxygen reduction, catalyzed by transition metal chelates

2.1. Introduction

An extensive review has been published by Van den Brink et al. [1a], Yeager [1b] and Van der Putten [1c]. Further, the literature on the absorption spectra of the water soluble metal tetrasulfonato-phthalocyanines and the influence of dioxygen on these spectra is summarized.

2.2. Dioxygen reduction

Dioxygen can be electrochemically reduced according to the following reactions [2]:



These reactions are written for acid solutions, but they can be easily converted into the corresponding ones for alkaline electrolytes by adding OH^- on both sides of the equations. The formal potentials are 1.229 V and 0.682 V (at $\text{pH} = 0$ vs. NHE: Normal Hydrogen Electrode) for, respectively, reaction (1) and (2) [2]. In both reactions, protons are involved and therefore a pH-dependency, as is given in the diagram of figure 2.1, is observed for the formal potentials. The formal potential of the one-electron reduction of dioxygen (3) is, of course, pH-independent and given in the diagram as a horizontal line ($E^\circ = -0.33$).

When CoPc is used as a catalyst, only reaction (2) is observed, both in alkaline [3,4,5] and in acid [3] solutions. On FePc, reaction (1) occurs predominantly in alkaline electrolytes [4,6,7]; while in acid solutions only reaction (2) is observed [8].

Contrary to the fact that the formal potential of reaction (2) is pH-dependent, for the dioxygen reduction catalyzed by CoPc a pH-independent behaviour is found [3], so that in alkaline solutions a small overpotential is

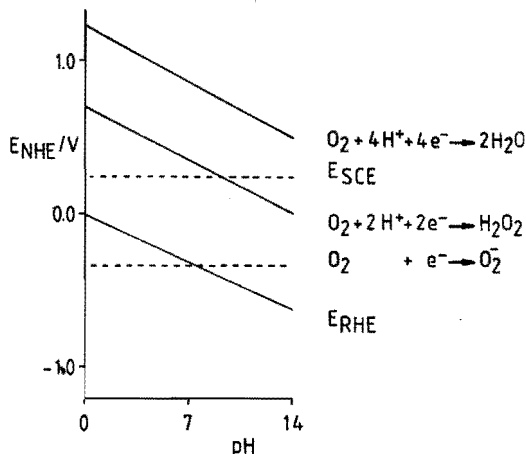


Fig. 2.1 Pourbaix diagram for dioxygen reduction (SCE: Saturated Calomel Electrode and RHE: Reversible Hydrogen Electrode).

observed for the dioxygen reduction to hydrogen peroxide, while in acid solutions, the reduction onset potential lies far more negative from the equilibrium potential. For FeTSPc a more complex, but in principal Nernstian pH-dependent behaviour is observed [9]; see also chapter 6 of this thesis.

Although the reduction of hydrogen peroxide (4) is energetically very favourable ($E_o = 1.776$ V), the reaction does not occur on CoPc in the potential region of interest. For FePc, however, a slow reaction (thus a large overpotential) is observed.



2.3. Light absorption spectroscopy

Co(II)TSPc dissolved in an alkaline solution (0.1 M KOH) shows a spectrum, mainly consisting of two peaks (see figure 2.2) [11,12]. These peaks, observed in deoxygenated solutions, are ascribed to monomer (at 663 nm) and dimer (at 626 nm) species of CoTSPc. When the concentration of the solution increases, the height of the dimer peak increases at the expense of the monomer peak [11]. Also, the addition of a salt, as for instance KCl, leads to an increase of the dimer absorption band. Because of the observation, that for high salt concentrations (10^{-1} M) the isosbestic behaviour is lost, it is even suggested that higher aggregates are formed in these concentrated solutions [12].

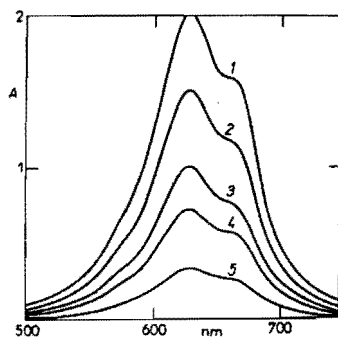


Fig. 2.2 Dependence of the change of absorption spectrum on the CoTSPc concentration in 0.1 M NaOH; $d = 1.0$ cm; the curves were recorded immediately after alkalinization; concentration of CoTSPc
 1) 4.0×10^{-5} M; 2) 3.0×10^{-5} M; 3) 2.0×10^{-5} M; 4) 1.5×10^{-5} M; 5) 7.0×10^{-6} M (from reference [11]).

Upon introduction of dioxygen a new peak appears at almost the same absorption wavelength as the monomer (670 nm) [11,12,13] (see figure 2.3).

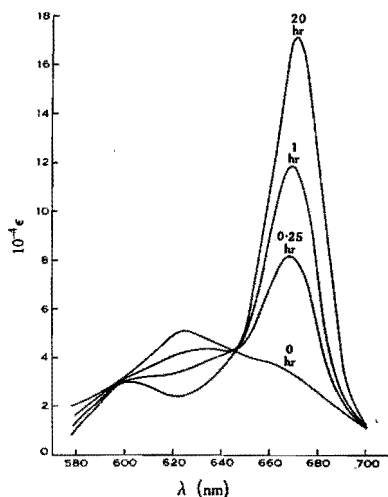


Fig. 2.3 Effect of dioxygen on the absorption spectrum of CoTSPc (5×10^{-6} M) in 0.1 M NaOH at 20°C after various periods of oxygenation (from reference [12]).

From dioxygen uptake measurements, it has been concluded that two CoTSPc molecules adsorb one dioxygen molecule, and therefore, the formation of a dioxygen bridged dimer has been proposed [11] (see also figure 2.4).

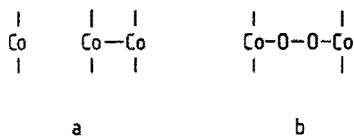


Fig. 2.4 CoTSPc species in a dioxygen-free solution (a) and a dioxygen-saturated solution (b).

Wagnerova et al. [11] claimed that OH^- has a promoting effect on the dioxygen adduct formation because only for solutions with a pH above twelve a dioxygen adduct has been observed [13,14]. However, more recently, it was reported [15] that also in acid solutions dioxygen adducts can be observed.

Kobayashi et al. [16] reported the spectra of several electrochemically prepared oxidation states of cobalt- and iron tetracarboxy-phthalocyanines (Co- and FeTCPc). These compounds are closely related to the sulfonated phthalocyanines and they are also soluble in water. From the spectra measured for CoTCPc (see figure 2.5), Kobayashi et al. have concluded that Co(II)- and

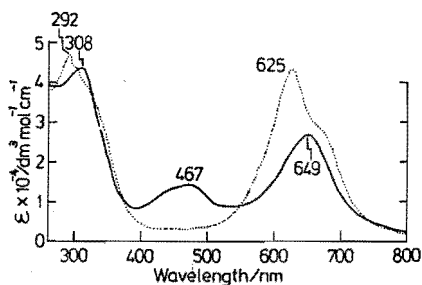


Fig. 2.5 UV-Vis. absorption spectra of Co(II)TCPc (...) and electrogenerated Co(I)TCPc (—) in 0.1 N bicarbonate solution (pH 9.0). $[\text{Co(II)TCPc}] = 1.20 \times 10^{-4}$ M, path length = 1.0 mm (from reference [16]).

Co(I)TCPC are well characterized by the peaks at respectively 625 and 649 nm.

For Fe(II)TSPC no equilibrium exists between the monomer and dimer form. For deoxygenated solutions of FeTSPC a spectrum has been recorded with a main absorption at 670 nm [17]. This band can be ascribed to a monomer species. Less intense peaks are found at 605, 425 and 330 nm. By bubbling dioxygen gas through the solution, the absorption at 670 nm disappears and a new one at 632 nm can be detected. From the measurement of the dioxygen uptake, again it is concluded, that a dioxygen bridged dimer is formed.

The spectrum of Fe(III)TSPC (no dioxygen present) has a main absorption band at a wavelength of 635 nm [17]. The oxidized compound was prepared by using a Fe(III) salt instead of a Fe(II) salt for the synthesis of the metal phthalocyanine [18]. The results of Kobayashi et al. [16] for FeTCPC confirm the main absorption wavelength of Fe(III)TSPC. They found for Fe(III)TCPC the spectrum of figure 2.6. The spectrum of the other possible oxidation state (Fe(II)TCPC) is also given in this figure.

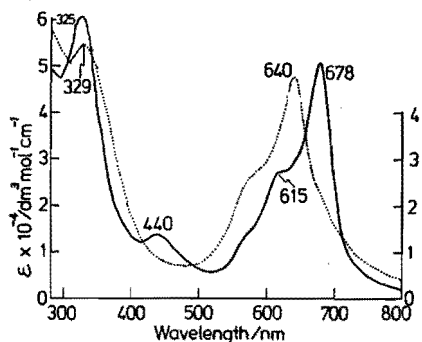


Fig. 2.6 UV-Vis. absorption spectra of Fe(III)TCPC (...) and electrogenerated Fe(II)TCPC (—) in 0.1 N bicarbonate solution (pH 9.0). [Fe(III)TCPC] = 1.14×10^{-4} M, path length = 1.0 mm (from reference [16]).

2.4. References

1. a. F. van den Brink, E. Barendrecht and W. Visscher, Recl. Trav. Chim. Pays-Bas 99 (1980) 253.
b. E. Yeager, Electrochim. Acta 29 (1984) 1527.
c. A. van der Putten, Thesis, Eindhoven University of Technology, Eindhoven (1986).

2. J.P. Hoare, 'Oxygen' in Encyclopedia of Electrochemistry of the Elements, vol. II, edited by A.J. Bard, Marcel Dekker, inc., New York (1974).
3. J. Zagal, R.K. Sen and E. Yeager, J. Electroanal. Chem. 83 (1977) 207.
4. J. Zagal, P. Bindra and E. Yeager, J. Electrochem. Soc. 127 (1980) 1506.
5. F. van den Brink, W. Visscher and E. Barendrecht, J. Electroanal. Chem. 157 (1983) 305.
6. A.J. Appleby, J. Fleisch and M. Savy, J. of Cat. 44 (1976) 281.
7. F. van den Brink, W. Visscher and E. Barendrecht, J. Electroanal. Chem. 172 (1984) 301.
8. H. Behret, W. Clauberg and G. Sandstede, Zeitschrift für Physikalische Chemie, Neue Folge, Bd. 113 (1978) 113.
9. J.H. Zagal-Moya, Thesis, Case Western Reserve University, Cleveland (1978).
10. F. van den Brink, Thesis, Eindhoven University of Technology, Eindhoven (1981).
11. D.M. Wagnerova, E. Schwertnerova and J. Veprek-Siska, Coll. Czech. Chem. Commun. 39 (1974) 1980.
12. L.C. Gruen and R.J. Blagrove, Aust. J. Chem. 26 (1973) 319.
13. J.H. Schutten, Thesis, Eindhoven University of Technology, Eindhoven (1981).
14. E.W. Abel, G.M. Pratt and R.J. Whelan, Chem. Soc. Dalton Trans. (1976) 509.
15. B. Simic-Glavaski, S. Zecevic and E. Yeager, J. Electroanal. Chem. 150 (1983) 469.
16. N. Kobayashi and Y. Nishiyama, J. Phys. Chem. 89 (1985) 1167.
17. D. Vonderschmitt, K. Bernauer and S. Fallab, Helv. Chim. Acta 48 (1965) 951.
18. J.H. Weber and D.H. Busch, J. Inorg. Chem. 4 (1965) 469.

3. Dioxygen adsorption on metal chelates.

Theoretical considerations

3.1. Introduction

Catalysis of the dioxygen reduction requires an interaction between the catalyst and dioxygen, i.e. adsorption of the latter on the catalyst [1]. It is to be expected that the adduct formed and its properties are essential for the type of the reduction process. Therefore, in this chapter some models for the description of the dioxygen adducts of metal chelates will be given.

Most of the models proposed in the literature have been developed to explain a specific aspect (as for instance the ESR signal) of the dioxygen binding to the metal chelates. Also, a number of theoretical studies have been focussed on dioxygen adsorption on porphyrin-type chelates, because iron porphyrin (FeP) is considered as the active centre of the hemoglobin molecule [2].

First, the Molecular Orbital (M.O.) description of dioxygen and a description of a metal chelate in the ligand field approximation, is given. Hereafter, qualitative models followed by quantitative calculation methods will be discussed. At the end of this chapter, dioxygen adducts of binuclear metal complexes are considered. The discussion about the possible consequences of the (electronic) structure of the dioxygen adduct on the reduction mechanism is postponed to the last chapter.

3.2. Electronic structure of dioxygen and of a metal chelate

The energy level diagram of a dioxygen molecule can be derived within the M.O. method (see figure 3.1). In the ground state the molecular orbitals are occupied in such a way that two unpaired electrons are in the two degenerated anti-bonding π -orbitals [3]. Therefore, the ground state is a triplet state and can be denoted by ${}^3\Sigma_g$. In the diagram three bonds are visualized: a two-electron σ -bond: $(3\sigma_g)^2$ and two three-electron π -bonds: $(1\pi_u)^2(1\pi_g)^1$.

The crystal field theory (sometimes called the ligand field theory) predicts the energy level scheme for the d-orbitals of a transition metal, surrounded by ligands [4,5]. For the metal phthalocyanines (MePc) the four ligands (the most inner nitrogen atoms of the phthalocyanine ring structure) are coordinated to the metal in a square planar geometry. For these planar

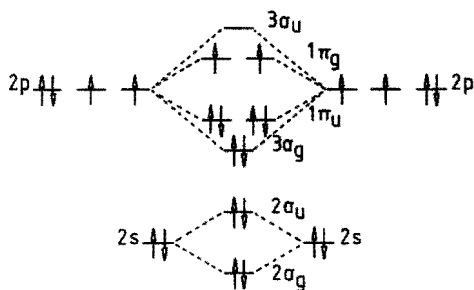


Fig. 3.1 M.O. diagram of dioxygen.

complexes a level splitting as given in figure 3.2 is expected. In this figure also the patterns of splitting for the octahedral and tetragonally distorted octahedral complex are given. For the latter a fifth ligand is necessary. When MePc is deposited onto an electrode, it is possible that basic surface groups of the substrate, or water, or even another dioxygen molecule, act as a fifth ligand for the metal ion [6]. The ligand field theory predicts a general

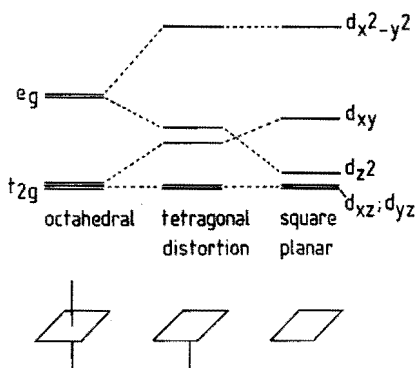


Fig. 3.2 Energy level diagram for 3d-metal orbitals in several geometries.

energy level diagram for the various geometries. In individual cases, depending on the ligands and the metal ion, some deviations of the general pattern are possible.

The next problem is: how do the electrons spread themselves over the orbitals of the diagram. Hund's Rule predicts that other conditions being equal, the states of the highest spin will have the lowest energy [7]. There are, respectively, 7 and 6 d-electrons in Co(II) and Fe(II) ions. In this

simple model CoPc and FePc are complexes with a strong ligand field, which means that the energy level splitting is such that the spins are paired as much as possible [8]. Thus, in principle, the MePc's are low spin complexes. The presence of a fifth ligand only affects the occupation of the dz^2 and dxy and has therefore no influence on the spin-multiplicity of CoPc. For FePc, it is possible that coordination of an extra fifth ligand causes a spin-multiplicity change from low to intermediate or even to high spin.

3.3. Electronic structure of dioxygen adducts.

Qualitative models

One of the first models for dioxygen adsorption on metal complexes has been proposed by Griffiths [9]. In his model, Griffiths assumed sp^2 -hybridization for the oxygen atom close to the metal ion [3,10]. When the geometry is as in figure 3.3a, the sp^2 -orbital χ can be described by

$$\chi = \frac{1}{\sqrt{3}} \psi(2s) - \frac{1}{\sqrt{2}} \psi(2p_x) + \frac{1}{\sqrt{6}} \psi(2p_y) \quad (1)$$

According to Griffiths the ionization energy of this orbital can be calculated from those of the atomic orbitals by using 1/3 of the value for the 2s-orbital and 2/3 of the value for the 2p-orbital. From the atomic spectra of oxygen an ionization energy of $0.216 \text{ kJ mol}^{-1}$ can be calculated for the orbital χ . For the alternative structure (see figure 3.3b), Griffiths found an

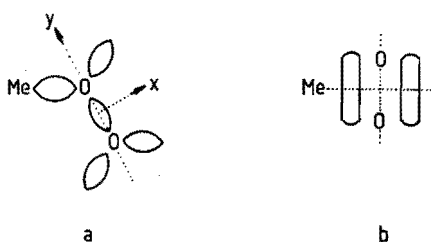


Fig. 3.3 Adsorption types of dioxygen
a) "end-on" (sp^2 -orbital); b) "side-on" ($1 \pi_u$ -orbital).

ionization energy of $0.172 \text{ kJ mol}^{-1}$ from molecular spectra for the $1 \pi_u$ molecular orbital. From this difference he concluded that the last structure is the most favourable one because in this structure the electrons of dioxygen

are more easily involved in the oxygen-metal bond, than for the structure of figure 3.3a. (The dioxygen orbitals are considered to be donating orbitals). The two adsorption types depicted in figure 3.3a and b are, respectively, called "end-on" (bent) and "side-on" adsorption. So, Griffiths came to the conclusion that dioxygen always adsorbs in the "side-on" configuration. For this reason this type of adsorption is often called "Griffiths adsorption". The model has the advantage that it presents an easy physical picture of the dioxygen adsorption, but it may be too crude because of the complete ignorance of the metal atomic orbitals. Also, the comparison between atomic and molecular orbitals is questionable.

The "end-on" adsorption was first proposed by Pauling [11,12]. Using the same concepts as described above, an extension of Griffiths model can be made by also considering the metal atomic orbitals [10]. For a transition metal in a relatively high oxidation state, the d-orbitals will be considerably contracted, compared with the zero-valent state; thus the overlap with the bonding and anti-bonding π -orbital of dioxygen will be small in the "side-on" adsorption case. Therefore, the dioxygen ligand coordinated to iron(II) and cobalt(II) complexes prefers the "end-on" orientation.

For the charges on the dioxygen ligand and the metal ion, Weiss proposed that the dioxygen in oxyhemoglobin is present as a superoxide ion with the iron being in a ferric state, i.e. $\text{Fe(III)} - \text{O}_2^-$ [13].

The following, more sophisticated, model to discuss is the spin-pairing model [14,15,16]. The pertaining theory has both qualitative and quantitative aspects, and is developed to explain the results of ESR spectroscopy. In the spin-pairing model the metal ion and the dioxygen molecule are both considered to be free radicals, whose spins have paired up in the dioxygen adducts [14]. Within the framework of this spin-pairing theory, Drago and Corden [14] give a description of the binding of dioxygen to five-coordinated cobalt(II) complexes. The energy level diagram of the cobalt(II) complex is given in the left part of figure 3.4. The level splitting pattern is predicted by simple ligand field theory and is, of course, the same as given in figure 3.2 for the tetragonally distorted octahedral complex. A $1 \pi_g^*$ -orbital (the asterix denotes that the orbital is anti-bonding), which contains one of the two unpaired dioxygen electrons, overlaps with the d_{z^2} -orbital of the cobalt(II) ion. This results in a σ -bonding orbital containing two electrons. The corresponding σ^* anti-bonding orbital is empty. The other $1 \pi_g^*$ -orbital is orthogonal to the d_{z^2} -orbital and it remains essentially unaltered in the

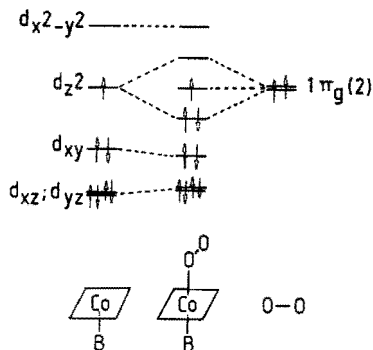


Fig. 3.4 Energy level scheme for dioxygen binding to a Co(II) complex within the spin-pairing model. Only stabilizing interactions are depicted.

adduct. The unpaired electron of the adduct resides in the unaltered $1\pi_g^*$ -orbital and belongs in principal to the dioxygen molecule. To maximize the σ -bonding interaction between the d_{z^2} - and the $1\pi_g^*$ -orbital, the adduct tends to have a bent configuration as shown in figure 3.4 [16]. The overlap of other d-orbitals with dioxygen molecular orbitals is neglected in this model.

An iron(II) ion has a d-electron configuration with one electron less than cobalt(II). As already mentioned before, the spin state of iron(II) complexes is not exactly known. Often, it is reported that coordination of an axial base to a four-coordinated iron(II) complex converts the complex in a high spin complex which thereafter reversibly picks up dioxygen [10,14,17,18,19]. Therefore, in the spin-pairing model high spin five-coordinated iron(II) is used as starting point. From the energy level schemes of the iron ion and the dioxygen molecule, as depicted in, respectively, the left and right part of figure 3.5, two types of molecular orbital schemes can be constructed for the dioxygen adduct. The first one is given in figure 3.5a. The metal d_{z^2} -orbital overlaps with one of the anti-bonding $1\pi_g^*$ dioxygen orbitals. The combination results in a filled σ -bonding and an empty σ^* -anti-bonding orbital. One of the d_{xz} - or d_{yz} -orbitals is also partly occupied and the orbitals can overlap with the other anti-bonding $1\pi_g^*$ -orbital of the dioxygen molecule to form a bonding and anti-bonding combination with π -symmetry ($d\pi-p\pi$). The occupancy of the molecular orbitals is given in figure 3.5a. All levels are either fully populated or empty, and therefore, the adduct is diamagnetic as is observed for reversible iron(II) systems [15].

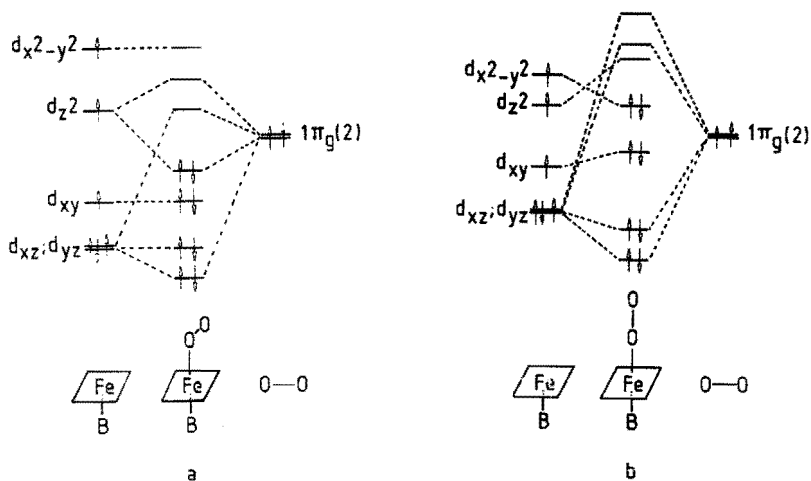


Fig. 3.5 Energy level scheme for dioxygen binding to a Fe(II) complex within the spin-pairing model. a) "end-on (bent)" adduct; b) "end-on (linear)" adduct. Only stabilizing interactions are depicted.

Also, an overlap of both $1\pi_g^*$ -orbitals with the dxz - and/or dyz -orbitals is possible. The dz^2 is now raised in energy by its strong interaction with the dioxygen ligand. This interaction is thought to be so strong that the dz^2 -orbital is driven higher in energy than the dx^2-y^2 (see figure 3.5b). The level scheme shows now two fully populated ($d\pi-p\pi$) bonding and two empty ($d\pi-p\pi$) anti-bonding combinations. Also this formalism of the dioxygen binding to the iron(II) complex leads to a diamagnetic complex.

For the first formulation, an adduct is expected which lies between the linear and the bent configuration. For the last case, with only $d\pi-p\pi$ interactions, a linear adduct is favoured, because this geometry results in maximum possible overlap between the metal dx^2 -, dy^2 - and the dioxygen $1\pi_g^*$ -orbitals [16] (see figure 3.5). Although a linear complex is possible within the spin-pairing model, a bent dioxygen adduct is reported for most iron(II) porphyrin complexes [16].

Another theory, which must be mentioned, is the increased valence theory [20,21] as applied by Harcourt to dioxygen bridged dimers of porphyrins [22]. Van der Putten [23] used this theory to explain the dioxygen reduction behaviour of a planar dicobalt chelate. Only the principles of the increased valence theory are outlined here. In the dioxygen bridged dimers of porphyrins

"bridge" adsorption of dioxygen occurs [24]. The dioxygen molecule interacts here with two metal atoms simultaneously, see figure 3.6 (c.f. with the "side-on" and "end-on" adsorption types). For noble metals such as platinum

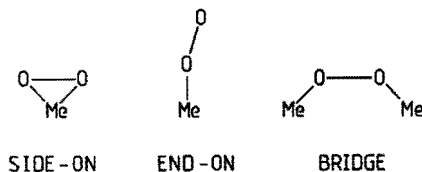


Fig. 3.6 Various adsorption types of dioxygen.

and silver often bridged adsorption is assumed [25,26]. In the cofacial dicobalt porphyrins synthesized by Collman and coworkers [27], the porphyrin rings are interconnected with two chains of atoms. For a chain of four atoms, the so created distance between the two cobalt ions makes bridge interaction of the dioxygen molecule possible.

The increased valence theory can be considered as an extension of the classical valence theory. Some quantum chemical concepts about one-electron bonds (for instance H_2^+) are added to the normal two-electron bonds (electron-pair binding) of the valence theory. The increased valence formulae are constructed from the normal valence formulae, but now the possibility that electrons occupy anti-bonding orbitals is also accounted for in the formulae. The theory is convenient for the description of a molecular system in which four electrons are delocalized over three atomic orbitals, belonging to three different atoms. (In the case of a dioxygen adduct the three atoms are, respectively, the metal and the two oxygen atoms). A more extensive treatment of the theory is given in reference [23].

3.4. Electronic structure of dioxygen adducts.

Quantitative models

The next theory to be treated, can be denoted as the spin crossover theory. It is based on a semi-quantitative model to be clarified as follows.

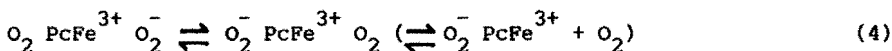
After dioxygen adsorption on an iron chelate molecule, resonance between the following configurations is possible [28]:



Appleby and coworkers proposed that in the bulk of for instance a vacuum deposited layer of iron phthalocyanine, the following chemisorption step occurs [29]:



From results of several spectroscopic techniques, such as Mössbauer and Optical Reflectance Spectroscopy, they concluded that the chemisorption of dioxygen is most favourable for Fe(III)-high spin or intermediate spin configurations. In the same way, Appleby et al. also explained the conduction mechanism of the phthalocyanine layer by supposing resonance (with chemisorption) and the existence of complete redox chains in the layer, in which charge transfer occurs by processes as given in the next equation.



Appleby et al. assumed that the existence of an easy multispin crossover is an important factor for a complex to bind dioxygen and to catalyse its reduction [28]. This assumption is based on the above given equations, in which for dioxygen both singlet and triplet states are possible.

The ground state wave functions (or vectors) for the $d^5(\text{Fe}^{3+})$ -configuration in N_4 -chelates have been determined [30]. A short description of the calculation technique will be given, focussed on the method to decide from ESR data whether spin crossover easily or not easily occurs for a certain complex.

The l 's (angular momentum quantum number of an individual electron) and the s 's (spin quantum number of an individual electron) can be added to one angular momentum quantum number L and one spin quantum number S . Now, the following terms (^{2s+1}L) can be derived for the d^5 -configuration: 6S , 4P , 4D , 4G , 2S , 2P , 2D , 2D , 2D , 2F , 2F , 2G , 2H , 2I . The energies of these terms are determined by interelectronic repulsion. Next, the spin-orbit coupling must be accounted for and a new quantum number $J = L + S$ can be defined (weak coupling limit). At this stage, the derived wave functions (or states) are orthogonal and are composed of functions which can be defined by SLJ . These are the ordinary states of the free ion.

The degeneracy of the states is further reduced through the crystal field operator. This operator can be expanded in spherical harmonics and for an octahedral we have:

$$V(r) = - \sum_{i=0}^6 \frac{Z_i e^2}{|R_i - r|} = - \sum_{i=1}^6 \sum_{n=0}^{\infty} \sum_{m=-n}^n \left(\frac{4\pi}{2n+1} \right) \left(\frac{Ze}{a} \right)^{2n} C_m^n(\theta, \phi) C_m^n(\theta_1, \phi_1) \quad (5)$$

where Z_i is the charge of the ligand on the place R_i , e is the unit of charge, $C_m^n(\theta, \phi)$ are the spherical harmonics, a is the distance of the ligands from the origin and (r, θ, ϕ) are the coordinates of the electron. For C_{4v} -symmetry the crystal field operator can be simplified to:

$$V = B_0^2 C_0^2 + B_0^4 C_0^4 + B_4^4 (C_{-4}^4 + C_4^4) \quad (6)$$

where B_i^j are crystal field parameters. The Hamiltonian can be diagonalized for several combinations of the crystal field parameters. The resulting ground state wave functions remain reasonably well characterized by the spin quantum number. Ground state spin diagrams can now be constructed, in which the ground state spin-multiplicity is given as a function of the crystal field parameters.

For the ground state wave functions of each spin-multiplicity domain, it is possible to calculate the electron g -values, which can be compared with the g -values measured by ESR spectroscopy. In this way, the place of a complex in the ground state spin diagram can be determined. An easy spin crossover can be expected when the complex lies close to the border between two multiplicities.

In short, the procedure is as follows: for a Fe(III) complex the g -values are determined by ESR spectroscopy. The wave function which belongs to these g -values and its place in the ground state spin diagram is determined. When the complex lies on the border of two multiplicities, it is expected that the complex is active in dioxygen reduction.

Three g -values, instead of two as for C_{4v} -symmetry, are found for many Fe(III) complexes. This indicates that the symmetry of the complex is even lower than C_{4v} -symmetry. To account for this, the above given calculation must be repeated for C_{2v} -symmetry.

One of the first quantum chemical calculations on iron porphyrin (FeP) has been published by Zerner et al. [31]. They have adapted the Hückel approximation until a method resulted, suitable to calculate the energies of the d -orbitals of the metal ion in the ligand field of the macrocycle. The method is called the Self Consistent Charge - Extended Hückel (SCC-EH) approximation. This means that the iterative calculations are stopped, as soon

as the charge distribution, which is each time determined, does not change during one calculation cycle.

They determined the sequence in increasing energy for the metal d-orbitals as, respectively, $dxy \leq dxz$, $dyz \leq dz^2 \leq dx^2-y^2$. In most cases this sequence did not change when they added a fifth (axial) ligand, as for instance water, to their calculation model. Also, the position of the iron ion (above or in the plane of the molecule) did not change the energy order of the d-orbitals. These modifications can, of course, change the energies of the orbitals and this influences their occupancy.

A FeP molecule with the Fe atom in the plane of the macrocycle resulted, in this model calculation, in an intermediate ($S = 1$) spin state with the occupancy: $(dxy)^2$; $(dxz, dyz)^3$; $(dz^2)^1$; $(dx^2-y^2)^0$. For the iron atom above the plane of the ligand, Zerner et al. found a high ($S = 2$) spin state, which belongs to the occupancy: $(dxy)^2$; $(dxz, dyz)^2$; $(dz^2)^1$; $(dx^2-y^2)^1$.

When the adduct formation of dioxygen is treated within the same model, a "side-on" adsorption geometry for the adduct is predicted and the molecular orbitals are filled in such a way that the dioxygen adduct is diamagnetic. The "end-on" adsorption appeared not to be stable within this extended Hückel calculation model.

The same approximation method has been applied to metal phthalocyanines (MePc) by Schaffer et al. [32]. The cage formed by the four nitrogen atoms is somewhat smaller for these complexes than for porphyrin complexes. This leads to a disturbance of the dxy-orbital, because the lobes of this orbital are pointing towards the nitrogen atoms of the ligand. To deal with this disturbance, a bonding and an anti-bonding combination of the dxy-orbital and the ligand orbitals can be constructed. These orbitals are, respectively, denoted by dxy and dxy*. The authors proposed, on the basis of this calculation, the following sequence in increasing energy for the d-orbitals: $dxy \leq dxz$, $dyz \leq dz^2 \leq dxy^* < dx^2-y^2$. ESR measurements showed that the unpaired electron of CoPc is placed in the dz^2 -orbital instead of the dxy*-orbital, as would be expected by using the above given energy order. Schaffer et al. give as possible explanation that in a phthalocyanine crystal the nitrogen atoms of the neighbour molecules, in adjacent layers above and below the phthalocyanine molecule, act as fifth (or sixth) ligand and drive the energy of the dz^2 above the energy of the dxy*-state. Also, for FePc the dxy* is occupied before the dz^2 . Based on their calculations, Schaffer et al. proposed a planar FePc molecule, with an intermediate ($S = 1$) spin state. A high ($S = 2$) spin complex is not attainable with FePc, because this requires a displacement from the

molecular plane considerably further than for the corresponding FeP complex. This will weaken the iron-nitrogen bonds too much and thus makes the high spin complex energetically unfavourable.

A related compound to the phthalocyanines is cobalt-acacen for which the structure is given in figure 3.7 [33]. Two of the four inner nitrogen atoms of

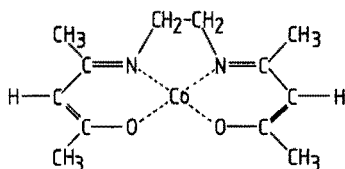


Fig. 3.7 The molecular structure of cobalt-acacen.

the phthalocyanine complex are replaced by oxygen atoms. Rohmer et al. [34] have carried out calculations to decide whether the dioxygen adsorption on the cobalt ion is "end-on" or "side-on". From ESR measurements with ^{17}O labeled dioxygen can be concluded that both oxygen atoms are magnetically equivalent. This result is consistent either with a "side-on" structure or with a rapid flipping of the dioxygen group between two bent positions. The oxygen atoms rearrange as is visualized in figure 3.8.

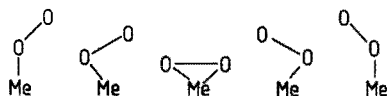


Fig. 3.8 Flipping of the dioxygen group between two "end-on" geometries.

The result is that for the "end-on" adsorption also a kind of average "side-on" structure is observed. Although the average structure is the same for both adsorption types, there is one fundamental difference: the average "side-on" structure represents for the "end-on" adsorption an energy maximum, while for the "side-on" adsorption this is a configuration which has just a minimum of energy.

The calculations of Rohmer et al. showed that the "end-on" adsorption is the most stable configuration. The introduction of a fifth axial ligand on the cobalt ion did not alter the energy sequence for the two adsorption types.

They also described the general principles and interactions, which determine the energies of the various ways of adsorption. A great part of this treatment is also valid for phthalocyanine molecules, and therefore, some more

attention will be paid to the description of cobalt-acacen. In the model calculation Rohmer et al. used the atomic orbitals of the involved atoms as a starting point. The 2px and 2pz atomic orbitals of oxygen are composed to a new orbital, denoted by π_g^a (or π_u^a , depending on the overlap between the orbitals of the two oxygen atoms). By this, only the atomic orbitals of oxygen are given in such a way that an easy description of the overlap between the involved orbitals is possible for the adsorption geometries of the figures 3.9, 3.10 and 3.11. It must be noted that the superscript a does not indicate that the orbital is anti-bonding. For some adsorption geometries this orbital consists almost entirely of the 2pz atomic orbital, while for other cases, it is a half and half mixture of the 2pz and 2px atomic orbitals. The remaining 2py-orbital of the oxygen atom is called π_g^b . These 2p-orbitals participate of course also in the oxygen-oxygen bond and the normal M.O. diagram for dioxygen, as given in figure 3.1, remains valid. For the metal ion the normal d-orbitals are used.

In the figures 3.9, 3.10 and 3.11 the orbital overlap is drawn for respectively "end-on" (bent); "end-on" (linear) and "side-on" adsorption. The

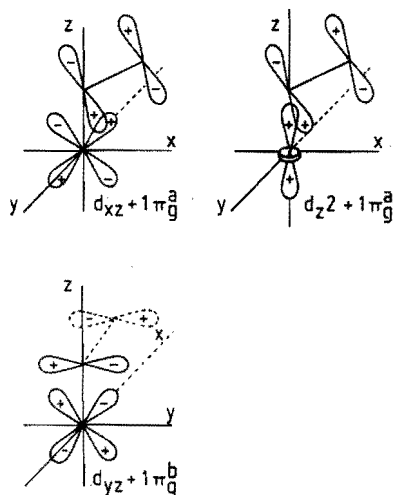


Fig. 3.9 Orbital overlap for "end-on (bent)" adsorption. To draw the d_{yz} - and $1\pi_g^b$ -orbitals the axes are rotated 90° counter clockwise.

strength of a bond is predicted not only by the overlap between two orbitals but also by the energy difference and the occupancy level of the orbitals. The interaction between two orbitals is only significant if the energy difference

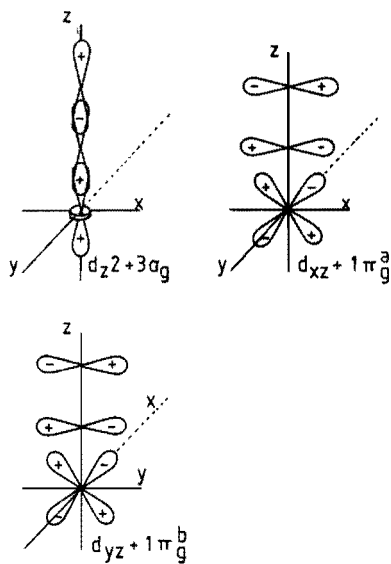


Fig. 3.10 Orbital overlap for "end-on (linear)" adsorption. Other conditions as in figure 3.9.

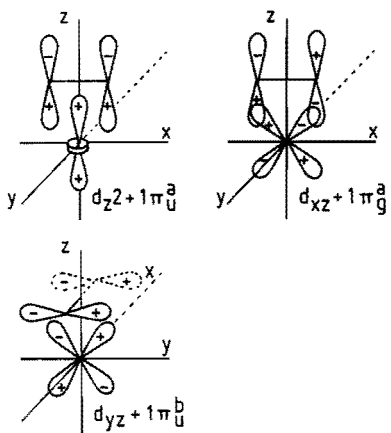


Fig. 3.11 Orbital overlap for "side-on" adsorption. Other conditions as in figure 3.9.

of them is small. Completely occupied orbitals destabilize the adduct when they overlap.

For cobalt-acacen the order in increasing energy for the d-orbitals is: $d_{xy} \leq d_{xz}, d_{yz} \leq d_{z^2} \leq d_{x^2-y^2}$, while according to Rohmer et al., the d_{z^2} -orbi-

tal has a higher energy than the anti-bonding $1 \pi_g^a$ -orbital of dioxygen. This metal dz^2 -orbital overlaps in the "end-on" (bent) geometry with $1 \pi_g^a$ (the orbital as constructed by Rohmer et al.), for the "end-on" (linear) case with $3\sigma_g$ and for the "side-on" structure with the bonding $1 \pi_u^a$ -orbital of the dioxygen molecule (see figure 3.9 - 3.11). For these orbitals the smallest energy difference can be expected between the dz^2 - and the anti-bonding $1 \pi_g^a$ -orbital; therefore this combination has the most stabilizing effect on the adduct. The interactions of the metal dxz and dyz with the M.O. orbitals of dioxygen are comparable for the two "end-on" adsorption cases. Thus the "end-on" (bent) structure is more favourable than the linear one. In the "side-on" adsorption structure the dyz -orbital overlaps with the bonding $1 \pi_u^b$ -orbital of the dioxygen molecule and, because of the fact that both orbitals are filled, this overlap destabilizes the adduct (see figure 3.11).

When the same concepts are used for cobalt phthalocyanine, then an "end-on" (bent) structure is predicted for its dioxygen adduct, if at least also the metal dz^2 -orbital of this complex is in energy above the $1 \pi_g^a$ -orbital of the dioxygen molecule.

In the last decade several ab initio calculation methods were developed to reveal the electronic structure of the porphyrins and of their dioxygen adducts. Especially, the dioxygen adduct of an iron porphyrin has often been a subject of study, because this compound is considered to be a model compound for the active centre of the hemoglobin molecule, as already has been mentioned in the introduction of this chapter. Many research workers are also puzzled by the observed cooperativity phenomenon for the hemoglobin molecule. The molecule possesses four iron porphyrin groups and after dioxygen adsorption on one of these the others are activated to adsorb also a dioxygen molecule [35]. In normal deoxyhemoglobin the iron ion is displaced out of the plane of the porphyrin ring and this out-of-plane-displacement has been estimated from an X-ray diffraction study to be 0.06 nm [36]. When dioxygen binds to deoxyhemoglobin, the iron ion moves into the plane of the porphyrin ring. After this, a sequential process is suggested which causes conformation changes in the four heme subunits. These changes are held responsible for the cooperativity of dioxygen bonding to hemoglobin [37,38]. Many quantum chemical calculations are undertaken on iron porphyrin to reveal the mechanism of the movement of the iron ion into the plane of the porphyrin ring as a result of dioxygen adsorption [39]. Only the electronic structures of the dioxygen adducts of cobalt and iron porphyrin predicted by most of these methods, will

be considered here. For the dioxygen adduct of cobalt porphyrin, with NH_3 as fifth (axial) ligand, the energy sequence and occupancy of orbitals is calculated by Dedieu et al. to be: $(d_{xy})^2 (d_{xz})^2 (d_{yz})^2 (\pi_g^a)^2 (\pi_g^b)^1$ [39]. Here π_g^a and π_g^b have the same meaning as in the discussion of the electronic structure of cobalt-acacen. Besides, NH_3 is used in many computations to simulate the effect of imidazole. In biological systems, often this base is encountered as a fifth (or sixth) axial ligand to the porphyrin [19]. For a catalyst as CoPc or FePc adsorbed on graphite probably basic groups of the surface occupy the fifth axially coordination site as was already stated in section 3.1., and dioxygen can bind on the sixth coordination place [40,41]. Therefore, the dioxygen binding to four- as well as to five-coordinated CoPc must be treated. The ground state electronic configuration, as given by Dedieu et al., indicates a charge transfer from cobalt to the dioxygen group, and a formal description as Co(III)-O_2^- is possible for the cobalt porphyrin-dioxygen adduct. Another result of their calculations is that the "end-on" (bent) structure is the most favoured one. Recent calculations of Newton et al. [42] for $\text{Co(O}_2\text{)P NH}_3$ confirm the electronic structure proposed by Dedieu et al.

Several authors give a ground state configuration for $\text{Fe(O}_2\text{)P NH}_3$, which corresponds with the formal description of the system, as Fe(II)O_2 , i.e. a neutral dioxygen group [39,43,44,45]. From the Mulliken population analysis, indeed a neutral dioxygen group is obtained, but in reference [44], a net negative charge for the dioxygen unit results. Most of the ab initio calculations predict a bent Fe-O-O moiety for the iron porphyrin complexes [45] in agreement with X-ray structure data [46]. A simplified M.O. diagram showing the main interactions in $\text{Fe(O}_2\text{)P}_3\text{NH}_3$, as follows from the ab initio calculations, is presented in figure 3.12 [46].

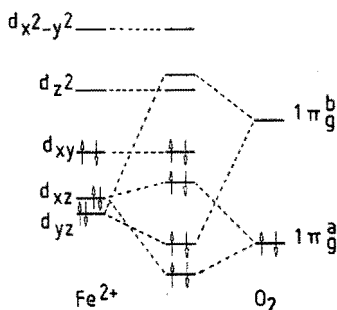


Fig. 3.12 Simplified M.O. diagram of $\text{Fe(O}_2\text{)PNH}_3$.

One of the most recent model calculations on phthalocyanine is due to Sabelli et al. [40]. For the di-anions of Pc and P, they used a procedure which is called CNDO-CI (Complete Neglect of Differential Overlap-Configuration Interaction), and for the corresponding iron complexes a method called INDO-CI (Intermediate Neglect of Differential Overlap-Configuration Interaction) was employed. They found that for FePc both planar d-orbitals (d_{xy} and $d_{x^2-y^2}$) are destabilized with respect to FeP. The reason for this is that in the first compound the inner ring structure is smaller. Also, the higher negative charge on the bridge nitrogen atom of the phthalocyanine molecule compared with the corresponding bridge carbon atom of the porphyrin macrocycle plays an important role. The result of this destabilization is an intermediate spin ($S = 1$) for the iron ion instead of the high spin state ($S = 2$) often reported for FeP.

Sabelli et al. found as a result of their calculations a very striking difference in the structures of the dioxygen adducts of FePc and FeP. For the porphyrin compound "end-on" binding of the dioxygen to the iron atom is preferred at an angle of 119° . For the FePc model, on the other hand, the "side-on" configuration is most favourable. Their calculations show that in the case of FePc very little charge transfer occurs between the iron ion and the dioxygen molecule, with almost zero net charge on the oxygen atoms.

Sabelli et al. also carried out the calculation with CO as a sixth ligand, to simulate the effect of a carbon support on the FeTSPc molecule. The macrocycle adsorbs on the carbon support such that possibly a basic group of the support occupies the sixth coordination site. The basic group must be an electron donor, possibly an adsorbed oxygen atom or oxidized carbon and therefore, CO is used in the calculation as extra ligand. The result of the introduction of CO is an increase in binding energy of the dioxygen molecule by about a factor 2.

At the end of this section, the proposed structures for the dioxygen adducts are summarized in table 3.1 and 3.2. The structures claimed in section 3.3. are also included.

Author [ref.]	"end-on (bent)"	"side-on"	Co(III)-O ₂ ⁻	Co(II)-O ₂
Griffiths [9]		+	-	-
Pauling [11]	+		-	-
Drago [14]	+		+	
Wayland [16]	+		+	
Rohmer [34]	+		+	
Dedieu [39]	+		+	
Newton [42]	+		+	

Table 3.1.: The structure of the dioxygen adducts of cobalt chelates. + denotes the predicted structure; - no predictions made.

Author [ref.]	"end-on (bent)"	"side-on"	Fe(III)-O ₂ ⁻	Fe(II)-O ₂
Griffiths [9]		+	-	-
Pauling [11,12]	+		-	-
Weiss [13]	-	-	+	
Wayland [16]	+			+
Zerner [31]		+		+
Dedieu [39]	+			+
Kirchner [43]	+			+
Case [44]	+			+
Olafson [45b]	+			+
Boca [46]	+			+
Sabelli [40] ^a	+			+
Sabelli [40] ^b		+		+

Table 3.2.: The structure of the dioxygen adducts of iron chelates. + denotes the predicted structure; - no predictions made. a: FeP b: FePc.

3.5. Dioxygen bridged metal complexes

As shown in this thesis, dioxygen bridged phthalocyanine dimers most likely play an important role in the reduction mechanism of the dioxygen molecule. Therefore, the electronic structure of such complexes will now be discussed. Up till now little attention has been paid to the theoretical considerations of dioxygen bridged metal complexes. It can be explained with the increased valence theory that breaking of the dioxygen bond occurs with only FeP and not with CoP, in agreement with experiments. The cleavage of this bond is often concluded from the fact that in a dioxygen-saturated solution of FeP (but also of FePc) oxo-bridged dimers (PcFe-O-FePc) are present [47].

Ochiai [48] has attempted to explain these observations by using more standard quantum chemical concepts. He argued that the dioxygen bond splitting would present a high potential barrier when going from the dioxygen to the oxygen bridged dimer. The probable transition state species M^+O^- (or MO) should facilitate the bond cleavage. In an energy diagram for octahedral coordination of the metal ion, as given in figure 3.13, he visualized the interactions between the $d\pi$ -electrons on M^+ and the odd electron on O^- . Other interactions, as the important σ -bonding interactions, are omitted. For a metal ion as iron with a d^5 -configuration for the iron(III) state all low lying levels are just occupied and the M^+O^- -species is stabilized. For cobalt the extra electron has to occupy the anti-bonding orbital (Ψ_2), thus no stabilization of the system is expected.

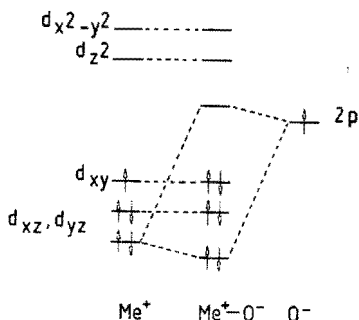


Fig. 3.13 Energy level diagram scheme for the transition state species M^+O^- .

The electronic structure of a cobalt μ -peroxo complex $[(\text{NH}_3)_5\text{Co}-\text{O}_2-\text{Co}(\text{NH}_3)_5]^{4+}$ or a cobalt μ -superoxo complex $[(\text{NH}_3)_5\text{Co}-\text{O}_2-\text{Co}(\text{NH}_3)_5]^{5+}$ have been analyzed by Vlcek [49] and Hyla-Kryspin et al. [50]. Unfortunately, Vlcek assumed a structure with the dioxygen axis perpendicular to the cobalt-cobalt axis, but a recent X-ray analysis revealed a structure for the complex with the oxygen-oxygen axis more parallel to the cobalt-cobalt axis [51]. Hyla-Kryspin et al. [50] applied the self consistent charge and configuration molecular orbital method to explain qualitatively some of the properties of the binuclear cobalt complexes. Because of the complexity of the electronic structure, it is not easy to draw an energy level diagram in which the interactions are visualized. The unpaired electron, responsible for the observed paramagnetism of the μ -superoxo cobalt complex occupies a molecular orbital containing mainly oxygen atomic orbitals. This orbital is anti-bonding and lies between the practically non-bonding $d\pi$ (d_{xy}, d_{yz}, d_{xz})- and the anti-bonding $d\sigma$ ($d_{z^2}, d_{x^2-y^2}$)-orbitals of the cobalt ions. When in an energy level scheme only the molecular orbitals containing mainly oxygen atomic orbitals are depicted, approximately a scheme results of a dioxygen molecule with an extra electron in an anti-bonding orbital: i.e. a superoxo (O_2^-) group. These authors also predict that, when the complex is reduced, the cobalt ions will stay in the +3 oxidation state, while the superoxo (O_2^-) group is reduced to the peroxo (O_2^{2-}) group. The additional electron is also placed in an anti-bonding orbital and therefore, the former (unreduced) complex is more stable than the latter complex. Although, Vlcek used a different geometry, he also concluded that the reduced complex has an additional electron in an anti-bonding orbital.

3.6. References

1. E. Yeager, *Electrochim. Acta* 29 (1984) 1527.
2. J.P. Collman, T.R. Halbert and K.S. Suslick, ' O_2 -binding to Heme Proteins and Their Synthetic Analogs' in '*Metal Ion Activation of Dioxygen*' edited by T.G. Spiro, J. Wiley, New York (1980).
3. A.V. Savitskii and V.I. Nelyubin, *Russ. Chem. Rev.* 44 (1975) 110.
4. F.A. Cotton and G. Wilkinson, '*Advanced Inorganic Chemistry. A Comprehensive Text*', J. Wiley, New York (1966).
5. H.L. Schäfer and G. Gliemann, '*Basic Principles of Ligand Field Theory*', J. Wiley, New York (1969).

6. F. van den Brink, Thesis, Eindhoven University of Technology, Eindhoven (1981).
7. S. Gasiorowicz, 'Quantum Physics', J. Wiley, New York (1974).
8. W.J. Moore, 'Physical Chemistry', Longman Group Limited, London (1972).
9. J.S. Griffiths, Proc. Roy. Soc. (A) 235 (1956) 73.
10. R.W. Erskine and B.O. Field, 'Reversible Oxygenation' in Structure and Bonding, Vol. 28, Springer Verlag Berlin (1976).
11. L. Pauling and C.D. Coryell, Proc. Natl. Acad. Sci. USA 22 (1936) 210.
12. L. Pauling, Nature 203 (1964) 182.
13. J.J. Weiss, Nature 202 (1964) 83.
14. R.S. Drago and B.B. Corden, Acc. Chem. Res. 13 (1980) 353.
15. B.S. Tovrog, D.J. Kitko and R.S. Drago, J. Am. Chem. Soc. 98 (1976) 5144.
16. B.B. Wayland, J.V. Minkiewicz and M.E. Abd-Elmageed, J. Am. Chem. Soc. 96 (1974) 2795.
17. R.D. Jones, D.A. Summerville and F. Basolo, Chem. Rev. 79 (1979) 139.
18. J. Manassen, Cat. Rev. Sci. Eng. 9 (1974) 223.
19. J.E. Linard, P.E. Ellis Jr., J.R. Budge, R.D. Jones and F. Basolo, J. Am. Chem. Soc. 102 (1980) 1896.
20. R.D. Harcourt, J. Mol. Struct. 9 (1971) 221.
21. R.D. Harcourt, 'Qualitative Valence Bond Descriptions of Electron-Rich Molecules: Pauling "3-Electron Bonds" and "Increased Valence" Theory' in 'Lecture Notes in Chemistry', edited by G. Berthier, M.J.S. Dewar, H. Fischer, K. Fukui, G.G. Hall, H. Hartmann, H.M. Jaffé, J. Jortner, W. Kutzelnigg, K. Ruedenberg and E. Scrocco, Springer Verlag, Berlin-Heidelberg-New York (1982).
22. R.D. Harcourt, J. Inorg. Nucl. Chem. 39 (1977) 243.
23. A. van der Putten, Thesis, Eindhoven University of Technology, Eindhoven (1986).
24. E. Yeager, 'Electrocatalysis on Non-metallic Surfaces', N.B.S. Spec. Publ. 455 (1976) 203.
25. P. Fischer and J. Heitbaum, J. Electroanal. Chem. 112 (1980) 231.
26. V. Jalan and E.J. Taylor, J. Electrochem. Soc. 130 (1983) 2299.
27. J.P. Collman, P. Denisevich, Y. Konai, M. Marocco, C. Koval and F.C. Anson, J. Am. Chem. Soc. 102 (1980) 6027.
28. A.J. Appleby, M. Savy and P. Caro, J. Electroanal. Chem. 111 (1980) 91.
29. A.J. Appleby, J. Fleisch and M. Savy, J. Cat. 44 (1976) 281.
30. P. Caro, M. Faucher, M. Savy and H. Pankowska, J. Chem. Phys. 68 (1978) 1045.

31. M. Zerner, M. Gouterman and H. Kobayashi, *Theo. Chim. Acta* 6 (1966) 363.
32. A.M. Schaffer, M. Gouterman and E.R. Davidson, *Theo. Chim. Acta* 30 (1973) 9.
33. A. Dedieu and A. Veillard, *Theo. Chim. Acta* 36 (1975) 231.
34. M.M. Rohmer, A. Dedieu and A. Veillard, *Theo. Chim. Acta* 39 (1975) 189.
35. G.L. Zubay, 'Biochemistry', Addison-Wesley Publishing Company Inc., Reading (Massachusetts) (1983).
36. G. Fermi, *J. Mol. Bio.* 97 (1975) 237.
37. M.F. Perutz, *Nature (London)* 228 (1970) 734.
38. M.F. Perutz, *Nature (London)* 237 (1972) 495.
39. A. Dedieu, M.M. Rohmer and A. Veillard, *Adv. Quant. Chem.* 16 (1982) 43.
40. N.H. Sabelli, L.K. Lee and C.A. Melendres, *Proc. of the Symp. on Electro-catal.* (edited by W.E. O'Grady, P.N. Ross Jr. and F.G. Will), Minneapolis (1981), *The Electrochemical Soc.*, Vol. 82-2 (1982).
41. P.A. Forshey, T. Kuwana, N. Kobayashi and T. Osa, *Adv. in Chem. Series* 201 (Electrochem. and Spectrochem. studies of biol. redox components, ed. by K.M. Kadisch) (1982) 601.
42. J.E. Newton and M.B. Hall, *Inorg. Chem.* 23 (1984) 4627.
43. R.F. Kirchner and G.H. Loew, *J. Am. Chem. Soc.* 99 (1977) 4639.
44. D.A. Case, B.H. Huynh and M. Karplus, *J. Am. Chem. Soc.* 101 (1979) 4433.
45. a. A. Dedieu, M.M. Rohmer, M. Bernard and A. Veillard, *J. Am. Chem. Soc.* 98 (1976) 3717.
b. B.D. Olafson and W.A. Goddard, *Proc. Natl. Acad. Sci. USA* 74 (1977) 1315.
46. R. Boca, *Coord. Chem. Rev.* 50 (1983) 1.
47. B.J. Kennedy, K.S. Murray, P.R. Zwack, H. Homburg and W. Kalz, *Inorg. Chem.* 24 (1985) 3302.
48. E.-I. Ochiai, *Inorg. Nucl. Chem. Lett.* 10 (1974) 453.
49. A.A. Vlcek, *Trans. Faraday Soc.* 56 (1960) 1137.
50. I. Hyla-Kryspin, L. Natkaniec and B. Jezowska-Trzebiatowska, *Chem. Phys. Lett.* 35 (1975) 311.
51. W.P. Schaefer and R.E. Marsh, *Acta Cryst.* 21 (1966) 735.

4. Dioxygen adsorption on metal chelates.

Experimental part

4.1. Introduction

In this chapter the electrochemical and spectroscopic techniques, used to obtain the results described in this thesis, are discussed. These techniques are:

- the Rotating Ring Disc Electrode (RRDE) technique, to measure quantitatively the activity and selectivity of a particular catalyst (4.2.)
- cyclic voltammetry, to characterize the general electrocatalytic behaviour over the applied potential domain (4.3.)
- in situ light absorption spectroscopy, to study the state of the metal chelates (4.4.)
- polarography, to study the electrochemical reactions in solutions of MeTSPc (4.5.).

The preparation methods used to apply the catalyst molecules to the electrode will be given in chapter 5, where the influence of electrode preparation on electrocatalysis is described.

4.2. The Rotating Ring Disc Electrode (RRDE)

In electrocatalysis, like in catalysis, the reaction rate depends on both the rate constant and the concentration of the reacting species. Electrochemical reactions are heterogeneous and thus the surface concentration of the reactant at the electrode is the pertaining variable. During the reaction (reduction or oxidation) its surface concentration decreases until an equilibrium is reached between its reaction rate and its transport rate to the electrode. The mass-transport rate depends on the diffusion coefficient of the reacting species and on the convection conditions. By using the Rotating Disc Electrode (RDE) technique, the natural convection, which is very ill-defined [1], is eliminated. Due to the rotation of the electrode, a well-defined forced convection is achieved, which results in a relatively simple expression for the mass-transport limited reduction current [2]:

$$i_L = -0.61 nF D^{2/3} \nu^{-1/6} c^S \omega^{1/2} = -nF k_d c^S \quad (1)$$

with i_L the limiting current density (mA cm^{-2}), D and c^S respectively the diffusion coefficient ($\text{cm}^2 \text{s}^{-1}$) and the bulk concentration of the reacting species (mol cm^{-3}), ν the kinematic viscosity ($\text{cm}^2 \text{s}^{-1}$), ω the angular velocity of the electrode (rad s^{-1}), n the number of electrons per reacting species, F the Faraday number (96495 C mol^{-1}) and k_d the rate constant of mass-transport (cm s^{-1}).

The activity of a particular catalyst can thus be measured by applying it to a disc electrode. In practice, the activity is determined by measuring the reaction rate (= current) as a function of the electrode potential. The reaction rate of an irreversible electrochemical reduction depends on the potential in the following way [2]:

$$k = k_o \exp \frac{-\alpha F \eta}{RT} \quad (2)$$

with k_o the heterogeneous rate constant (= the value of k at $E = E_{eq}$), E_{eq} the Nernst equilibrium potential (V), k the heterogeneous rate of the electron transfer (cm s^{-1}), η the overpotential defined by $E - E_{eq}$ and α the transfer coefficient, while F , R and T have their usual meaning. For the current density (mA cm^{-2}) the following relation holds:

$$i = -nFk C^{\sigma} \quad (3)$$

where C^{σ} is the surface concentration (mol cm^{-3}) of the reacting species.

At large overpotential values, the reaction rate is so high that all species which reach the electrode surface react and the mass-transport limited current, defined in relation (1), is achieved. The value of k_o then determines the potential where this will happen: for a small k_o , a large overpotential is necessary, while for a high k_o -value already a small overpotential is sufficient.

In practice, the observed i - E curve is characterized by the half-wave potential ($E_{1/2}$) at which the current is equal to one half of the mass-transport limited current ($i = 1/2 i_L$). Relations (1) and (3) (together with the diffusion equation of Fick: $i = nFD (c^S - c^{\delta}) / \delta_N$, with δ_N the Nernst diffusion layer thickness (cm)) can be used to derive:

$$\frac{i}{i_L} = \frac{1}{1 + k_d/k} \quad (4)$$

From this relation, it can be concluded that at the half-wave potential k is equal to k_d . By substitution of k by k_d in equation (2), it is possible to derive for the half-wave potential:

$$E_{1/2} = E_{eq} - \frac{RT}{\alpha F} \ln \frac{k_d}{k_o} \quad (5)$$

From this relation, it is obvious that the catalytic activity of a catalyst for the dioxygen reduction can be characterized by its half-wave potential. For an active catalyst, k_o is large and approaches k_d and the half-wave potential then approaches the equilibrium potential.

In a number of experiments a Rotating Ring Disc Electrode (RRDE) was used to determine the possible production of hydrogen peroxide or other possible intermediates of the dioxygen reduction reaction. The RRDE is schematically drawn in figure 4.1 (for more details see reference [3]). The compound

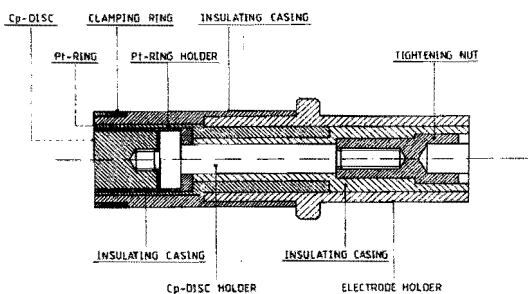


Fig. 4.1 The Rotating Ring Disc Electrode (RRDE).

produced at the disc is for a certain part swept to the ring, where it can be determined; the other part disappears into the bulk of the solution. By solving the concerning hydrodynamic equations, it can be shown that the fraction, which reaches the ring, only depends on the dimensions of the ring and disc and on the gap between them. This fraction is called the collection efficiency (N) of the electrode [1,2,4]. By using this method, it is possible to discriminate between dioxygen reduction to hydrogen peroxide or water. If dioxygen is reduced to hydrogen peroxide, a ring current is observed at a ring potential selected such, that all hydrogen peroxide is oxidized. For dioxygen reduction to water no ring current is observed. The selectivity of a dioxygen reducing catalyst can be defined as the fraction of the dioxygen, which is reduced to water.

4.3. Cyclic voltammetry

A three-compartment electrochemical cell, as drawn in figure 4.2, is used to perform RRDE experiments and to record cyclic voltammograms of the electrodes. These cyclic voltammograms are measured in a dinitrogen-saturated solution to characterize the electrodes onto which the catalysts (CoPc or FePC) are deposited. These compounds show redox activity: they are reduced and

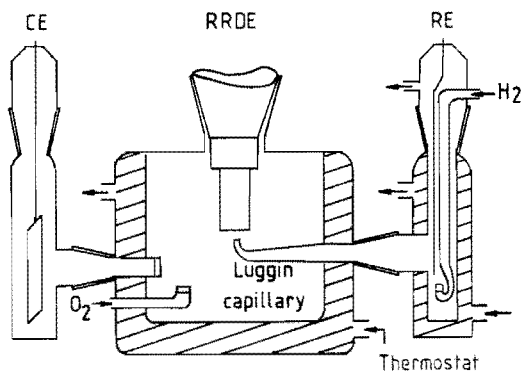


Fig. 4.2 The electrochemical cell.

oxidized back during a cyclic potential sweep in the potential range between 1 and 0 V (vs. a Reversible Hydrogen Electrode).

The RDE is the working electrode (WE), and as reference (RE) and counter electrode (CE), respectively, a Reversible Pt-Hydrogen Electrode (RHE) and a Pt foil are used. In a few cases a Saturated Calomel Electrode (SCE) or a Mercury Sulphate Electrode is used as RE.

A potentiostat (Tacussel, type bipad) in combination with a function generator (Wenking VSG 72) was used to establish the potential between the WE and the RE. The RRDE or RDE was fixed in a holder attached to an electromotor (Motomatic, Electrocraft Corporation). With a control unit (Electrocraft Corporation) the rotation frequency could be varied between 0 - 64 s⁻¹. The voltammetric $I_D, I_R = f(E)$ -curves were recorded on an XYX' -recorder (Hewlett Packard 7076A).

4.4. In situ light absorption spectroscopy

Light absorption spectra of solutions of CoTSPc and FeTSPc were recorded by using a double beam Pye Unicam spectrophotometer. In order to investigate the influence of dioxygen on the spectra, a cuvette was constructed which allows for deoxygenation of the solution with helium (cell thickness: 0.5 cm). Traces of dioxygen were removed from the helium gas by leading the helium stream over a BTS catalyst (BASF) at a temperature of 170°C.

To combine the electrochemical and spectroscopic measurements two cells were constructed, in which the spectra could be recorded while simultaneously the potential of the electrode could be controlled. The first cell (see figure 4.3) is used to obtain in situ absorption spectra of polypyrrole/Co- (or Fe-)TSPc layers [see chapter 5] attached to a transparent gold electrode. This electrode is also drawn schematically in the figure and consists of a thin glass plate, onto which a thin gold layer is vacuum deposited. Before depositing the gold film, the plate was covered with a very thin titanium layer to assure a good adherence of the gold film. The thickness of the electrode is a compromise between its conduction properties and its transparency. The resulting transparency was about 10%.

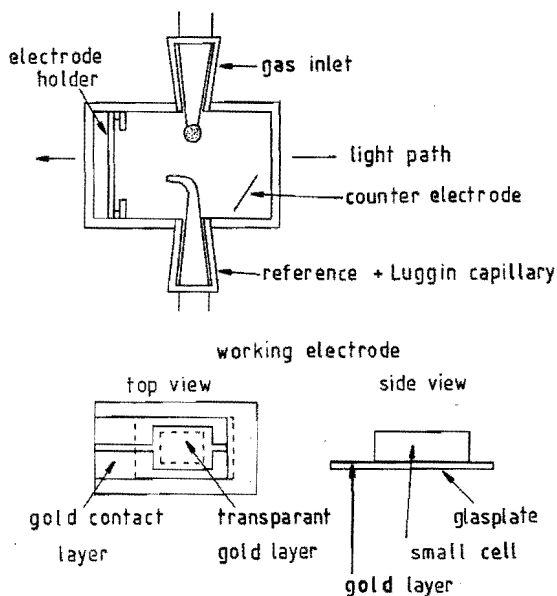


Fig. 4.3 Cell to record in situ absorption spectra of polypyrrole layers.

The application of a polypyrrole film onto this electrode was carried out in a small perspex cell, which is glued on the glass plate. Its place and dimensions are given by the broken lines in figure 4.3. A platinum sheet is covering the perspex box over the gold layer and the result is a small electrochemical cell, in which the electropolymerization of pyrrole [see chapter 5] was carried out. After this modification process, the electrode was placed into the holder in the optical cell and in situ absorption spectra of the polypyrrole film were recorded.

The second cell is schematically drawn in figure 4.4. An Optical Transpa-

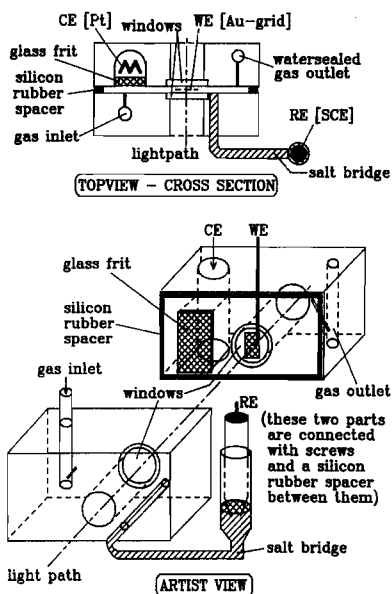


Fig. 4.4 Optical transparent thin layer cell (OTTLC).

rent Thin Layer Electrode (OTTLE) [5,6,7] was placed in the cell to study the spectra of several redox states of the metal phthalocyanine molecules. This electrode consists of a nickel minigrad (100 mesh) covered with a thin layer of gold (2 μm) and has a transmission of approximately 60% (VECO). Unfortunately, after using this electrode in acid solutions for some time, the nickel grid was no longer completely covered with a gold layer, as could be concluded from the increased anodic current, observed in a cyclic voltammogram, due to the oxidation of the nickel. A gold plate, in which small holes (0.2 mm) were drilled at about the same distance from each other as the hole size, has a lower transparency (about 30%) but a superior electrochemical

behaviour as compared to the nickel grid. Therefore, this home-made grid was used for the spectro-electrochemical experiments. The cell thickness is approximately 0.4 mm, giving a cell volume, small enough to convert all species in the solution between the quartz plates within a few minutes. The transport of unreacted species from the counter-electrode compartment and other reservoirs (see also figure 4.4) can be neglected on the time scale of the experiment.

Electroreflectance spectra were recorded in the Laboratoire d'Electrochimie Interfaciale (Meudon-Bellevue). The ER spectroscopic technique and the experimental set-up are described in detail in reference [8]. For these measurements an electrode with a reflecting surface must be used. In our case, the reflecting electrode was a piece of the basal plane of stress-annealed pyrolytic graphite (BP of SA-Cp), kindly given by Dr. A.W. Moore of Union Carbide. To obtain a clean surface, the upper layers of the graphite were removed before each experiment by using adhesive tape.

As usually in ER experiments, the geometry was such that the incident light beam and the reflected light beam make a small angle with each other. (See figure 4.5, where the principles of the experimental set-up are given). A monochromator was placed in the incident beam to enable the recording of an ER spectrum in the wavelength range of 300 to 700 nm.

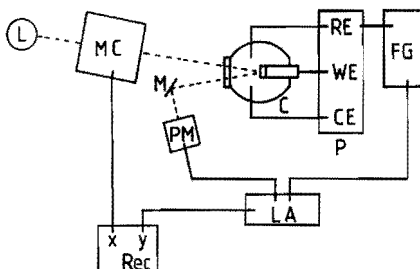


Fig. 4.5 Set-up to record electroreflectance spectra. (L = Light source; Mc = Monochromator; C = Cell; P = Potentiostat; FG = Function Generator; M = Mirror; Pm = Photomultiplier; LA = Lock-in Amplifier; Rec = Recorder).

In ER spectroscopy, an ac-potential is superimposed on the applied dc electrode potential. When this dc-potential lies in the domain of an electro-

chemical change of the electrode surface, as for instance oxide layer formation or a redox reaction, then the intensity of the reflected light will show the same modulation as the potential. For FeTSPc, adsorbed on graphite an ER spectrum could be expected in the potential domains of the redox couples Fe(I)TSPc/Fe(II)TSPc and Fe(II)TSPc/Fe(III)TSPc.

The spectral amplitude at a certain wavelength depends on [9]:

$$1/R \partial R/\partial E = 1/R \partial R/\partial q \times \partial q/\partial E \quad (6)$$

(R denotes the reflection coefficient of the electrode, E is the potential (V) and q is the transferred charge (C)). The equation shows that the spectral amplitude depends on dq/dE and thus is proportional to the differential capacitance. The other term of the equation $1/R \times \partial R/\partial q$ contains the optical properties of the redox species, or in the other case, of the bare surface and the oxide layer. For FeTSPc, adsorbed on graphite, it is the difference between the light absorption in the mono- and divalent, or the di- and trivalent oxidation states.

To account for the observed wavelength-dependence of both the reflection coefficient and the sensitivity of the photomultiplier, a feed-back system was used to obtain a constant mean-value for the output of the photomultiplier. The (rapid) oscillating (15 Hz) component of the photomultiplier signal was analyzed by using a lock-in amplifier. As a reference signal, the ac-potential was used, which simultaneously modulated the electrode potential.

4.5. Polarography

The polarographic measurements were carried out in solutions of CoTSPc (or FeTSPc), with a polarographic analyzer of Princeton Applied Research (model 174A). The observed polarograms (dc or pulse) were recorded on an XY-recorder (Hewlett Packard 7044A).

4.6. References

1. W.J. Albery, 'Electrode Kinetics', Clarendon Press, Oxford (1975).
2. A.J. Bard and L.R. Faulkner, 'Electrochemical methods, Fundamentals and Application', J. Wiley, New York (1980).

3. A. van der Putten, Thesis, Eindhoven University of Technology, Eindhoven (1986).
4. W.J. Albery and M.L. Hitchman, 'Ring-Disc Electrodes', Clarendon Press, Oxford (1971).
5. T.P. De Angelis and W.R. Heineman, J. of Chem. Education 53 (1976) 594.
6. C.W. Anderson, H.B. Halsall and W.R. Heineman, Anal. Biochem. 93 (1979) 366.
7. N. Kobayashi and Y. Nishiyama, J. Phys. Chem. 89 (1985) 1167.
8. J.P. Dalbera, C. Hinnen and A. Rousseau, J. de Phys. C5; 38 (1977) 185.
9. D. van den Ham, C. Hinnen, G. Magner and M. Savy, to be published.

5. The cathodic reduction of dioxygen at cobalt phthalocyanine: influence of electrode preparation on electrocatalysis

5.1. Introduction

In recent years a considerable number of papers have been published on dioxygen reduction. In many of these investigations a metal chelate is used as a catalyst. These catalysts are attached to the electrode with the aid of different methods, such as irreversible adsorption [1]; vacuum deposition [2]; incorporation into a conducting polymer, as polypyrrole [3]; impregnation of porous carbon [4] and evaporation of the solvent [5]. All these preparation techniques result in electrodes with different activity, even if the same catalyst and the same amount of catalyst are used. One of the most striking examples is the difference in activity between an electrode prepared by vacuum deposition of cobalt phthalocyanine (CoPc) and by incorporation of water-soluble cobalt tetrasulfonato-phthalocyanine, abbreviated as CoTSPc, in polypyrrole [3]. Especially in acid media, the catalyst incorporated in polypyrrole is much more active than the vacuum-deposited one, while in both cases a thick layer containing the catalyst is present. To explain the difference in activity, we have to take into account the conductivity of the catalyst layer and the possibility of the diffusion of dioxygen through this layer. Both the conductivity of, and the dioxygen diffusion velocity in the catalyst/polypyrrole layer is so high that all attached catalyst molecules can take part in the electrocatalysis, which is not the case for the vacuum-deposited film, as will be shown later in this chapter. A comprehensive theoretical description of this phenomenon is given in a paper by Savéant et al. [6].

The purpose of the present chapter is to demonstrate how preparation conditions affect the activity. This will be illustrated for the reduction of dioxygen on CoPc or, in some cases, the water-soluble modification CoTSPc. The following preparation methods were investigated: a. Irreversible adsorption; b. Vacuum deposition; c. Incorporation in polypyrrole; d. Impregnation of porous carbon; e. Evaporation of the solvent. For a precise description see the section 'experimental' [5.3.].

5.2. Theoretical aspects

CoPc (or CoTSPc) gives under all circumstances a first reduction wave of dioxygen to hydrogen peroxide. The kinetics for the reaction is in general

much faster in alkaline solutions than in acid solutions. The main reason is that the probable intermediate O_2^- , or an O_2^- -like species, is relatively more stable in alkaline solutions than in acid solutions, as was stressed by Yeager [7]. With this in mind, we expect the effect of the preparation method on the activity to be more dramatic in acid than in alkaline solutions, therefore, for comparison, measurements were carried out in both electrolytes.

Clearly, the number of active sites is an important parameter determining the i - E relationship, characterized by the half-wave potential $E_{1/2}$, as determined with the Rotating Disc Electrode technique. It can be shown that this half-wave potential shifts when the number of active sites at an electrode is increased. Suppose, we have an irreversible electrochemical reaction with a rate-determining electron transfer as the first step. For the current density measured with a Rotating Disc Electrode the following relation has been derived by Albery [8] for a first-order reaction:

$$\frac{i}{i_L} = \frac{1}{1 + k_d/k} \quad (1)$$

i : current density (mA cm^{-2})

i_L : transport-limited current density (mA cm^{-2})

k_d : heterogeneous rate constant describing mass-transport (cm s^{-1})

k : observed heterogeneous rate constant of the electron transfer (cm s^{-1})

At the half-wave potential ($i = 1/2 i_L$), $k_d = k$. Rate constant k corresponds to a surface with a certain number of active sites. If this number of active sites on the surface increases by a factor p , then the rate constant k also increases by this factor, because k is based on the geometric surface area. Increasing the number of active sites neither affects the size of this geometric area nor the diffusion to this surface. Therefore, for the original and the new surface (1 and 2, respectively), we have, in the case of a cathodic reaction, the following relations:

$$\text{surface 1: } k_d = k_o \exp \frac{-\alpha F \eta_1}{RT} \quad (2)$$

$$\text{surface 2: } k_d = p \cdot k_o \exp \frac{-\alpha F \eta_2}{RT} \quad (3)$$

with k_o : the value of k at $E = E_{eq}$
 E_{eq} : the equilibrium electrode potential

η_1, η_2 : $(E_{1/2})_1 - E_{eq}, (E_{1/2})_2 - E_{eq}$: overpotential for surface 1 and 2, respectively
 $(E_{1/2})_1, (E_{1/2})_2$: half-wave potential of surface 1 and 2, respectively

The difference between the two half-wave potentials is:

$$(E_{1/2})_2 - (E_{1/2})_1 = \Delta E_{1/2} = \frac{RT}{\alpha F} \ln p \quad (4)$$

For $\alpha = 1/2$ the lowering of the half-wave overpotential is 118 mV for a tenfold increase of the number of active sites. Generally, the shift of the half-wave potential for a tenfold increase of the number of active sites is equal to the Tafel slope.

5.3. Experimental

CoPc was obtained from Eastman Kodak. The sodium salt of CoTSPC was synthesized according to the method described by Weber and Busch [9]. All other chemicals were commercially available and used without further purification, except the pyrrole which was distilled before use. As will be explained below, five different electrode systems (a-e) were prepared. For electrode system b and d, a gold disc with a surface area of 0.50 cm^2 and for system a, c and e, a pyrolytic graphite (C_p) disc with a surface area of 0.52 cm^2 was used. Before the preparation of the electrode systems the electrodes were polished with $0.3 \mu\text{m}$ alumina, rinsed with doubly distilled water and cleaned in an ultrasonic water bath for one minute.

a. Irreversible adsorption. A pyrolytic graphite electrode (C_p) is dipped into a solution of CoPc or CoTSPC, resulting in the irreversible adsorption of the complex on the electrode [1]. A (sub)monolayer of catalyst is obtained. Characterization by cyclic voltammetry is possible with these electrodes, so the exact number of active sites can be determined. It is also possible to produce electrodes with different surface coverages by dipping the C_p electrode in solutions of CoPc in pyridine (or CoTSPC in water) with concentrations ranging from 10^{-3} to 10^{-5} mol/l. The time of exposure (dipping time) was about one minute.

b. Vacuum deposition. This technique has already been previously employed in our laboratory [2]. In this way, it is possible to produce an electrode which is covered with a large amount of catalyst. The thickness of the layer was determined spectroscopically, as described in the same paper.

c. Incorporation in polypyrrole. The sodium salt of CoTSPc is soluble in water. The electro-oxidation of pyrrole gives a polymer with positive charges, which must be compensated by negatively charged ions [8]. When the polymerization is carried out in the presence of the CoTSPc⁴⁻ anion, incorporation of this ion in the film is obtained. For the preparation of this type of electrode systems, a 10⁻³ M CoTSPc solution in water, containing 1 vol.% pyrrole, was used. The electro-oxidation was carried out galvanostatically with a current of 0.2 mA. By varying the time, layers of different thickness can be produced.

d. Impregnation of porous carbon. The impregnation of the carbon support (Norit BRX) was realized by dissolving 10 mg of CoPc in 20 ml THF, adding 40 mg of the carbon, then refluxing and stirring for 30 minutes. The carbon particles were attached to the Au-disc of the electrode via incorporation in a polypyrrole film, according to a previously described procedure [11]. The carbon support has a high conductivity and a high specific surface area, so many catalyst molecules can be adsorbed on the surface.

e. Evaporation of the solvent. A drop (several microliters) of a CoPc solution in pyridine is placed on a C_p electrode; thereafter, the solvent is allowed to evaporate, yielding electrodes with relatively thick layers of catalyst. By changing the concentration of the solution from 10⁻³ to 10⁻⁵ mol/l, the thickness of the layer can be regulated.

The electrochemical experiments were carried out in a standard three-compartment electrochemical cell, filled with 100 ml electrolyte. As electrolyte both acid (0.5 M H₂SO₄ or 0.05 M H₂SO₄) and alkaline (1 M KOH or 0.1 M KOH) solutions were used. The polypyrrole electrodes were tested only in 0.1 M KOH and not in 1 M KOH, because of the lack of stability of polypyrrole in alkaline solutions [12]. For characterization of the electrode, cyclic voltammetry was conducted in dioxygen-free solutions. The dioxygen reduction was measured in dioxygen-saturated solutions, with the Rotating Disc Electrode technique. The electrochemical measurements were carried out using a Tacussel bipotentiostat (Bipad). As reference electrode a Reversible Hydrogen Electrode (RHE) was used. All potentials in this chapter are given versus the RHE.

The reduction curves of electrode systems in which polypyrrole was used, are corrected for the high capacitive current of the polypyrrole itself.

5.4. Results and discussion

a. Acid media

Figure 5.1 gives the result for the dioxygen reduction on the electrode systems (a-e). In table 5.1 the amounts of attached catalyst for the different electrode systems are given. It is obvious that each electrode system cata-

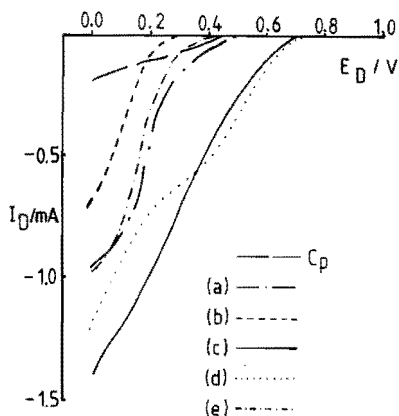


Fig. 5.1 Effect of electrode preparation on the dioxygen reduction. For notation see table 5.1. Electrolyte: 0.5 M H_2SO_4 , dioxygen-saturated; scan rate: 50 mV s^{-1} ; rotation frequency: 16 s^{-1} .

Table 5.1 The amounts of attached catalyst for the electrode systems of figure 5.1.

Electrode type	Description	Amount of catalyst (mol cm^{-2})
a	irreversible adsorption (10^{-3} M CoPc)	2.6×10^{-10}
b	vacuum deposition (180 nm)	6.3×10^{-8}
c	incorporation in polypyrrole (30 mC)	1.7×10^{-8}
d	impregnation of porous carbon (20%)	1.8×10^{-7}
e	evaporation of the solvent	4.0×10^{-8}

lyses the reduction of dioxygen, however, to a different extent, indicating that the number of active sites is not automatically the same as the total number of catalyst molecules present; an electrode prepared via irreversible

adsorption is even more active than a thick vacuum-deposited film.

To illustrate the shift in half-wave potential due to a change in active sites, as derived in equation (4), the dioxygen reduction was investigated as a function of the CoTSPc/polypyrrole layer thickness (type c). Since the polymer layer is very thin compared to the thickness of the diffusion layer, k_d will remain unchanged for all layer thicknesses. In figure 5.2 the dioxygen reduction on CoTSPc adsorbed on C_p (curve 1), and on various CoTSPc/polypyrrole layers (curves 2-6) in $0.05\text{ M H}_2\text{SO}_4$ is shown. In this figure, the

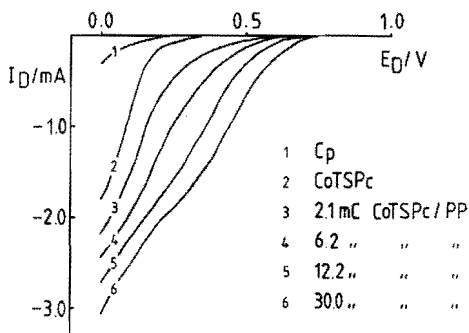


Fig. 5.2 Dioxygen reduction as a function of the CoTSPc/polypyrrole layer thickness. Electrolyte: $0.05\text{ M H}_2\text{SO}_4$, dioxygen-saturated; scan rate: 50 mV s^{-1} ; rotation frequency: 64 s^{-1} . For comparison the dioxygen reduction on an irreversibly adsorbed layer of CoTSPc on C_p is also included (curve 2).

thickness of the layer is expressed as the charge passed during the electropolymerization of pyrrole. In order to determine the amount of catalyst in a film, a cyclic voltammogram in dioxygen-free solution was measured for a 30 mC thick layer; see figure 5.3. In this figure the cyclic voltammogram of CoTSPc adsorbed on C_p is also given (a). The characterization of the electrodes is somewhat hampered by the instability of CoTSPc in acid solutions. Moreover, at potentials above 1 volt versus RHE, the polypyrrole degrades rapidly. Despite these difficulties, for an electrode obtained from irreversible adsorption, a surface coverage of $1.4 \times 10^{-10}\text{ mol cm}^{-2}$ can be determined from the area under the reduction peak at 1.1 V. The 30 mC CoTSPc/polypyrrole layer (b) gives a coverage of $7.8 \times 10^{-9}\text{ mol cm}^{-2}$. If it is assumed that for the oxidation of pyrrole to neutral polypyrrole 2 electrons per molecule are involved, and that in the oxidized form of polypyrrole, every four pyrrole units carry one posi-

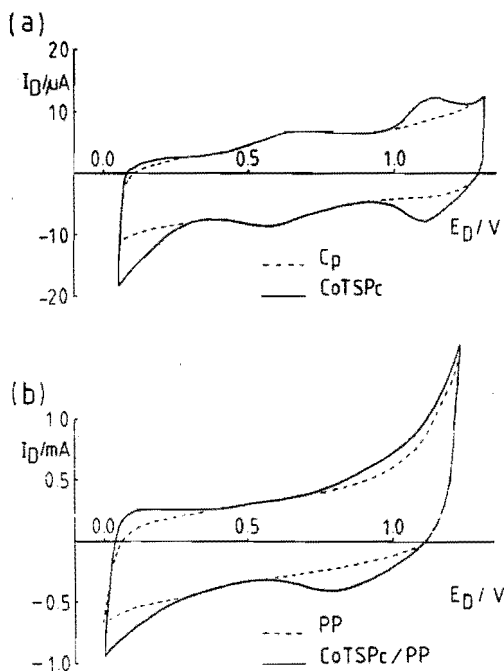


Fig. 5.3 Cyclic voltammograms of CoTSPc adsorbed on C_p (a) and of a 30 mC CoTSPc/polypyrrole layer (b). Electrolyte: 0.05 M H₂SO₄, dioxygen-free; scan rate: 100 mV s⁻¹.

tive charge [10], a coverage of 1.67×10^{-8} mol cm⁻² can be calculated for a 30 mC CoTSPc/polypyrrole layer. In this chapter this theoretical value will be used.

A limiting current of 2.5 mA is reached below 0 V versus RHE in curve 2, figure 5.2. (The plateau is not shown in the figure). This value equals the theoretical diffusion limiting current for the reaction of dioxygen to hydrogen peroxide. Curve 6, in the same figure, shows, although not very clearly, a first wave and the start of a second wave. In our view, the first wave corresponds to the reaction of dioxygen to hydrogen peroxide; the second wave is attributed to the further reduction of hydrogen peroxide to water. With this in mind, the half-wave potentials for the curves 2 and 6 can be determined with reasonable accuracy if only the reaction of dioxygen to hydrogen peroxide is considered. The results are respectively 70 and 395 mV. With the use of these values, and the surface coverage in the two cases, the shift in half-wave potential as a function of the number of active sites can be calculated. The result is 155 mV/decade of active sites.

For the Tafel slope of the first wave of curve 6 (figure 5.2) a value of -155 mV has been determined. Notwithstanding the difficulty of the determination, this is the same value as reported by Zagal-Moya [7], for the dioxygen reduction on CoTSPc adsorbed on C_p . The value of the Tafel slope corresponds very well with the observed shift in the half-wave potential. This agreement may be somewhat flattered because of two "each-other" compensating effects. First, the amount of catalyst in the film is probably taken too high, if we compare this with the results of the cyclic voltammetric measurements; secondly, it is probably not correct to neglect the dioxygen reduction on the polypyrrole matrix completely.

Returning to the results for the five different electrode systems as presented in figure 5.1, we note that a vacuum-deposited layer (b) has a lower activity than an irreversibly adsorbed layer (a), notwithstanding its thickness. Since the film has a relative low conductivity, the reaction must take place mainly at the interface between the substrate and the phthalocyanine film. Dioxygen must diffuse through the inactive outer parts of the film to reach the active sites at the interface. The electrode obtained by evaporation of the solvent (e) has a comparable physical structure, but probably a somewhat higher porosity and/or conductivity, resulting in a slightly increased activity for this electrode system as compared with system b.

The two other electrode systems consist of a catalyst dispersed on a matrix with high porosity and high conductivity, so that the whole layer, or at least a major part of it, is involved in the electrocatalysis. The direct incorporation in polypyrrole results in the most efficient utilization of the catalyst.

b. Alkaline media

Electrode systems a, b and e all show about the same activity in 1 M KOH, as can be concluded from the figures 5.4 and 5.5. Due to the greater stability of CoPc (or CoTSPc) in alkaline as compared with acid solutions, a more precise characterization of the electrode is now possible. In figure 5.4a, the results are given for an irreversibly adsorbed layer prepared by using solutions of different concentrations. The surface coverage increases from $6.4 \times 10^{-11} \text{ mol cm}^{-2}$ (for a concentration of 10^{-5} M CoPc) to $2.6 \times 10^{-10} \text{ mol cm}^{-2}$ (for a concentration of 10^{-3} M CoPc). Figure 5.4b demonstrates that the increased coverage is accompanied only by a slight increase in activity. The vacuum-deposited film (110 nm) also drawn in figure 5.4b has the same activity as the above mentioned a-type electrode prepared from a 10^{-3} M solution.

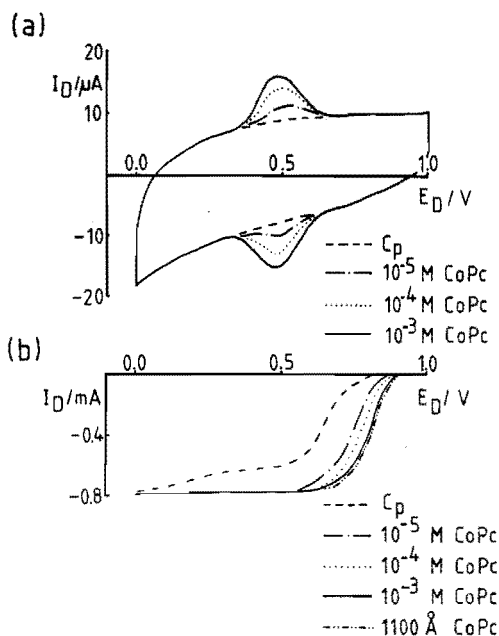


Fig. 5.4 a) Cyclic voltammogram of CoPc adsorbed on C_p . The concentrations of the dip solutions are given in the figure. Electrolyte: 1 M KOH, dioxygen-free; scan rate: 100 mV s^{-1} .
 b) Dioxygen reduction on the electrodes of a, compared with a vacuum-deposited layer of CoPc. Electrolyte: 1 M KOH, dioxygen-saturated; scan rate: 50 mV s^{-1} ; rotation frequency: 16 s^{-1} .

An electrode with a vacuum-deposited film gives non-reproducible and featureless cyclic voltammograms in dioxygen-free solutions. From the measured activity, it can be concluded that the conductivity and porosity of the layer are such, that about the same activity as that obtained for a monolayer is realized. On comparing figures 5.1 and 5.4b, it appears that the vacuum-deposited films show a relative higher activity in alkaline than in acid solution. In our view, this difference is not caused by the electrolytes themselves, but due to the used preparation method. It is difficult to obtain films with identical physical properties. Different films have a somewhat different conductivity and/or porosity, depending on the exact preparation conditions; these conditions cannot be kept constant with the applied method. Nevertheless, in both electrolytes only one monolayer or even less, is electrochemically active.

With electrode system e (deposition of CoPc by evaporation of the sol-

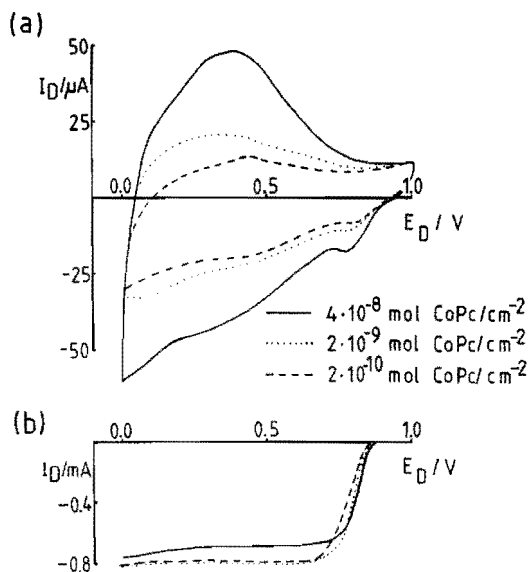


Fig. 5.5 a) Cyclic voltammogram of electrode system e (evaporation of the solvent). The amounts of deposited catalyst are given in the figure. Electrolyte: 1 M KOH, dioxxygen-free; scan rate: 100 mV s^{-1} . b) Dioxxygen reduction on the same electrodes as in a. Electrolyte: 1 M KOH, dioxxygen-saturated; scan rate: 50 mV s^{-1} ; rotation frequency: 16 s^{-1} .

vent), the characterization also results in a featureless cyclic voltammogram, as can be observed in figure 5.5a. The amount of catalyst has almost no effect on the activity, as is demonstrated in figure 5.5b.

The dioxxygen reduction on electrode system c (CoTSPc incorporated in polypyrrole) has been examined in 0.1 M KOH solutions. The result is shown in figure 5.6. For comparison, the dioxxygen reduction curve measured on a layer prepared from irreversible adsorption of CoTSPc (coverage $1.4 \times 10^{-10} \text{ mol cm}^{-2}$) has been drawn in the same figure. As can be seen from these curves, there is almost no difference in activity, in spite of the high catalyst loading in the case of the 30 mC CoTSPc/polypyrrole film ($1.67 \times 10^{-8} \text{ mol cm}^{-2}$). With the CoTSPc/polypyrrole layer again a second wave appears. This wave can be ascribed, as is also done for acid electrolytes, to the further reduction of hydrogen peroxide to water. The appearance of the second wave is due to the great number of active catalyst molecules. For the vacuum-deposited layer, there is no second wave, again suggesting that only part of the vacuum-

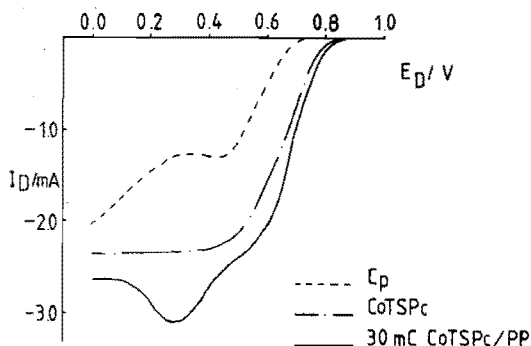


Fig. 5.6: Dioxygen reduction on CoTSPc, adsorbed on C_p , compared with a 30 mC CoTSPc/polypyrrole layer. Electrolyte: 0.1 M KOH, dioxygen-saturated; scan rate: 50 mV s^{-1} ; rotation frequency: 64 s^{-1} .

deposited layer is active. At high overpotential, the current decreases due to the change of polypyrrole to a reduced, non-conducting, form.

It is difficult to determine one unique Tafel slope for the first wave of the dioxygen reduction on a 30 mC CoTSPc/polypyrrole layer in 0.1 M KOH: the results vary from -60 mV at low overpotentials to -130 mV at higher overpotentials. Tafel slopes of -120 mV have been reported by Zagal-Moya for an irreversibly adsorbed layer of CoTSPc [7]. Figure 5.6 shows that the shift of the half-wave potential as a function of the amount of catalyst, is not equal to the observed Tafel slope. The reason for this is that an adsorbed monolayer already accomplishes a reversible (or quasi-reversible) reduction of dioxygen to hydrogen peroxide in 0.1 M KOH. Any further increase of the number of active sites does not bring about an enhanced activity, as is characteristic for reversible reactions.

Electrode system d has not been examined in alkaline solutions.

5.5. Conclusions

The investigations of five electrode systems demonstrate that the number of active sites is an important factor determining the activity of an electrode. This number is by no means the same as the total amount of catalyst present on the surface. A layer prepared by irreversible adsorption on an inert electrode material is recommended to study electrocatalysis, because of the possibility of determining the exact number of active sites and, moreover, the diffusion to the surface is well-defined. The use of this electrode system enables the

determination of the "intrinsic catalytic activity" of a catalyst. With "intrinsic catalytic activity" is meant the (catalytic) activity of a surface expressed by an exchange current density and corrected for the number of the active sites on this surface. The obtained quantity can be called turnover number.

The use of this turnover number instead of the exchange current density will not give very different results for metal electrodes, since they all have about the same number of surface atoms per unit surface area. However, this is not the case with large organic molecules as catalyst, containing only one active site per molecule. For instance, when the catalytic activity of a surface, covered with CoTSPc, is compared with the activity of platinum, the use of exchange current densities gives a false picture. If the same geometric surface area is taken into account, an adsorbed monolayer of CoTSPc contains 5×10^{13} molecules cm^{-2} , assuming an area of 2 nm^2 per molecule with the molecules lying parallel to the surface. For platinum, however, a number of 1.35×10^{15} atoms cm^{-2} can be calculated using a density of 21.45 g/cm^3 . Thus, a platinum electrode has 27 times more active sites than an adsorbed monolayer of CoTSPc. An (imaginary) CoTSPc electrode that would contain the same number of active sites as platinum per unit surface area (and which, therefore, allows a fair comparison), would show in acid electrolytes a half-wave potential, that is shifted 220 mV in anodic direction, compared with the electrode, described by curve 2 in figure 5.2.

5.6. References

1. J. Zagal, R.K. Sen and E. Yeager, J. Electroanal. Chem. 83 (1977) 207.
2. F. van den Brink, W. Visscher and E. Barendrecht, J. Electroanal. Chem. 157 (1983) 283.
3. M.I. Florit, W.E. O'Grady, C.A. Linkous, T. Skotheim and M. Rosenthal, Published, Abstract N415, Extended Abstracts, Vol. 84-1, The Electrochem. Soc. (1984).
R.A. Bull, F.R. Fan and A.J. Bard, J. Electrochem. Soc. 131 (1984) 687.
4. L. Kreja and A. Plewka, Electrochim. Acta 27 (1982) 251.
5. H. Behret, W. Clauberg and G. Sandstede, Ber. Bunsenges. Phys. Chem. 81 (1977) 54.
H. Behret, W. Clauberg and G. Sandstede, Zeitschrift für Physikalische Chemie, Neue Folge, Bd. 113 (1978) 97.

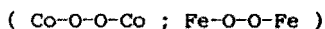
6. C.P. Andrieux, J.M. Dumas-Bouchiat and J.M. Savéant, *J. Electroanal. Chem.* 131 (1982) 1.
7. E. Yeager, *Electrochim. Acta* 29 (1984) 1527.
J.H. Zagal-Moya, Thesis, Case Western Reserve University, Cleveland (1978).
8. J. Albery, *Electrode Kinetics*, Clarendon Press, Oxford (1975).
9. J.H. Weber and D.H. Busch, *J. Inorg. Chem.* 4 (1965) 469.
10. A.F. Diaz, J.I. Castillo, J.A. Logan and W.Y. Lee, *J. Electroanal. Chem.* 129 (1981) 115.
11. A. van der Putten, W. Visscher and E. Barendrecht, *J. Electroanal. Chem.* 195 (1985) 63.
12. E.M. Genies and A.A. Syed, *Synth. Met.* 10 (1984) 21.

6. The cathodic reduction of dioxygen at metal tetrasulfonato-phthalocyanines: influence of adsorption conditions on electrocatalysis

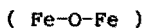
6.1. Introduction

In a number of papers, the dioxygen reduction at electrodes, prepared by irreversible adsorption of metal chelates on graphite has been described [1-8]. It was discovered more or less accidentally that electrodes, that had been used in an electrolyte in which a water-soluble porphyrin or phthalocyanine was dissolved, showed the same dioxygen reduction behaviour when they were thereafter investigated in the electrolyte free of dissolved metal chelate [7,9]. So, the adsorption of these complexes is so strong that measurements in electrolytes devoided of the metal chelate are possible, without desorption of the complex on the time scale of the experiment. In which way the molecules are adsorbed on the surface is not completely understood [8,10,11]. Also the conditions which affect the establishment of the adsorption equilibrium are not fully known. In some cases, the adsorption is a fast process, while in other cases adsorption occurred only as the result of cycling of the electrode for half an hour in a solution of the complex [8,12].

To get more insight into the adsorption phenomena, we have investigated the adsorption process in more detail and also the effect of ageing on phthalocyanine solutions has been investigated. The first question was: under which conditions can the highest coverage of cobalt- or iron tetrasulfonato-phthalocyanine (Co- or FeTSPc) on pyrolytic graphite (Cp) be obtained. For comparison, also cobalt- or iron phthalocyanine (Co- or FePc) are investigated. Subsequently, the effect of different coverages on the dioxygen reduction has been studied. Also UV-Vis. spectra were recorded to determine the reaction of the water-soluble phthalocyanines with dioxygen. Generally, it is accepted that peroxy species are formed [13,14,15]:



For FePc even the subsequent forming of an oxo-bridged species has been reported [16,17]:



However, for CoPc an oxo-bridged dimer has never been reported [17,18].

In our experiments, we have concentrated our attention on the oxygenation behaviour of aged phthalocyanine solutions.

6.2. Experimental section

CoTSPc and FeTSPc were synthesized as described by Weber and Busch [19]. The chemicals CoPc and FePc were obtained from Eastman Kodak and used as such. As a solvent for CoPc and FePc pyridine, while for the tetrasulfonated form double distilled water, was used.

To determine the solution species in the case of the water soluble complexes, UV-Vis. spectra were recorded, using a double beam Pye-Unicam spectrophotometer. The spectra were recorded in dioxygen- or helium-saturated solutions. The helium was purified from traces of dioxygen by leading the gas over a BTS-copper type catalyst (obtained from BASF), at a temperature of 150°C. Preliminary experiments have shown that at room temperature the reaction with dioxygen is slow. For this reason, the spectra were recorded at a temperature of 70°C.

All electrochemical experiments were performed in a standard three-compartment electrochemical cell. In the case of cyclic voltammetry, the electrolyte, 1 M KOH, was made free of dioxygen by bubbling nitrogen through it. The dioxygen reduction was measured with the Rotating Disc Electrode technique in the same, but now dioxygen-saturated, electrolyte. A Tacussel bipotentiostat was used.

The working electrode was a disc electrode made of Cp, with a surface area of 0.52 cm². The electrode was polished with 0.3 μm alumina before use, to obtain a flat surface, free from adsorbed species. The alumina was removed from the disc by cleaning in an ultrasonic bath for 1 minute or by rinsing in a powerful stream of water. No difference was observed for the two procedures. The complexes were applied onto the disc by dipping the polished electrode for 1 minute into a solution of the corresponding complex and thereafter flushing with distilled water. A Reversible Pt-Hydrogen Electrode (RHE) was used, to which all potentials are referred. The counter electrode was made of a Pt-foil.

6.3. Results and discussion

6.3.1. The adsorption process

For the description of the adsorption process the following experiments are relevant:

- The difference between CoTSPc and FeTSPc. From a freshly prepared 10^{-4} M solution of CoTSPc in distilled water, adsorption of CoTSPc on graphite is possible in one minute or less. The presence of CoTSPc on graphite is indicated by the redox peaks in the cyclic voltammogram (figure 6.1). For FeTSPc no

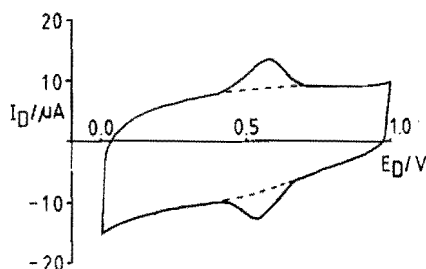


Fig. 6.1 Cyclic voltammogram of CoTSPc adsorbed on Cp from a 10^{-4} M solution. The dashed curve is for Cp only. Electrolyte: 1 M KOH, dioxygen-free; scan rate: 100 mV s^{-1} .

adsorption is observed under these conditions. Adsorption of the latter could only be achieved by addition to the solution of a salt like LiClO_4 , a base (KOH) or an acid (H_2SO_4), figure 6.2. If the concentration of one of these

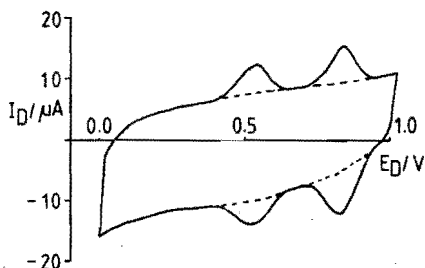


Fig. 6.2 Cyclic voltammogram of FeTSPc adsorbed on Cp from a 10^{-4} M solution in 1 M KOH. Other specifications as in figure 6.1.

supporting electrolytes is increased, then also the coverage of FeTSPc increases; for a concentration of 1 M a saturation value for coverage is obtained. Therefore, all solutions, used for the achievement of the adsorption of FeTSPc, were prepared from 1 M KOH. For CoTSPc, however, no effect of type and concentration of the supporting electrolyte was observed.

• Crystallization in the presence of ions. CoTSPc is soluble in 1 M KOH.

After a few days, however, small crystals are observed in the solution and the colour changes gradually from dark blue to green. After a week a deposit is formed and the colour of the solution has become light green. If the deposit is dissolved in distilled water, the original CoTSPc spectrum is obtained anew. The light green colour of the remaining solution is probably caused by an impurity or by some degradation of the complex. A CoTSPc solution in distilled water is stable for months; it still retains its blue colour. FeTSPc shows the same behaviour.

• Irreversible oxygenation. A freshly prepared solution of CoTSPc (circa 10^{-5} M) in dioxygen-free 0.1 M KOH shows a spectrum as depicted by the solid curve in figure 6.3A. This spectrum was recorded immediately after addition of CoTSPc to the dioxygen-free 0.1 M KOH solution. Two peaks are visible and are ascribed to a monomer (670 nm) and a dimer species (626 nm) [14,15].

By bubbling of dioxygen through the solution for one hour, a new peak appears at a wavelength of 670 nm and this peak has been ascribed to a peroxo-bridged dimer [14,15], figure 6.3A. This figure also shows that after helium saturation the original spectrum did not restore. If we use shorter times for dioxygen and helium saturation a more reversible oxygenation is observed. For longer times, a few hours and more, however, and depending on the measuring temperature, oxygenation is quite irreversible. This means that the spectra of the dioxygen-free species could not be converted into the spectra of the dioxygen-containing species, vice versa, with the same rate as at the beginning of the experiment. So the rearrangement is irreversible.

In figure 6.3B, with helium first and then dioxygen, the slowing down of the oxygenation is already visible. By comparing figure 6.3A and B, it is evident that the dioxygen adduct is formed with a higher rate when the solution is directly saturated with dioxygen. Although the initial conditions are a little different (for figure 6.3B the concentration of the freshly prepared solution appeared to be somewhat higher than for figure 6.3A, leading to relatively more dimer species in the solution), this does not influence the drawn conclusions.

For the recorded spectra of FeTSPc, it is even more difficult to draw

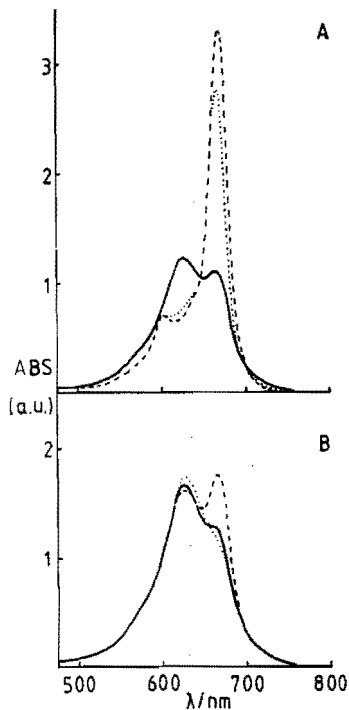


Fig. 6.3 UV-Vis. spectra for CoTSPc (10^{-5} M).

- A) — recorded immediately after addition of CoTSPc to 0.1 M KOH (dioxygen-free).
 ----- after 1 hour of dioxygen saturation
 and, thereafter, 1 hour of helium saturation.
- B) The same notation is used but the time sequence of dioxygen and helium saturation has been reversed.

conclusions. These experiments are complicated by the fast degradation of the complex in the presence of dioxygen as can be observed in figure 6.4. Contrary to CoTSPc, with FeTSPc a dioxygen-containing species is detected immediately after addition of FeTSPc to the dioxygen-free solution. Probably, the dioxygen-FeTSPc bond is so strong, that dioxygen is already irreversibly adsorbed on FeTSPc in the solid form.

In acid media the effects are qualitatively the same, but somewhat smaller.

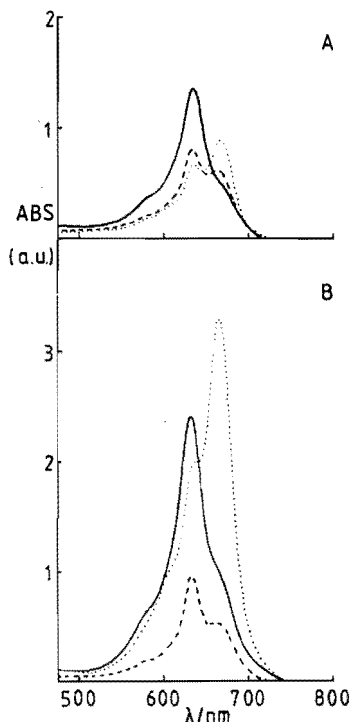


Fig. 6.4 UV-Vis. spectra for FeTSPc (10^{-5} M) (see for notation figure 6.3).

• Concentration dependence. In the figures 6.5 (and 6.6) the results for three different concentrations of CoTSPc (and FeTSPc) dip solutions are given. As can be concluded from these figures, increasing the concentration leads to a higher coverage.

If for the redox process observed for CoTSPc (figure 6.5) $n = 1$ is supposed, one can calculate the following coverages from the charge under the oxidation or reduction peak: 1.4×10^{-10} ; 5.5×10^{-11} and 1.5×10^{-11} mol cm^{-2} for concentrations of 10^{-4} , 10^{-5} and 10^{-6} M, respectively. A limiting surface coverage appears to be reached with concentrations of 10^{-4} M or higher, because this coverage (1.4×10^{-10} mol cm^{-2}) is equivalent to a monolayer of CoTSPc (or FeTSPc), assuming that the molecules lie parallel to the surface and occupy 2 nm^2 per molecule.

An increase of the diptime to one hour for the 10^{-6} M solution leads to the same coverage as observed for the 10^{-4} M solution after 1 minute, indicating a diffusion controlled process. However, kinetic control for the

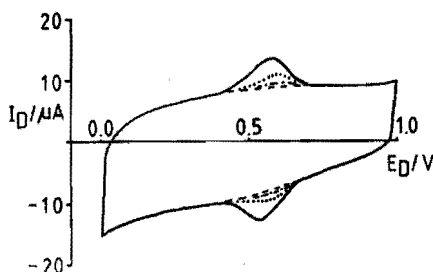


Fig. 6.5 Cyclic voltammograms of CoTSPC adsorbed on Cp from solutions of different concentrations. — 10^{-4} M; 10^{-5} M; -.-.- 10^{-6} M and ----- Cp. Other specifications as in figure 6.1.

adsorption process [8] cannot be completely ruled out on the basis of these facts alone.

The cyclic voltammogram of FeTSPC adsorbed on Cp shows two redox processes (see figure 6.6). From the charges under these peaks, and again

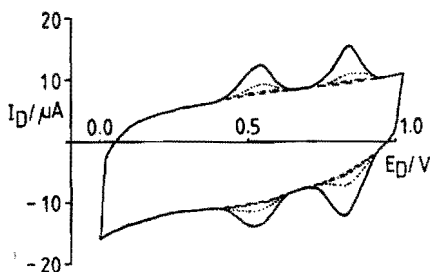


Fig. 6.6 Cyclic voltammograms of FeTSPC adsorbed on Cp from solutions of different concentrations. Specifications are the same as in figure 6.5.

assuming a process for which $n = 1$, the following coverages are calculated: 1.3×10^{-10} and 3.5×10^{-11} mol cm $^{-2}$ for, respectively, 10^{-4} and 10^{-5} M solutions. For the 10^{-6} M solution no surface concentration is given, because for this low coverage hardly a redox peak is detectable. A similar influence of the concentrations of FePc and CoPc, dissolved in pyridine, on the adsorption process is observed.

The phenomena can be explained as follows: it has been reported [14,15]

that increasing the ionic strength of a solution of CoTSPc increases the dimer peak in the UV-Vis. spectrum. The extra ions most probably compensate the expected large electrostatic repulsion between two CoTSPc⁴⁻ ions. We now suppose that in alkaline solutions the dimerization process is followed by aggregation of the dimers. After some time these species have grown to such dimensions that the accessibility for dioxygen and so the oxygenation rate is decreased. It is to be expected that aggregation does not affect the absorption behaviour; and the recorded spectra are therefore not changed. Further, we suppose that the aggregation happens for dioxygen-free species as well as for dioxygen-containing species. The new formed species show a considerable longer time for dioxygen uptake or release as compared with the original monomers or dimers. A possible reaction scheme is given in figure 6.7 for both CoTSPc and FeTSPc. In this scheme, the reactions with dioxygen are written in

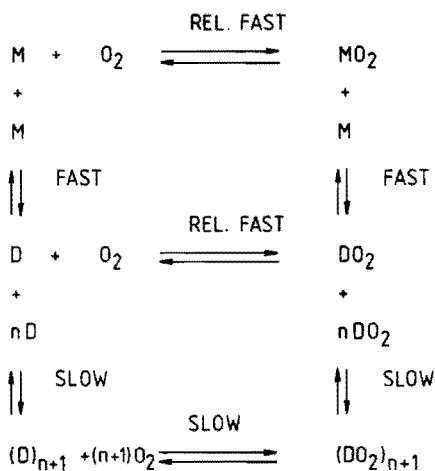


Fig. 6.7 Reaction scheme: M is monomer; D is dimer, MO₂ and DO₂ are species containing dioxygen, and (D)_{n+1} and (DO₂)_{n+1} are aggregates.

the horizontal direction, while vertical the dimerization and the aggregation are given. The aggregation and the oxygenation of the aggregates occur slowly. For FeTSPc no dioxygen-free dimer is detected. The acceptable reason for this is, that the equilibrium between the monomer and dimer form lies completely on the monomer site.

In 1 M KOH, the aggregation continues and after some days the tetra-sulfonato-phthalocyanine starts to precipitate until finally a clear solution is obtained.

For FeTSPc solutions, at first a peroxo-bridged species is formed, as can be concluded from the fact that with helium saturation a spectrum of the dioxygen-free FeTSPc monomer is obtained. It is not likely that an oxo-bridged species is converted into a dioxygen-free species by helium saturation alone. Besides the aggregation (as is also observed for FeTSPc in 1 M KOH), after some time some peroxo species are probably converted into oxo-bridged species, and this could also partly explain the observed irreversible oxygenation of FeTSPc.

The adsorption of FeTSPc on Cp is probably promoted in the same way as the aggregation in solution, by increasing the ionic strength of the solution. The large negative charge of the FeTSPc-ring hinders the adsorption of FeTSPc on the graphite surface. By compensation for this charge by cations, adsorption of the FeTSPc molecule is made possible.

The difference between the adsorption behaviour of CoTSPc and FeTSPc leads to the conclusion that the metal centre is involved in the bonding to the graphite surface. Perhaps an association of this centre to a dioxygen functionality on the graphite takes place, as was already previously suggested by Zagal [7], based upon the different observed coverages for the ordinary and the basal plane of pyrolytic graphite. On the latter substrate less surface groups are available.

Contrary to our observations, Zecevic et al. [8] reported that the pH has no effect on the adsorption process of FeTSPc. In their experiments they used solutions, which were prepared from stock solutions. It is evident that their solutions must be aged. Especially with FeTSPc, we observed a drastic decrease in surface coverage of the Cp when solutions of several days old were used. In that case hardly any redox peaks were detectable. The same behaviour was found with FePc, dissolved in pyridine.

6.3.2. Dioxygen reduction on CoTSPc

The fact that different coverages are achieved when solutions of varying dip concentrations are used, enables us to study the electrocatalysis of the dioxygen reduction as a function of the electrode coverages with phthalocyanines.

Figure 6.8 shows the dioxygen reduction behaviour for the three coverages of CoTSPc, as calculated in the preceding section. As already described in chapter 5 or reference [20], the half-wave potential increases as the coverage increases. In this chapter, we want to focus our attention to the values of

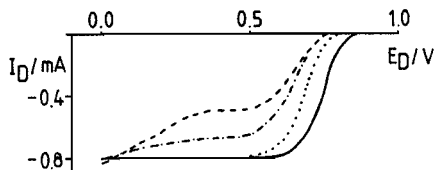


Fig. 6.8 Dioxygen reduction at electrodes covered with different amounts of CoTSPc. — 1.4×10^{-10} , 5.5×10^{-11} , -.-.- 1.5×10^{-11} mol cm^{-2} , ----- Cp. Electrolyte: 1 M KOH, dioxygen-saturated; scan rate: 50 mV s^{-1} ; rotation frequency: 16 s^{-1} .

the limiting current. For the electrodes with surface concentrations from 1.4×10^{-10} to 5.5×10^{-11} mol cm^{-2} , a current of 0.8 mA is measured in the diffusion controlled region. This is equal to the diffusion limiting current, determined according to the Levich equation for the reduction of dioxygen to hydrogen peroxide, at a rotation frequency of 16 s^{-1} and an electrode surface area of 0.52 cm^2 . The limiting currents observed for different rotation frequencies are depicted as Levich plots in figure 6.9A. For the smallest coverage, curve 3, a deviation from Levich behaviour is observed. Plotting these results as Koutecky-Levich plots (i_L^{-1} versus $\omega^{-1/2}$), in figure 6.9B, the extrapolated line for the smallest coverage (curve 3) does not go through the origin, indicating the occurrence of "kinetic limitation". This is attributed by Durand et

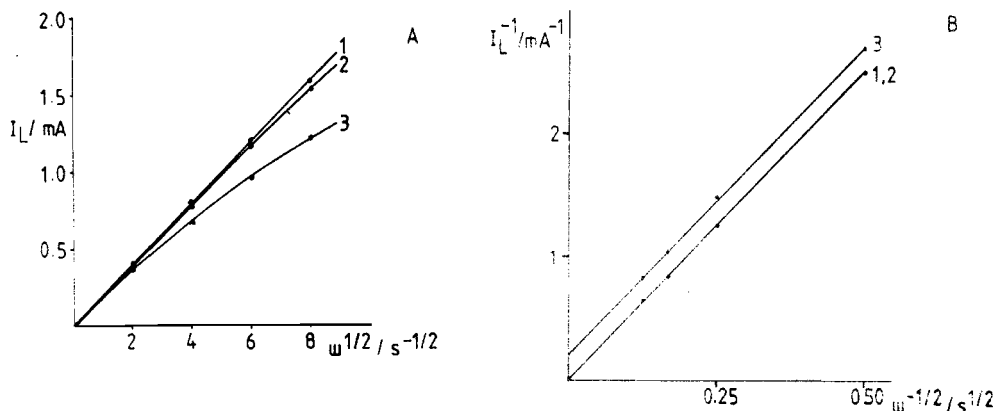


Fig. 6.9 Levich (A) and Koutecky-Levich (B) plot for the dioxygen reduction at the electrodes of figure 6.8. Again the amounts of CoTSPc are 1) 1.4×10^{-10} ; 2) 5.5×10^{-11} ; 3) 1.5×10^{-11} mol cm^{-2} .

al. [21], to a rate determining chemical reaction between dioxygen and the catalyst. In their experiments, they used cobalt porphyrin as a catalyst. In our case a similar explanation can be given.

However, in the case of very small coverages an alternative explanation based upon a theory about surface diffusion, as has been developed by McIntyre and Peck, Jr. for gold [22], is also possible. When only few catalyst molecules are present on the surface, it must be realized that approach of the electrode by a dioxygen molecule not automatically means that an active site is encountered. According to McIntyre and Peck, Jr. "current or kinetic saturation" occurs as the time for a dioxygen molecule to traverse through the convective diffusion layer becomes comparable to the time, required to diffuse across the surface to an active site [22]. The thickness (δ) of the convective diffusion layer at a Rotating Disc Electrode (RDE) is given by:

$$\delta = 1.61 D^{1/3} \nu^{1/6} \omega^{-1/2} \quad (1)$$

where D is the diffusion coefficient of the electroactive species, ν is the kinematic viscosity of the electrolyte and ω is the rotational speed of the electrode. The time (τ) to traverse this layer can be calculated as:

$$\tau = 1.3 D^{-1/3} \nu^{1/3} \omega^{-1} \quad (2)$$

For curve 3 of figure 6.9 a deviation of the Levich behaviour is already visible for a rotation frequency of 16 s^{-1} . For this rotation frequency the time required to pass the diffusion layer is 0.12 s, with $\nu = 1.065 \times 10^{-2} \text{ cm}^2 \text{ s}^{-1}$ and $D = 1.36 \times 10^{-5} \text{ cm}^2 \text{ s}^{-1}$ [23]. The chosen onset point of the "kinetic saturation" is rather arbitrary; whereas McIntyre et al. took the value at complete saturation, we have chosen a rotation frequency, where only a small deviation of the Levich behaviour is observed. Thus, the surface diffusion time (t) must be smaller than the solution diffusion time (τ) for the case of a rotation frequency of 16 s^{-1} . Therefore, it is reasonable to assume that t is in the range of $(0.01-0.1)\tau$.

When the surface diffusion is treated as a random walk, with the above mentioned assumption, an estimate of the surface diffusion coefficient, D_s , can be made from the following relation:

$$\langle x^2 \rangle = 2 D_s t \quad (3)$$

where $\langle x^2 \rangle$ is the mean square displacement. If it is assumed that CoTSPc is randomly distributed over the graphite surface, then a loading of 1.5×10^{-11} mol cm^{-2} is equivalent to a surface domain of 11 nm^2 for one CoTSPc molecule, i.e. a circle with a radius of 1.9 nm. The time available to travel this distance is 0.0012-0.012 s (i.e. 1-10% of the time necessary to pass through the diffusion layer), so a surface diffusion coefficient of 1.5×10^{-11} - $1.5 \times 10^{-12} \text{ cm}^2 \text{ s}^{-1}$ is determined. This value is in the same range as the value for the surface diffusion coefficient for a gold (111) face, which has been calculated by McIntyre et al. ($7 \times 10^{-11} \text{ cm}^2 \text{ s}^{-1}$). For both surfaces only a weak interaction is expected to occur between dioxygen and the surface [22,24]. Association of the catalyst molecules on the graphite surface will result in a higher surface diffusion coefficient. In this chapter only a random distribution will be taken into account. Thus, the above given calculation demonstrates that surface diffusion can explain the "kinetic limitation". Both explanations (a rate determining chemical step or surface diffusion) are equally probable; the second explanation has, however, the advantage that it does not require introduction of a rate determining chemical step.

6.3.3. Dioxygen reduction on FeTSPc

The resulting dioxygen reduction behaviour for the three different coverages, is depicted in figure 6.10. It is clear that the dioxygen reduction wave is composed of two different waves, as previously published by Zagal et al. [6,7,25]. When the coverage decreases, the first wave (or the wave at low

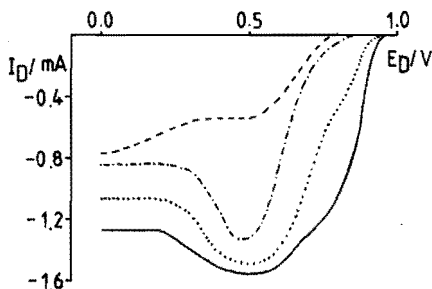


Fig. 6.10 Dioxygen reduction at electrodes covered with different amounts of FeTSPc. — 1.3×10^{-10} , $3.5 \times 10^{-11} \text{ mol cm}^{-2}$, -.-.- no coverage determinable, -.-.- Cp. Other specifications as in figure 6.8.

overpotential) disappears more rapidly than the second wave (main wave), see figure 6.10. For FePc, the same observations have been made [26].

The results of a study of the dioxygen reduction on electrodes, covered with different amounts of FeTSPc, as a function of the rotation frequency are summarized in a Levich plot, figure 6.11. The points in this figure are the obtained current maxima (see also figure 6.10). These maxima are characteristic for both FeTSPc [7] and FePc [26]. The decrease in current in figure 6.10 is caused by the competition between FePc (or FeTSPc) sites and the graphite surface at high overpotentials. The graphite surface itself, gives hydrogen peroxide as a reduction product, and compared with the reduction of dioxygen to water at FePc (or FeTSPc), this causes a decrease in current.

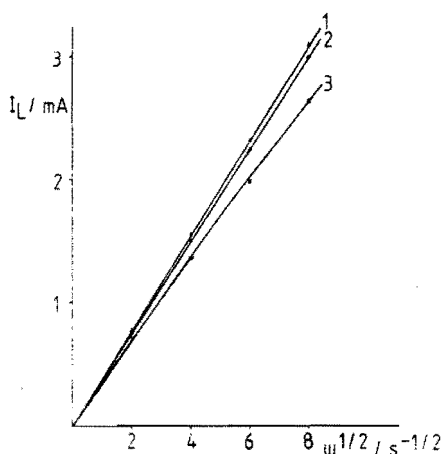


Fig. 6.11 Levich plots for the dioxygen reduction at electrodes covered with the same amounts of FeTSPc as in figure 6.10. 1) 1.3×10^{-10} ; 2) $3.5 \times 10^{-11} \text{ mol cm}^{-2}$; 3) no coverage determinable.

Curves 1 and 2 in figure 6.11 demonstrate that the dioxygen reduction at the two highest coverages satisfies the Levich equation, while for the other case, curve 3, a deviation of this behaviour is observed. The diffusion limiting currents are a factor of two higher for FeTSPc as compared with CoTSPc, because of the dioxygen reduction to water at FeTSPc instead of hydrogen peroxide. When the results are plotted in a Koutecky-Levich plot, we obtain, as in figure 6.9B for CoTSPc, parallel lines, of which the line for the smallest coverage does not pass the origin, indicating again "kinetic limitation"; the same explanations, as before for CoTSPc, are now possible.

If the FeTSPc coverage of the electrode decreases, then the prewave shows more severe "kinetic limitation" than the main wave, as can be concluded from figure 6.10. For this "kinetic limitation" an explanation based on surface diffusion is also possible, but here the conclusion must be drawn, that we are dealing with two different FeTSPc sites. One type of site is then responsible for the main wave, while the other, in minority present, should cause the prewave.

The possibility of the existence of two different sites (monomeric and dimeric) has already been suggested by us earlier and was based on analogies [26]. A survey of the literature shows that direct reduction of dioxygen to water without formation of hydrogen peroxide as an intermediate is occurring on noble metals as platinum and silver [27], electrodes prepared by UPD (Under Potential Deposition) of some metals [28] and cofacial dicobalt porphyrins [29]. In all cases, this behaviour is explained, assuming bridge adsorption. For FeTSPc (or FePc) a direct reduction of dioxygen is occurring at low overpotentials, as is demonstrated by the fact that with Rotating Ring Disc Electrode (RRDE) experiments no ring current due to the production of hydrogen peroxide is detected at the potentials of the prewave [25]. As stated previously, the prewave must be associated with dimer sites for which bridge adsorption of dioxygen is possible, while the main wave is due to monomer sites.

The dioxygen reduction behaviour at the highest coverage of FeTSPc is given for four different rotation frequencies in figure 6.12A. In this figure also an extension of the prewave is constructed (dashed lines). Of course, this extrapolation is questionable, but the extrapolated curves show the onset of "kinetic limitation" (see figure 6.12B) and this agrees with the fact that the prewave rather critically depends on the coverage. In figure 6.12B a deviation of the Levich equation for a rotation frequency from 16 s^{-1} onwards is observed. If again the assumption is made that for this rotation frequency the time required for the surface diffusion is 10% of the time necessary for passing the diffusion layer, then a time of 0.012 s is available for surface diffusion. In this time, a distance of 1.9 nm could be covered according to equation (3) when as surface diffusion coefficient $1.5 \times 10^{-12} \text{ cm}^2 \text{ s}^{-1}$ is used. From this distance, it can be calculated that, in the case of a uniform distribution of the sites over the surface, the coverage is $1.5 \times 10^{-11} \text{ mol cm}^{-2}$. Compared with the total amount of $1.3 \times 10^{-10} \text{ mol cm}^{-2}$ of FeTSPc present on the surface, this corresponds to 12% of it. Taking 1% of the time necessary for passing the diffusion layer as the surface diffusion time, then

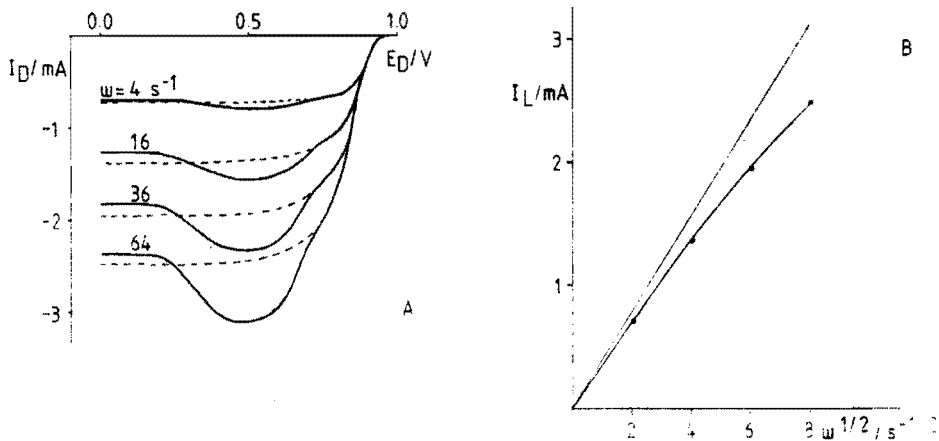


Fig. 6.12 A. Dioxygen reduction at FeTSPC adsorbed on Cp for the highest coverage ($1.3 \times 10^{-10} \text{ mol cm}^{-2}$) only. The rotation frequencies are given in the figure. The dashed lines represent the extrapolations of the prewave. Other specifications as in figure 6.8.

B. Levich plots for the extrapolated prewave. The straight line also drawn in this figure is the Levich behaviour of the current maxima for the highest coverage (see also figure 6.10; line 1).

the corresponding surface diffusion coefficient of $1.5 \times 10^{-11} \text{ cm}^2 \text{ s}^{-1}$ must be used and the same amount of dimer sites is calculated.

To prove the existence of dimer sites, independent evidence is necessary. Unfortunately, it is not possible to carry out reflectance spectroscopy with electrodes made of ordinary pyrolytic graphite, because the surface of these electrodes is not reflective enough. Reflectance spectroscopy has been performed on the basal plane of pyrolytic graphite by Nikolic et al. [12], which shows a higher reflectivity. However, this basal plane pyrolytic graphite does not behave identical with ordinary pyrolytic graphite. Zagal, for example, reported an almost completely vanished prewave [7]. Going from ordinary to basal plane pyrolytic graphite, the coverage has decreased 4 to 5 times. From the dramatic effect on the prewave of a 3 to 4 times decrease in coverage, as can be seen in figure 6.10, we can imagine that the prewave completely vanishes when the basal plane instead of ordinary pyrolytic graphite is used. Perhaps, there is also an influence of the surface roughness on the probabili-

ty of the occurrence of dimer sites, as has been suggested in a previous publication [26].

As to the results of Nikolic et al. for the basal plane, they recorded spectra at a potential of 0.9 V vs. RHE, where the adsorbed FeTSPc molecule is in the oxidized Fe(III)-state (see figure 6.2). The spectrum shows a main peak at 635 nm, ascribed to a dioxygen-containing dimer species. It may, however, also be argued that the peak corresponds to a monomer Fe(III)TSPc species which has almost the same absorption wavelength (632 nm) as a dioxygen-containing dimer in the solution [30]. Experiments are planned to solve this question by studying the spectra at potentials below 0.9 V, where the Fe ion is in the Fe(II)-state. For the moment, we will take the dimer model of Nikolic et al. as valid. In their view, a structure with the phthalocyanine rings perpendicular to the surface belongs to the possibilities. This model gets some evidence from Raman spectroscopy [10,31].

The estimate of 12% dimer sites seems to be in contradiction with the spectroscopic results. We must keep in mind, however, that for each dimer site there are two monomer sites available. Between two molecules bridge adsorption can occur, while outside the region between the two molecules two places remain for the formation of monomeric dioxygen adducts. So, even if we are dealing with only FeTSPc dimers and assuming that the adsorption model of Nikolic et al. is valid, we must keep in mind that bridge adsorption is occurring on only 33% of the available sites. The estimated number of 12% should be considered as an indication of the value which can be expected for the amount of dimers; so an agreement with the results of Nikolic et al. is still possible.

The model, presented here, explains the observed "kinetic limitation" for the prewave solely by the small number of dimer sites. The advantage with respect to other models is that there is no need for the introduction of a rate determining chemical step.

6.3.4. FePc compared with FeTSPc

Until now, no distinction is made between CoTSPc (or FeTSPc) and CoPc (or FePc) in the observed cathodic dioxygen reduction behaviour. The differences between CoPc and CoTSPc are so small that they can be neglected. However, although most results are qualitatively also the same for FeTSPc and FePc, there are some differences, which need a closer examination.

The already previously published results obtained for FePc, irreversibly

adsorbed on graphite from a pyridine solution [26], are repeated in figure 6.13. First of all, it must be noted that with FePc slightly higher coverages are obtained as compared with FeTSPc. The coverages for FePc, calculated in the same manner as for FeTSPc, are 1.6×10^{-10} and 2×10^{-11} mol cm⁻² for

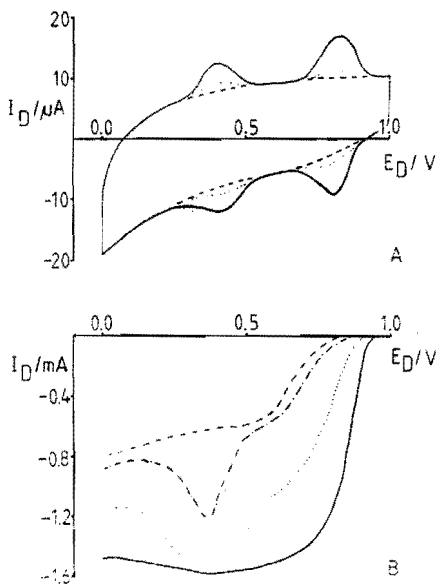


Fig. 6.13 A. Cyclic voltammograms of FePc adsorbed on Cp from pyridine solutions with different concentrations. — 10^{-3} M, 10^{-4} M, -.-.- 10^{-5} M, ----- Cp. Other specifications as in figure 6.1.

B. Dioxxygen reduction at the electrodes of A. Other specifications as in figure 6.8.

10^{-3} and 10^{-4} M solutions, respectively. For the 10^{-5} M solution no peaks are detected.

In the potential region of the prewave hardly any differences are observable (figures 6.10 and 6.13). Perhaps, due to the slightly higher coverage for FePc, less "kinetic limitation" occurs in the case of a 10^{-3} M FePc solution as compared with a 10^{-4} M FeTSPc solution. The observed current maxima in the i-E curves for the dioxxygen reduction are shifted circa 100 mV in cathodic direction, going from FeTSPc to FePc. This shift is not due to a difference in coverage because the figures 6.10 and 6.13 for FeTSPc and FePc,

respectively, show that this maximum does not shift as the coverage is altered. A comparison of the cyclic voltammograms measured for FePc and FeTSPc in dioxygen-free electrolytes leads to the conclusion that the shift of the current maximum is accompanied by a shift in the potential for the second, most cathodic, redox process. These results concur with the statement made by Zagal et al. that the current maximum is associated with the second redox process [25].

It is amazing that the sulfonation of the ligand has such a great effect on the redox potentials, as observed for the metal chelates. The reason why only the most cathodic redox process is affected, is not completely understood, especially if one ascribes both redox processes to the central metal ion, as is done by Zecevic et al. [8].

Further investigations are necessary to explain the difference in the redox behaviour between FeTSPc and FePc, and to draw conclusions about the way of adsorption of the complexes on the electrode. Hopefully, this will lead to more insight into the mechanism of dioxygen reduction on FeTSPc or FePc, irreversibly adsorbed on pyrolytic graphite.

6.4. References

1. R.J.H. Chan, Y.O. Su and T. Kuwana, *J. Inorg. Chem.* 24 (1985) 3777.
2. A. Bettelheim, R.J.H. Chan and T. Kuwana, *J. Electroanal. Chem.* 99 (1979) 391.
3. R.R. Durand and F.C. Anson, *J. Electroanal. Chem.* 134 (1982) 273.
4. N. Kobayashi, M. Fujihira, T. Osa and S. Dong, *Chem. Lett.* (1982) 575.
5. J.H. Zagal, R.K. Sen and E. Yeager, *J. Electroanal. Chem.* 83 (1977) 207.
6. J.H. Zagal, M. Pacz, J. Sturm and S. Ureta-Zanartu, *J. Electroanal. Chem.* 182 (1984) 295.
7. J.H. Zagal, Thesis, Case Western Reserve University, Cleveland (1978).
8. S. Zecevic, B. Simic-Glavaski and E. Yeager, *J. Electroanal. Chem.* 196 (1985) 339.
9. D. Ozer, R. Parash, F. Broitman, U. Mor and A. Bettelheim, *J. Chem. Soc. Faraday Trans. I* 80 (1984) 1139.
10. B. Simic-Glavaski, S. Zecevic and E. Yeager, *J. Phys. Chem.* 87 (1983) 4555.
11. B. Simic-Glavaski, S. Zecevic and E. Yeager, *J. Electroanal. Chem.* 150 (1983) 469.

12. B.Z. Nikolic, R.R. Adzic and E.B. Yeager, *J. Electroanal. Chem.* 103 (1979) 281.
13. I. Collamati, *Inorg. Chim. Acta* 35 (1979) 303.
14. L.C. Gruen and R.J. Blagrove, *Aust. J. Chem.* 26 (1973) 319.
15. D.M. Wagnerova, E. Schwertnerova and J. Veprek-Siska, *Collect. Czech. Chem. Comm.* 39 (1974) 1980.
16. B.J. Kennedy, K.S. Murray, P.R. Zwack, H. Homborg and W. Kalz, *Inorg. Chem.* 24 (1985) 3302.
17. R.D. Harcourt, *J. Inorg. Nucl. Chem.* 39 (1977) 243 and references therein.
18. T.D. Smith and J.R. Pilbrow, *Coord. Chem. Rev.* 39 (1981) 295.
19. J.H. Weber and D.H. Busch, *J. Inorg. Chem.* 4 (1965) 469.
20. A. Elzing, A. van der Putten, W. Visscher and E. Barendrecht, *J. Electroanal. Chem.* 200 (1986) 313.
21. R.R. Durand and F.C. Anson, *J. Electroanal. Chem.* 134 (1982) 273.
22. J.D.E. McIntyre and W.F. Peck, Jr., *Proc. Electrochem. Soc. (The Chem. and Phys. of Electrocatal.)* 84 (1984) 102.
23. K.E. Gubbins and R.D. Walker, Jr., *J. Electrochem. Soc.* 112 (1965) 469.
24. A.V. Kiselev, *Quart. Rev.* 15 (1961) 99.
25. J. Zagal, P. Bindra and E. Yeager, *J. Electrochem. Soc.* 127 (1980) 1506.
26. A. van der Putten, A. Elzing, W. Visscher and E. Barendrecht, *J. Electroanal. Chem.* 214 (1986) 523.
27. P. Fischer and J. Heitbaum, *J. Electroanal. Chem.* 112 (1980) 231.
28. K. Jüttner, *Electrochim. Acta* 29 (1984) 1597.
29. J.P. Collman, M. Marocco, P. Denisevich, C. Koval and F.C. Anson, *J. Electroanal. Chem.* 101 (1979) 117.
30. D. Vonderschmitt, K. Bernauer and S. Fallab, *Helv. Chim. Acta.* 48 (1965) 951.
31. R. Adzic, B. Simic-Glavaski and E. Yeager, *J. Electroanal. Chem.* 194 (1985) 155.

7. The mechanism of the dioxygen reduction at iron tetrasulfonato-phthalocyanine incorporated in polypyrrole

7.1. Introduction

The dioxygen reduction at FeTSPc, adsorbed on pyrolytic graphite (Cp), in basic media is characterized by an i-E curve, consisting of two waves, as was observed by Zagal et al. [1]. For FePc (iron phthalocyanine), adsorbed on graphite, we observed a similar behaviour [2]. Recently, we [chapter 6 or ref. 3] proposed a mechanism, in which the wave at low overpotential (prewave) is ascribed to dimer species, while the second wave (main wave) is attributed to monomer species. The dioxygen reduction has also been investigated at FeTSPc, incorporated in polypyrrole, a conducting polymer, by Bull et al. [4]. For CoTSPc, incorporated in polypyrrole, measurements were published by Florit et al. [5] and also by us [chapter 5 or ref. 6].

The question arises whether we are dealing here with dimers or monomers of FeTSPc. To answer this question, we also investigated the dioxygen reduction at FeTSPc, incorporated in polypyrrole.

For the pH-dependence of the dioxygen reduction at FeTSPc, adsorbed on Cp, Zagal [7] found that the prewave potential shows a more or less pH-dependent Nernstian behaviour for the pH-range 3 to 12; this means that no shift in potential is observed, if as a reference electrode a pH-dependent electrode, such as the Reversible Pt-Hydrogen Electrode (RHE), is used. For the main wave, the experiments indicate a pH-independent process. Hence, a greater difference in potential can be expected for the two waves in acid media. For FeTSPc, adsorbed on Cp, this means that experiments at lower pH-values than those used in Zagal's experiments (even though the stability of the complexes therein is far less) are expected to give additional information.

For comparison, the dioxygen reduction is also studied at polypyrrole without catalyst and with CoTSPc molecularly dispersed in it.

7.2. Experimental

CoTSPc and FeTSPc were synthesized according to the methods described by Weber and Busch [8]. All other chemicals were commercially available and used without further purification, except the pyrrole, which was distilled before use.

A Rotating Ring Disc Electrode (RRDE) was used, with a Cp-disc (0.52 cm^2) and a Pt-ring. The electrode was polished with $0.3 \text{ }\mu\text{m}$ alumina before each experiment to obtain a flat surface, free of adsorbed species. The alumina was removed from the disc by cleaning in an ultrasonic bath for one minute.

In some cases the catalyst (FeTSPc) was applied onto the disc by dipping the electrode into a solution of 10^{-3} M FeTSPc in 1 M KOH for one minute and thereafter flushing with distilled water. The reason for using 1 M KOH solutions was outlined in chapter 6 [or ref. 3].

In other cases, the disc was modified with a polypyrrole/FeTSPc (or CoTSPc) layer by electro-oxidation of pyrrole (solution containing 1% pyrrole and 10^{-3} M FeTSPc⁴⁻ (or CoTSPc⁴⁻) anions in water) in a galvanostatic way with a current of 0.2 mA . Since the electro-oxidation of pyrrole gives a polymer with positive charges, these are compensated by negatively charged FeTSPc⁴⁻ (or CoTSPc⁴⁻) anions [4,5,9]. By varying the time, layers of different thickness are produced. For some experiments FeTSPc was replaced by LiClO_4 , which results in a polypyrrole layer without catalytically active material.

The electrochemical experiments were carried out in a standard three-compartment electrochemical cell, filled with 100 ml electrolyte. As electrolytes were used both acid (0.05 M H_2SO_4) and alkaline (0.1 M KOH) solutions or in some cases buffer solutions with the compositions shown in table 7.1. To the buffer solutions 1 M KNO_3 was added to assure a good conductivity. For characterization of the electrode, cyclic voltammetry was carried out in dioxygen-free solutions. The dioxygen reduction was measured in dioxygen-saturated solutions, with the Rotating Disc Electrode technique. In a few experiments the ring was used to detect the hydrogen peroxide possibly produced at the disc. To achieve a quantitative oxidation of the hydrogen peroxide, the ring was slightly platinized and maintained at a potential of 1.2 V versus RHE.

The electrochemical measurements were carried out using a Tacussel bipotentiostat (Bipad). The counter electrode consisted of a Pt-foil and as reference electrode a Reversible Pt-Hydrogen Electrode (RHE) was used. All potentials in this chapter are given versus this RHE.

7.3. Results and discussion

7.3.1. Dioxygen reduction at polypyrrole applied on Cp

Figure 7.1A shows a typical result of the measurement of the dioxygen

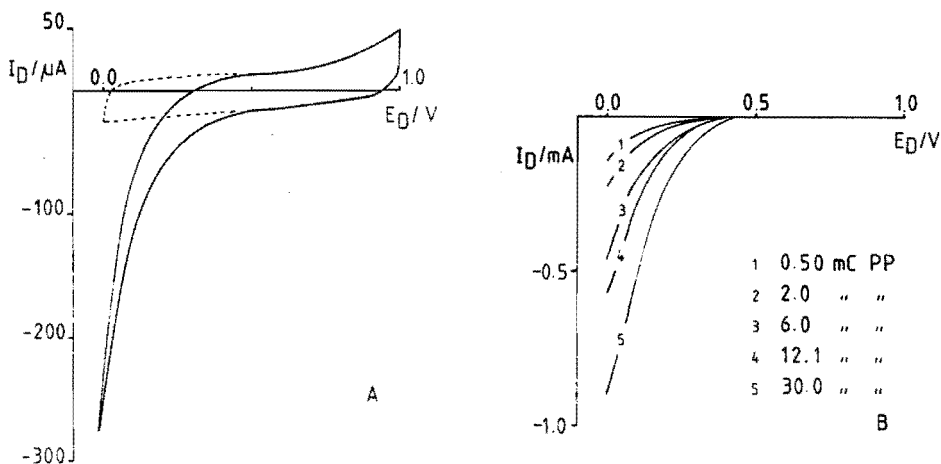


Fig. 7.1A Dioxygen reduction on a polypyrrole/FetSPc layer. Thickness of the layer: 2.0 mC. Electrolyte: 0.05 M H_2SO_4 , dioxygen-saturated; scan rate: 50 mV s^{-1} ; rotation frequency: 64 s^{-1} .

B Dioxygen reduction as a function of the thickness of the polypyrrole layer, attached to a Rotating Disc Electrode. Electrolyte: 0.05 M H_2SO_4 , dioxygen-saturated; scan rate: 50 mV s^{-1} ; rotation frequency: 64 s^{-1} .

reduction in acid solution (0.05 M H_2SO_4) for a polypyrrole layer with a thickness of 2.0 mC. In this figure, also the cyclic voltammogram (dotted line) for the layer in dioxygen-free solution is drawn, so the dioxygen reduction current includes a relatively high capacitive background current. To determine the true dioxygen reduction current, the curve measured in dioxygen-free solution is subtracted from the curve recorded in dioxygen-saturated solution.

Figure 7.1B displays the dioxygen reduction behaviour at polypyrrole, without any catalyst incorporated in it, as a function of the layer thickness. The layer thickness is expressed as the charge passed during the formation (electro-oxidation of pyrrole) of polypyrrole. According to Diaz et al. [10] 24 mC cm^{-2} corresponds to a thickness of 100 nm, which means that in our case 1 mC corresponds to a layer thickness of 8.3 nm. Figure 7.1B shows that polypyrrole is rather inactive for dioxygen reduction, though with increasing layer thickness the activity apparently rises, due to the increase of the

surface area of the film, as is shown by the higher capacitive currents obtained for the respective films in dioxygen-free solutions.

When the layer thickness is still further increased, we could expect that for larger values a dioxygen molecule cannot diffuse through the whole layer, on the time scale of the experiment. This leads to a situation where the reduction of dioxygen takes place only in the outer parts, i.e. the electrolyte side of the film. The result will be a limitation of the reduction current, if the conductivity of the layer does not become a limiting factor too. A general treatment of these phenomena is given in a paper by Andrieux et al. [11]. That this really happens, is shown in figure 7.2, where the dioxygen reduction currents, measured at a potential of 0 V, are plotted as a function of the layer thickness. These results indicate that a dioxygen molecule can diffuse through a polypyrrole layer up to a thickness of 20 mC (= 170 nm).

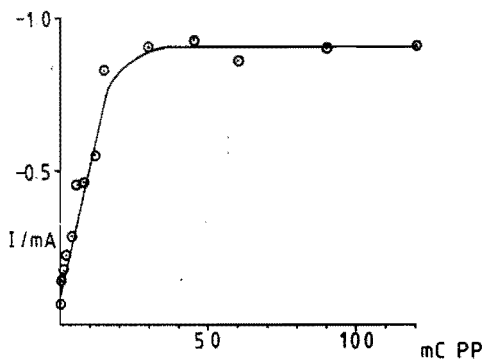


Fig. 7.2 The dioxygen reduction current at a potential of 0 V, plotted as a function of the thickness of the polypyrrole layer and corrected for the capacitive background current for the polypyrrole itself (see text).

Electrolyte: 0.05 M H_2SO_4 , dioxygen-saturated; scan rate: 50 mV s^{-1} ; rotation frequency: 64 s^{-1} .

7.3.2. Dioxygen reduction at FeTSPc incorporated in polypyrrole

In figure 7.3, cyclic voltammograms are given for FeTSPc, incorporated in polypyrrole (A), and for FeTSPc adsorbed on pyrolytic graphite (B). Both voltammograms were measured in dioxygen-free 0.05 M H_2SO_4 . Note the difference

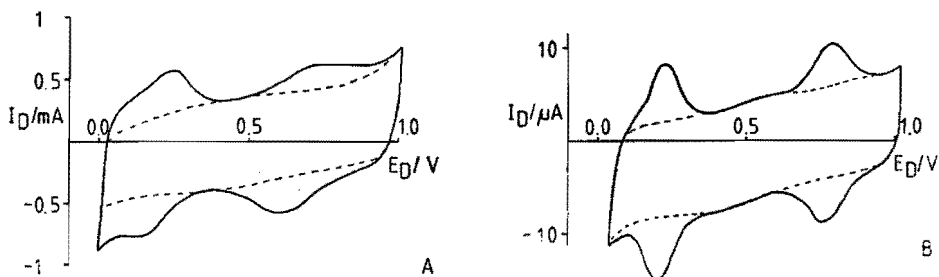


Fig. 7.3 Cyclic voltammograms recorded in dioxygen-free 0.05 M H_2SO_4 ; scan rate: 100 mV s^{-1} ; A) 30 mC FeTSPc/PP layer, B) FeTSPc adsorbed on Cp.

in current scales. The dotted lines indicate the background curves as measured for an evenso 30 mC polypyrrole film by recording its cyclic voltammogram with ClO_4^- as a counter ion instead of FeTSPc. For the adsorbed FeTSPc layer, the cyclic voltammogram of Cp without any catalyst is used as the background current. Just as for FeTSPc adsorbed on Cp [1,3], two redox processes are detected for FeTSPc, incorporated in polypyrrole, in the potential region of interest. In polypyrrole, the two redox processes are less reversible than those for the adsorbed FeTSPc. Perhaps, the conductivity of the polypyrrole layer is not high enough to enable a completely reversible process. It is also possible that the electron transfer from the polymer to the metal complex is a kinetically slow process. Also a shift to lower potentials of about 100 mV is observed for the redox process at the highest potential, for the polymer with incorporated vs. adsorbed FeTSPc. It is rather obvious that this must be ascribed to an interaction between the nitrogen atom of the pyrrole unit and the metal ion.

The amount of FeTSPc, present on the surface, can be calculated from the surface area under the redox peaks. For FeTSPc, incorporated in polypyrrole, a charge of approximately $600 \mu\text{C}$ is determined for each of the four redox peaks. When a redox process with $n = 1$ is assumed, this results in a coverage of $1.2 \times 10^{-8} \text{ mol cm}^{-2}$. This value is in reasonable agreement with the value of $1.67 \times 10^{-8} \text{ mol cm}^{-2}$ that can be calculated for the coverage of a 30 mC polypyrrole/FeTSPc layer. The basis of this calculation is the assumption [chapter 5 or ref. 6] that two electrons per molecule are involved in the oxidation of pyrrole to neutral polypyrrole and that in the oxidized form of polypyrrole every four pyrrole units carry one positive charge. As we have

shown earlier [chapter 6 or ref. 3], no adsorption of FeTSPc occurs on Cp under the conditions used for the electro-oxidation of pyrrole. This means that for a 1 μC thick layer, $4 \times 10^{-10} \text{ mol cm}^{-2}$ is the total coverage. The redox peaks in the cyclic voltammogram of figure 7.3B correspond with a coverage of $1.1 \times 10^{-10} \text{ mol cm}^{-2}$ for the adsorbed FeTSPc.

For different pH's, the dioxygen reduction results at FeTSPc, adsorbed on Cp, are given in figure 7.4. The figure clearly shows that, from pH = 13 to

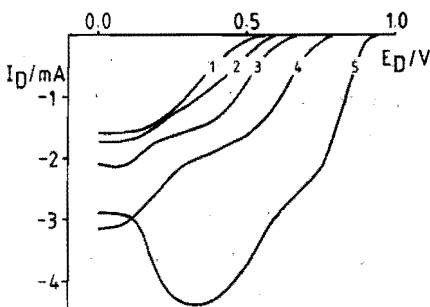


Fig. 7.4 Dioxygen reduction at different pH for FeTSPc, adsorbed on Cp. Curves 1 to 5 are, respectively, measured at a pH of 0, 2, 4, 6 and 13. For the curves 1 to 4 the buffer solutions of table 7.1 are used. Curve 5 has been recorded in 0.1 M KOH. Dioxygen-saturated electrolyte; scan rate: 50 mV s^{-1} ; rotation frequency: 64 s^{-1} .

pH = 6, the main wave, as indicated by the half-wave potential, shifts from about 600 mV to 200 mV, while the prewave shifts from about 800 mV to 650 mV. From pH = 6 to lower values, the two waves merge gradually, and it is not easy to say if the main wave or the prewave will become dominating, especially in the pH-range from 2 to 0. It follows from Rotating Ring Disc experiments, that in alkaline solutions both waves yield water, while in acid solution hydrogen peroxide is the endproduct.

The study of the influence of the layer thickness on the dioxygen reduction at FeTSPc, incorporated in polypyrrole, resulted in the i - E curves of figure 7.5. The i - E curve obtained for FeTSPc, adsorbed on Cp, is also given in this figure, to enable comparison. A problem, encountered here, is the instability of the film. With repeated scanning, the activity decreases, being most pronounced for very thin films; e.g. for the 0.58 μC film the second scan gave a 40% smaller current at a scan rate of 200 mV s^{-1} , whereas a 15 μC

pH = 0: 1 M HClO₄

pH = 2: 125 ml 0.2 M KCl + 65 ml 0.1 M HCl

pH = 4: 250 ml 0.1 M KH-phthalate + 0.5 ml 0.1 M HCl

pH = 6: 250 ml 0.1 M KH₂PO₄ + 28 ml 0.1 M NaOH

Table 7.1: Compositions of the used buffer solutions. Double distilled water was added to the mixtures until a volume of 500 ml. The buffer solutions were made 1 M in KNO₃.

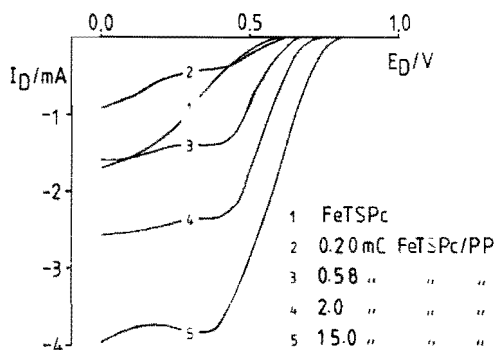


Fig. 7.5 I-E curves for the dioxygen reduction at FeTSPc/polypyrrole layers of different thicknesses; curve 1: FeTSPc adsorbed on Cp. Electrolyte: 0.05 M H₂SO₄, dioxygen-saturated; scan rate: 200 mV s⁻¹; rotation frequency: 64 s⁻¹.

film showed only a 10% decrease in current after a few scans. The better stability of the thicker layer is due to the higher coverage with catalyst molecules for this layer. Therefore, a high scan rate (200 mV s⁻¹) was chosen and only the first scan is given in figure 7.5. The behaviour of FeTSPc, with regard to the influence of layer thickness, differs from that of CoTSPc (figure 7.6) which was previously investigated by us [chapter 5 or ref. 6]. There, a theoretical description for the improvement of the activity based upon the increased number of active sites is given. It was concluded on theoretical arguments that a tenfold increase of the number of active catalyst molecules caused a shift of the half-wave potential with a value equal to the

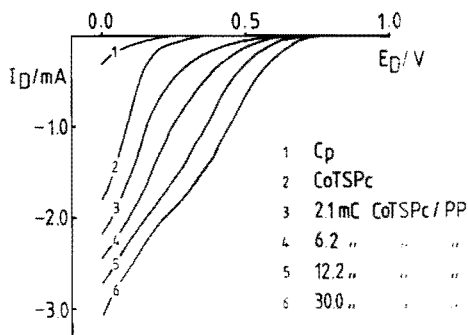


Fig. 7.6 The dioxxygen reduction behaviour at CoTSPc/polypyrrole layers of different thicknesses. In the same figure are also given the results for pyrolytic graphite (Cp) itself (curve 1) and CoTSPc adsorbed on Cp (curve 2). Electrolyte: 0.05 M H_2SO_4 , dioxxygen-saturated; scan rate: 50 mV s^{-1} ; rotation frequency: 64 s^{-1} .

Tafel slope for the same reaction. For CoTSPc in polypyrrole the Tafel slope of -155 mV in $0.05 \text{ M } H_2SO_4$ agrees well with the observed shift (155 mV) in half-wave potential for a tenfold increase of the number of active sites.

By comparing the curves for FeTSPc, incorporated in polypyrrole, (fig. 7.5 curves 2 to 5) with each other, an increasing limiting current is observed as the layer thickness increases. Half-wave potentials can be determined, if each curve is considered to be a complete wave. The resulting shift in half-wave potential on going from curve 2 to curve 5 is small and has a value of 42 mV for a tenfold increase of the number of active sites. This is less than the Tafel slope of FeTSPc, incorporated in polypyrrole (about -100 mV), which could be determined for curve 5, for instance. This points to a quasi-reversible reaction, because for a completely irreversible reaction (as for CoTSPc), the observed shift in half-wave potential for a tenfold increase of active sites should be equal and not less to the Tafel slope.

When the same calculation model is applied to adsorbed FeTSPc in comparison with FeTSPc, incorporated in polypyrrole, then from the difference of about 170 mV for the half-wave potentials of curve 1 (i.e. the adsorbed layer with $1.1 \times 10^{-10} \text{ mol cm}^{-2}$), and curve 3 (with coverage of $2.4 \times 10^{-10} \text{ mol cm}^{-2}$), a shift of 780 mV for a tenfold increase of the number of active sites could be determined. This leads to a very unlikely high value for the Tafel slope. So, the mechanism of dioxxygen reduction at FeTSPc, incorporated in polypyr-

role, must be different from that of the adsorbed layer. In this last case, in 0.05 M H_2SO_4 , the prewave has almost completely disappeared (curve 1). For FeTSPc/polypyrrole layers, this prewave reappears and this causes the considerable increase in activity.

We have argued that the "kinetic limitation", as observed for the prewave in basic media, is caused by the fact that there are only few dimers present on the surface [3]. The same arguments, applied here, lead to the conclusion that, in 0.05 M H_2SO_4 , FeTSPc is almost not present in the dimer form on the graphite surface. For FeTSPc/polypyrrole films two explanations are now possible:

1: The ratio of dimer to monomer species is the same as for FeTSPc, adsorbed on Cp. By increasing the amount of FeTSPc on the electrode via incorporation in polypyrrole, also the number of dimer sites increases and the prewave is reinforced.

2: The dimerization is favoured in polypyrrole, so relatively more dimers are present in FeTSPc/polypyrrole films, which also results in a stronger prewave.

A closer examination of figure 7.5 reveals that the results are in favour of the second explanation. For curve 2 (0.2 mC), a slightly higher activity is observed at low overpotential than for FeTSPc, adsorbed on graphite (curve 1), in spite of the lower coverage in the first case (0.8×10^{-10} compared with 1.1×10^{-10} mol cm^{-2}). In the potential region, where the second wave is dominant, the electrode prepared by adsorption acts as the more active electrode. This means that the prewave is relatively more important for FeTSPc, incorporated in polypyrrole; hence, in polypyrrole relatively more dimer sites of FeTSPc are present than in an adsorption layer.

In figure 7.7, the dioxygen reduction in 0.05 M H_2SO_4 is given as a function of the rotation frequency for a 1 mC FeTSPc/polypyrrole layer. For each rotation frequency a freshly prepared layer is used, because of the already mentioned rapid deactivation. As in the preceding experiments, again a high scan rate of 200 $mV s^{-1}$ is chosen to prevent a deactivation during the scan. The instability of the FeTSPc/polypyrrole film severely hampers the investigations, but it also gives a clue to the mechanism of dioxygen reduction. Electrodes prepared by irreversible adsorption of FeTSPc on graphite and electrodes covered with CoTSPc/polypyrrole layers show a greater stability. Therefore, it is the combination of FeTSPc and polypyrrole, which is the cause of the strong deactivation. If we realize that small configurational changes of the polymer are probably enough to destroy a dimer site, we can expect a rapid decrease in activity.

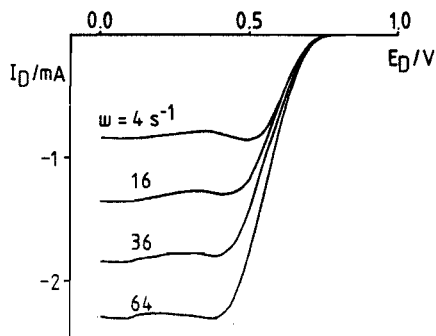


Fig. 7.7 Rotation frequency dependence of the dioxygen reduction at a 1 mC FeTSPc/polypyrrole layer. The different frequencies are given in the figure. Electrolyte: 0.05 M H_2SO_4 , dioxygen-saturated; scan rate: 200 mV s^{-1} .

From figure 7.7, a half-wave potential of about 570 mV can be determined for a 1 mC FeTSPc/polypyrrole layer. For the substrate, Cp (without catalysts), it is not possible to determine a half-wave potential under these conditions, but it can be argued that the half-wave potential must be below 0 V. In our view a catalyst which causes such a large increase in activity deserves some attention, and this justifies these experiments, notwithstanding the high instability of the layer.

The curves, depicted in figure 7.7, display almost no "kinetic limitation", which means that a 1 mC thick layer contains enough dimer sites to obtain a Levich diffusion behaviour [chapter 6 or ref. 3]. In figure 7.8, the rotation frequency dependence for FeTSPc, irreversibly adsorbed on Cp, is given. This shows again, if compared with figure 7.7, the almost complete lack of the prewave in the case of electrodes prepared by irreversible adsorption.

For a thin FeTSPc/polypyrrole layer (0.58 mC), the ring current has also been measured as a function of the disc potential. These results are given in figure 7.9. With a value of 0.145 for the collection efficiency, it follows that 84% of the dioxygen is reduced to hydrogen peroxide. As the layer thickness increases, also that part of the dioxygen, which is reduced to water, increases. Figure 7.5 shows a disc current of about 4 mA for a 15 mC FeTSPc/polypyrrole layer (curve 5). If it is assumed that the same ratio of water to hydrogen peroxide production is occurring as for the 0.58 mC layer, then a limiting current of 6.9 mA can be determined for the quantitative reduction of

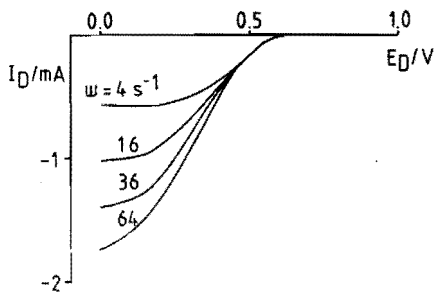


Fig. 7.8 Rotation frequency dependence of the dioxxygen reduction at FeTSPc, adsorbed on Cp. The different frequencies are given in the figure. Electrolyte: 0.05 M H_2SO_4 , dioxxygen-saturated; scan rate: 200 mV s^{-1} .

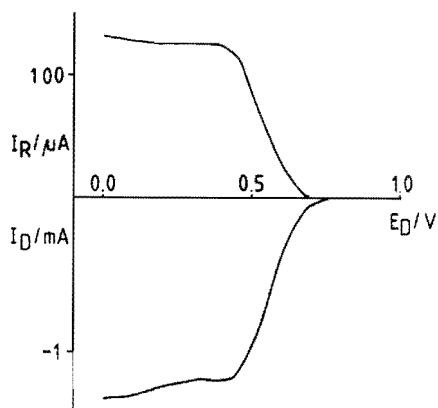


Fig. 7.9 Disc and ring current as a function of the disc potential for a 0.58 mC FeTSPc/polypyrrole layer. Electrolyte: 0.05 M H_2SO_4 , dioxxygen-saturated; scan rate: 200 mV s^{-1} ; rotation frequency: 64 s^{-1} .

dioxxygen to water. This value far exceeds the theoretical value of 5.2 mA, as can be calculated from the diffusion coefficient [12] and the solubility [13] of dioxxygen in 0.05 M H_2SO_4 . The difference between the values can only be explained by an increase in that part of the dioxxygen, which is reduced to water.

To present a complete treatment of the dioxxygen reduction on FeTSPc, incorporated in polypyrrole, in figure 7.10 some results obtained in 0.1 M KOH

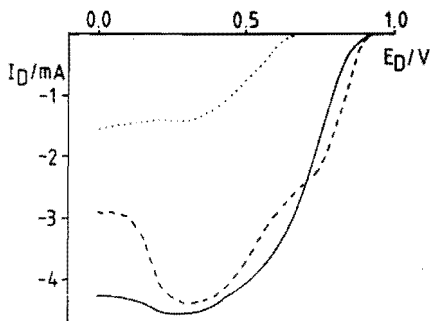


Fig. 7.10 Comparison between the dioxygen reduction at FeTSPc adsorbed on Cp, respectively, incorporated in polypyrrole and at polypyrrole itself in 0.1 M KOH. — 15 mC FeTSPc/polypyrrole; 30 mC polypyrrole; - - - - FeTSPc adsorbed on Cp; dioxygen-saturated electrolyte; scan rate: 50 mV s^{-1} ; rotation frequency: 64 s^{-1} .

are given, together with the results for FeTSPc, irreversibly adsorbed on Cp. For the FeTSPc/polypyrrole layer only one wave is observed. The higher activity of the adsorbed FeTSPc at low overpotential, compared with the vast amount of FeTSPc, incorporated in polypyrrole, is probably due to a limited conductivity of the polypyrrole layer. Perhaps, also the instability in alkaline media of polypyrrole itself, as reported by some authors [14], plays a role. Since the prewave and the main wave almost coincide in alkaline media, it is not expected that a more detailed study of the dioxygen reduction on FeTSPc/polypyrrole films in these media will give more insight into the mechanism of dioxygen reduction on FeTSPc.

7.4. Concluding remarks

We have given some evidence for a dioxygen reduction mechanism operating by dimers at FeTSPc, incorporated in polypyrrole. To prove this mechanism completely, more experiments are necessary. Currently, investigations are in progress to detect the postulated dimer species [see chapter 11]. With respect to the proposed mechanism, the dioxygen reduction behaviour of a di-iron phthalocyanine, analogous to the cofacial-dicobalt porphyrin complexes of Collman et al. [15], if possible to synthesize, would be interesting. The cofacial-dicobalt porphyrin complex gives reduction of dioxygen to water at relatively

low overpotential in acid media. Perhaps, the same results can be obtained for a comparable di-iron phthalocyanine complex.

7.5. References

1. J. Zagal, P. Bindra and E. Yeager, *J. Electrochem. Soc.* 127 (1980) 1506.
2. A. van der Putten, A. Elzing, W. Visscher and E. Barendrecht, *J. Electroanal. Chem.* 214 (1986) 523.
3. A. Elzing, A. van der Putten, W. Visscher and E. Barendrecht, *J. Electroanal. Chem.* 233 (1987) 113.
4. R.A. Bull, F.R. Fan and A.J. Bard, *J. Electrochem. Soc.* 131 (1984) 687.
5. M.I. Florit, W.E. O'Grady, C.A. Linkous, T. Skotheim and M. Rosenthal, Abstract N 415, Extended Abstracts, Vol. 84-1, The Electrochem. Soc. (1984).
6. A. Elzing, A. van der Putten, W. Visscher and E. Barendrecht, *J. Electroanal. Chem.* 200 (1986) 313.
7. J.H. Zagal-Moya, Thesis, Case Western Reserve University, Cleveland (1978).
8. J.H. Weber and D.H. Busch, *J. Inorg. Chem.* 4 (1965) 469.
9. A.F. Diaz, J.I. Castillo, J.A. Logan and W.Y. Lee, *J. Electroanal. Chem.* 129 (1981) 115.
10. A.F. Diaz and J.I. Castillo, *J. Chem. Soc. Chem. Commun.* (1980) 397.
11. C.P. Andrieux, J.M. Dumas-Bouchiat and J.M. Savéant, *J. Electroanal. Chem.* 131 (1982) 1.
12. K.E. Gubbins and R.D. Walker, Jr., *J. Electrochem. Soc.* 112 (1965) 469.
13. R.J. Millington, *Science* 122 (1955) 1090.
14. E.M. Genies and A.A. Syed, *Synth. Met.* 10 (1984) 21.
15. J.P. Collman, P. Denisevich, Y. Konai, M. Marrocco, C. Koval and F.C. Anson, *J. Am. Chem. Soc.* 102 (1980) 6027.

8. The electrocatalysis of dioxygen reduction in an acidic solution of iron tetrasulfonato-phthalocyanine

8.1. Introduction

Usually, to let occur catalysis the electrocatalyst is applied onto the electrode by irreversible adsorption, or vacuum deposition, or evaporation of the catalyst containing solvent, or some other procedure. Its behaviour is then studied in an electrolyte, free of the catalyst. When the catalyst is also dissolved in the electrolyte, it depends on the value of its diffusion coefficient whether the dissolved species contributes significantly to the total catalytic current. For instance, in the case of dioxygen, the major contribution to the reduction current will be the current due to the reduction of dioxygen on the immobilized catalyst molecules. For, because of the size of the involved dissolved catalyst molecules, its transport rate to the electrode is, compared to that of dioxygen, too slow to result in a considerable extra dioxygen reduction current [1,2,3].

Preliminary experiments in 0.05 M H_2SO_4 showed a difference in dioxygen reduction behaviour between FeTSPc, only irreversibly adsorbed onto a graphite surface, and FeTSPc, also dissolved (10^{-3} M) in the electrolyte. Thus, the ratio of the diffusion coefficients of dioxygen and the dissolved FeTSPc in 0.05 M H_2SO_4 is such, that the dissolved species contribute in a small, but noteworthy amount to the dioxygen reduction current.

The adsorbed FeTSPc species are predominantly monomer species [as was discussed in chapter 6 and 7], while dioxygen bridged dimers are present when FeTSPc is dissolved in 0.05 M H_2SO_4 [4]. Moreover, these two species could show a different catalytic activity. Thus, electrochemical measurements were carried out to investigate the role of dioxygen bridged FeTSPc dimers in the reduction mechanism of dioxygen, together with UV-Vis. spectroscopy to establish the species present in the applied potential range. Use was made of an Optical Transparent Thin Layer Cell (OTTLC), as described in chapter 4.

8.2. Results and discussion

8.2.1. (Spectro-)electrochemical measurements in a dinitrogen-saturated solution of FeTSPc

The voltammogram of dissolved FeTSPc (1.03×10^{-3} M in 0.05 M H_2SO_4 ,

dinitrogen-saturated) shows the onset of a cathodic reaction at $E < 0.8$ V, see figure 8.1. For these measurements a rotating electrode with a Cp-disc and a Pt-ring (A disc = 0.52 cm^{-2} , $N = 0.268$) was used, but qualitatively the same results were obtained for other disc and ring materials, as e.g. glassy carbon (Cg). It is obvious that dissolved FeTSPc takes part in the reaction because

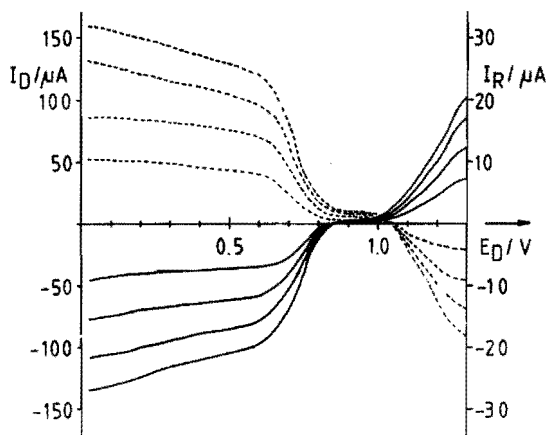


Fig. 8.1 I-E curves measured with a Pt/Cp (ring/disc) electrode in a dinitrogen-saturated solution of FeTSPc ($1.03 \times 10^{-3} \text{ M}$) at different rotation frequencies. The broken lines indicate the ring currents ($E_R = 0.93 \text{ V}$). Electrolyte: $0.05 \text{ M H}_2\text{SO}_4$. Rotation frequencies: 4, 16, 36 and 64 s^{-1} . Scan rate: 10 mV s^{-1} .

the disc current shows Levich behaviour. The ring current at $E_R = 0.93 \text{ V}$ reveals an almost quantitative back oxidation of the reduced species, produced at the disc. At disc potentials $E > 1.0 \text{ V}$, an oxidation reaction is observed, which is then accompanied by a back reduction at the ring at $E_R = 0.93 \text{ V}$.

The combined spectro-electrochemical investigations were carried out in an OTTLC. The cyclic voltammogram for the FeTSPc solution, as measured in this cell, is given in figure 8.2A. Thereafter, the solution was refreshed and spectra were recorded at fixed potentials after a rest time of about 3 min. at the O-marked potentials; in between these potentials a scan rate of 2 mV s^{-1} was applied. During the rest period of 3 min. the current gradually drops to zero as can be seen in figure 8.2B.

The spectra recorded during the cathodic scan at the O-denoted potentials in figure 8.2B (0.83; 0.63; 0.43 and 0.03 V), are given in figure 8.3. The

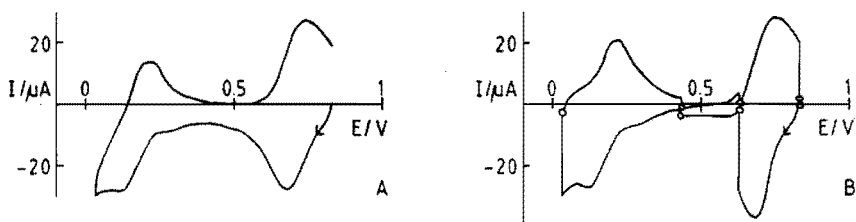


Fig. 8.2A Cyclic voltammogram measured in a dinitrogen-saturated solution of FeTSPc (1.03×10^{-3} M), with an optical transparent gold electrode in a thin layer cell (0.4 mm).

B As A; however, at the potentials indicated with a circle a rest time of 3 min. was applied, thereafter a spectrum was recorded (see figure 8.3) before the potential scan was continued.

For both: scan rate 2 mV s^{-1} ; electrolyte $0.05 \text{ M H}_2\text{SO}_4$.

spectrum recorded at 0.43 V is omitted, because it does not differ significantly from the spectrum recorded at 0.63 V. At $E_D = 0.83 \text{ V}$ (i.e. the potential at zero current, see figure 8.1) a spectrum is observed with a main absorption at 637 nm and a shoulder at 670 nm. In the UV-range of the spectrum, a peak is observed at 330 nm. The peak at 637 nm is close to the absorption wavelengths reported for a dioxygen bridged FeTSPc dimer (632 nm) and a Fe(III)TSPc species (635 nm) [chapter 2]. After having maintained the potential for 3 min. at 0.63 V, the peak at 637 nm has decreased, while the peaks at 670 and 330 nm have increased, resulting in a spectrum with two peaks (637 and 670 nm) of approximately the same height. The peak at 670 nm, which can be attributed to Fe(II)TSPc [chapter 2], shows a little shoulder at 700 nm.

When the potential is set at 0.03 V, i.e. more cathodic than the redox peak at about 0.2 V (figure 8.2), the absorption peaks disappear and two new ones at 470 and 270 nm appear. These last peaks can be attributed to Fe(I)TSPc [see chapter 2].

After this cathodic scan spectra are recorded during an anodic scan from 0.03 V to 0.83 V and they are given in figure 8.4. The spectra at 0.43 V and 0.63 V are again very similar. In contrast with the spectra taken during the cathodic scan, the spectrum at 0.63 V now consists of one main peak at 670 nm in the wavelength range between 600 and 800 nm. The peak at 637 nm has disappeared. Therefore, it must be concluded that after reduction of Fe(II)TSPc

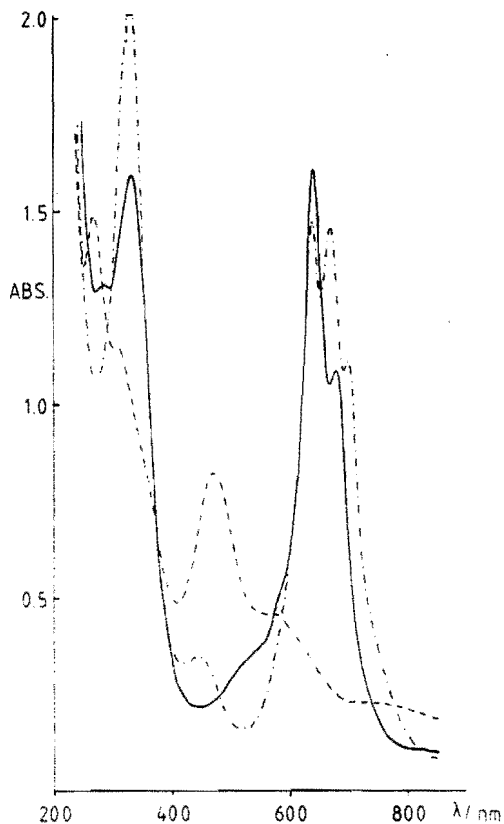


Fig. 8.3 Spectra recorded during the cathodic scan from 0.83 to 0.03 V, using the same cell and solution as in figure 8.2. — spectrum at 0.83 V, -.-.- spectrum at 0.63 V and ---- spectrum at 0.03 V. (All spectra are recorded after a rest time of 3 min. at the applied potential).

to Fe(I)TSPc an existing oxygen bridged dimer (both μ -oxo and μ -peroxo complexes are possible) dissociates, and the back oxidation to the second valence state results in a free Fe(II)TSPc monomer molecule.

After this series, the solution was refreshed and the potential was then raised from 0.83 V to higher values. Figure 8.5 shows the cyclic voltammogram and figure 8.6 gives the recorded spectra. The spectra show an oxidation of the metal chelate, but also a decrease in the intensity of the absorption bands. After having maintained the potential at 1.23 V for 3 min., a spectrum

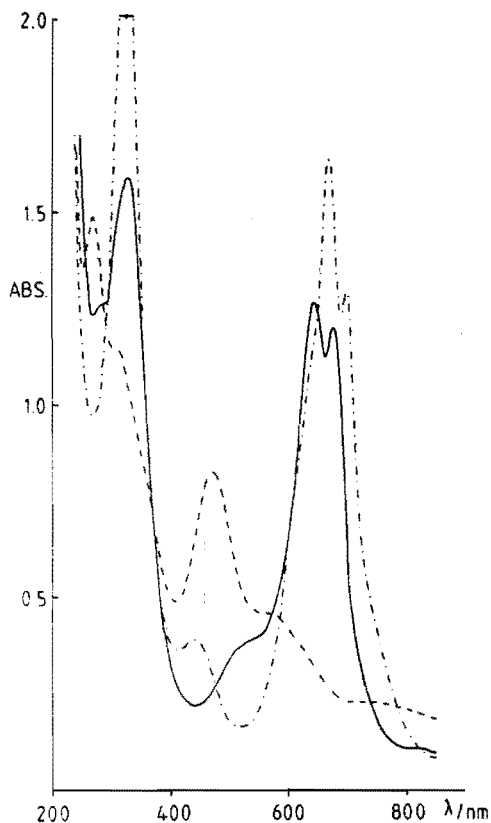


Fig. 8.4 Spectra recorded during the anodic scan from 0.03 to 0.83 V, using the same cell and solution as in figure 8.2. — spectrum at 0.83 V, -.- spectrum at 0.63 V and -.-.- spectrum at 0.03 V. (All spectra are recorded after a rest time of 3 min at the applied potential).

is recorded, which is not characteristic for Fe(III)TSPc, but must be attributed to Fe(IV)TSPc or Fe(III)TSPc⁺: in general, it is very difficult to assign the location of the charge to either the metal or the organic ring structure. When in this chapter Fe(IV)TSPc is written, then also the possible oxidation of the ligand is included. Lowering of the potential to 0.83 V again, leads to a spectrum with an absorption peak at 637 nm; however, also a drastic decrease in intensity is observed. Surprisingly, it was not possible, by further lowering of the potential, to re-obtain the spectrum of Fe(II)TSPc.

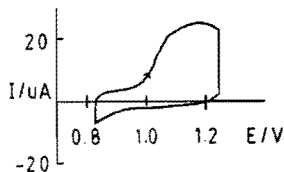


Fig. 8.5 Cyclic voltammogram under the same conditions as in figure 8.2, but now measured in the anodic potential region.

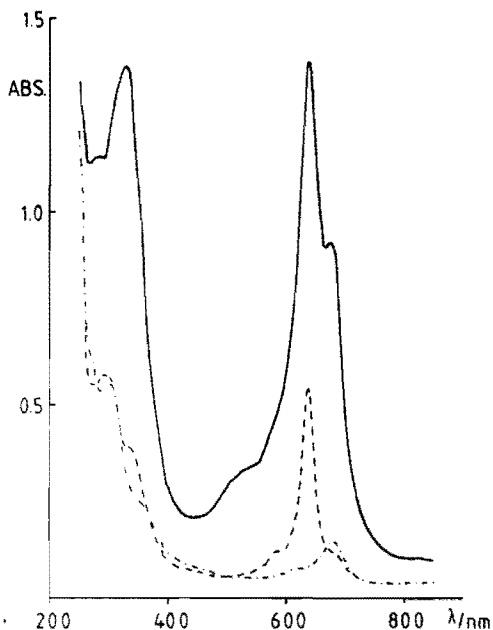
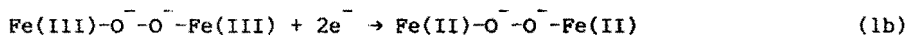
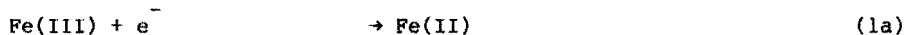


Fig. 8.6 The spectral change caused by keeping the potential at 1.23 V for 3 min. Curves — and ---- were both recorded at 0.83 V, respectively, before and after having maintained the potential at 1.23 V for 3 min.; -.- recorded at 1.23 V after 3 min. at this potential.

Bottomley et al. [5] reported that a μ -oxo bridged Fe(III)-phthalocyanine dimer ($\text{Fe(III)-O}^{2-}\text{-Fe(III)}$), dissolved in pyridine, is reduced at a lower potential than the free Fe(III)Pc monomer and that only one of the two Fe(III) ions is reduced to Fe(II). Analogously, we propose that the spectrum at 0.83 V

(obtained after oxidation at 1.23 V) can be attributed to a μ -oxo bridged dimer, which cannot be reduced at the potential where Fe(III)TSPc is converted to Fe(II)TSPc. Due to the oxidation at 1.23 V all FeTSPc species, except the μ -oxo bridged species, are decomposed and the spectrum at 0.83 V should be solely due to the absorption of the μ -oxo species.

From the above given observations the following total picture of dissolved FeTSPc is proposed. In a solution of FeTSPc, part of the compound is present as μ -oxo dimers, in spite of the saturation with dinitrogen; even after saturation with helium, purified from traces of dioxygen, the μ -oxo dimer is demonstrable. From the absorption spectra, it is concluded that about 30% of the FeTSPc is present in the μ -oxo form. The rest of the FeTSPc is present as free Fe(III)TSPc molecules or as μ -peroxo dimers (Fe(III)-O⁻-O⁻-Fe(III)). At potentials below 0.8 V, these last two species are reduced as follows (in the equations Fe(III) stands for Fe(III)TSPc, and so on):



If a one-electron reduction of Fe(III)TSPc (reaction (1a)) is assumed, then a diffusion coefficient of $3 \times 10^{-6} \text{ cm}^2 \text{ s}^{-1}$ is calculated from the obtained limiting disc currents (see figure 8.1) for the Fe(III)TSPc molecule. For this calculation the concentration ($1.03 \times 10^{-3} \text{ M FeTSPc}$) is lowered by the part, which is in the not-reducible μ -oxo form (about 30%). This value of the diffusion coefficient agrees reasonably with the values reported for other metal chelates of comparable dimensions [6,7]. When the second reaction (1b) is supposed to occur, then, of course, the same value for the diffusion coefficient is calculated for the dimer species. From this, it can be concluded that most of the FeTSPc is present as free Fe(III)TSPc molecules, because otherwise the calculation should result in a much smaller diffusion coefficient. Thus, reaction (1b) is occurring to a small or negligible extent.

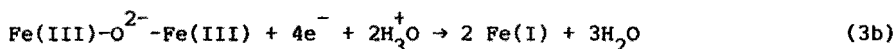
The ring currents of figure 8.1 reveal an almost quantitative back oxidation (85%).



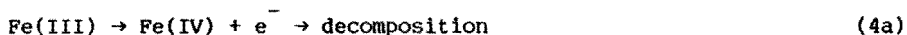
The second reduction process, only clearly observed in the cyclic voltammogram measured in the thin layer cell, is ascribed to the following reduction:



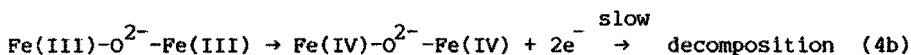
At potentials below 0.2 V, also the μ -oxo dimer is slowly reduced:



Oxidation of the solution leads to decomposition of most FeTSPc molecules as can be concluded from the spectra in figure 8.6 (to what and how is not known):



An oxidation of the μ -oxo bridged dimer is also observed (see figure 8.6); however, the oxidized μ -oxo species is more stable towards decomposition:



After having maintained the potential at 1.23 V for 3 min., the μ -oxo species is the only FeTSPc containing species left in the solution, as can be concluded from the absence of a spectral change, when the potential is lowered from 0.83 V to 0.63 V.

When the decomposition of most of the FeTSPc molecules is nearly completed, there is only a minor change in the redox peak observed at about 0.7 V, while the redox peak at about 0.3 V has almost completely disappeared. The explanation for this is that Fe(III)TSPc is reduced to Fe(II)TSPc close to the potentials where also Fe(III) ions are reduced to Fe(II) ions. This was verified by measuring this last reduction in an acidic solution (0.05 M H_2SO_4) of $\text{Fe}_2(\text{SO}_4)_3$. Contrary to FeTSPc, no reduction of Fe(II) ions to Fe(I) ions is observed. Thus, after decomposition of the FeTSPc, the redox peak at 0.3 V (Fe(II)TSPc \rightarrow Fe(I)TSPc) must have disappeared also.

The statement that the μ -oxo dimer is not reduced at the same potential as Fe(III)TSPc, but only at potentials below 0.2 V, while simultaneously dissociation into Fe(I)TSPc and water occurs, could be proved as follows. In figure 8.7, the oxidation peak due to the conversion of Fe(II)TSPc to Fe(III)TSPc, realized in the thin layer cell, is given. The same figure shows that after having maintained the potential at 0.03 V for 3 min., the area under the

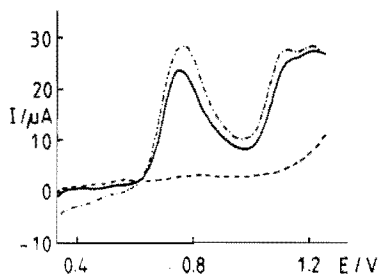


Fig. 8.7 Comparison between the oxidation peak observed for the conversion of Fe(II)TSPc into Fe(III)TSPc before — and after -.-.- having maintained the potential at 0.03 V for 3 min. Curve ----- obtained without FeTSPc present in the electrolyte. Electrolyte: 0.05 M H_2SO_4 , dinitrogen-saturated. Concentration FeTSPc: 1.03×10^{-3} M. Scan rate: 2 mV s^{-1} .

peak has increased. This increase indicates that, at a potential of 0.03 V, μ -oxo dimers dissociate into free FeTSPc molecules. From this increase of the area under the peak a value of 20% was calculated for the amount of the FeTSPc, which is originally present in the μ -oxo form.

8.2.2. (Spectro-)electrochemical measurements in a dioxygen-saturated solution of FeTSPc

The same solution, as used in the previous section, is now saturated with dioxygen and the potential and rotation frequency dependence of the dioxygen reduction is measured (see figure 8.8). At disc potentials higher than 0.7 V, the disc currents have the same shapes and values as those observed in the case of the dinitrogen-saturated solution (compare the inset of this figure with figure 8.1). Thus, in this potential domain, the same species is reduced as in the dinitrogen-saturated solution (Fe(III)TSPc, see section 8.2.1.).

Closer examination of the figure shows, however, the remarkable effect that the disc currents at the various rotation frequencies cross each other. For low rotation rates, the disc currents at potentials slightly more cathodic than 0.6 V are higher than for high rotation rates, despite of the higher dioxygen transport rate in the last case. The effect is small, but it was observed also at other electrode materials such as glassy carbon (Cg) and gold, and should thus be considered as significant.

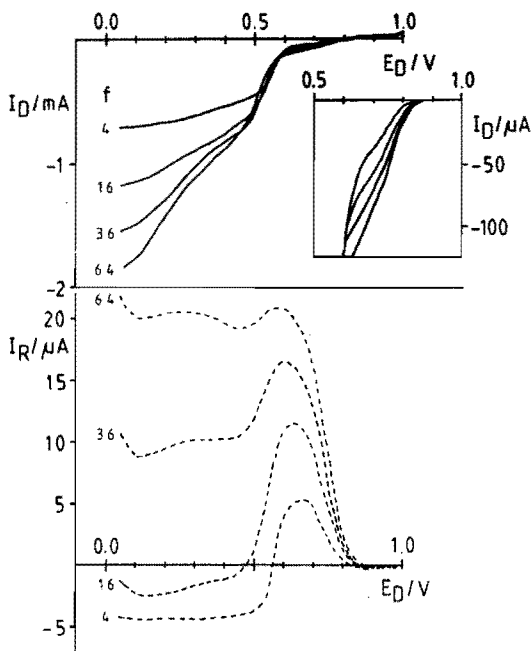


Fig. 8.8 I-E curves measured with a Pt/Cp (ring/disc) electrode in a dioxxygen-saturated solution of FeTSPc (1.03×10^{-3} M) at different rotation rates (4, 16, 36 and 64 s^{-1}). The broken lines indicate the ring current at $E_R = 0.93$ V. The inset of the figure shows I_D with a higher sensitivity for potentials above 0.6 V. Electrolyte: $0.05 \text{ M H}_2\text{SO}_4$. Scan rate: 10 mV s^{-1} .

For high rotation rates, the ring current (at $E_R = 0.93$ V) reaches a plateau with about the same height as in the dinitrogen-saturated solution, while for lower rotation rates, the positive ring current shows an increasingly pronounced maximum when measured as a function of the disc potential and even becomes negative at more cathodic disc potentials. This indicates that, especially at low rotation rates, dioxxygen reacts to a product which on arrival at the ring is reduced instead of oxidized. The reaction at the disc causes a higher disc current at low rotation rates than at higher rotation rates; see below for the possible product formed at the disc.

The catalytic effect due to the dissolved FeTSPc species is demonstrated in figure 8.9. The dissolved species cause a shift of the reduction wave of

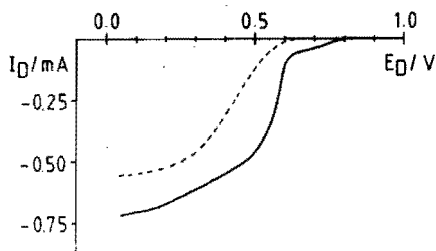


Fig. 8.9 Dioxygen reduction at FeTSPc adsorbed on a Cp-disc electrode. Curve —: solution with 1.03×10^{-3} M FeTSPc; ----: solution without FeTSPc. Electrolyte: 0.05 M H_2SO_4 , dioxygen-saturated. Rotation frequency: 4 s^{-1} . Scan rate: 10 mV s^{-1} .

dioxygen to a higher potential and the curve is more steep than the curve, observed for only immobilized catalyst molecules.

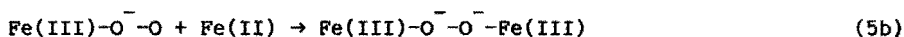
The spectrum observed at 0.83 V is almost equal to the corresponding spectrum recorded in the dinitrogen-saturated solution. This can be explained by the lack of interaction between Fe(III)TSPc and dioxygen. Also the μ -oxo species does not react with dioxygen.

The spectra recorded at other potentials show only minor changes with respect to the corresponding ones in the dioxygen-free solution. After holding the potential at 0.63 V or lower for 3 min., most of the dioxygen is also reduced (probably to hydrogen peroxide) with as a result that the spectra resemble those of the dioxygen-free solution. Perhaps, hydrogen peroxide slowly oxidizes Fe(II)TSPc to Fe(III)TSPc (or even Fe(IV)TSPc), but this species is converted back to Fe(II)TSPc at the gold electrode. It must be stressed that the invariability of the spectra upon the introduction of dioxygen, does not include that there is no interaction between dioxygen and Fe(II)TSPc or Fe(I)TSPc. In this experiment, we observe no reaction because the dioxygen is reduced at the metal chelate (or the gold electrode) and the metal chelate returns to the divalent or the monovalent oxidation state, depending on the applied potential of the gold electrode.

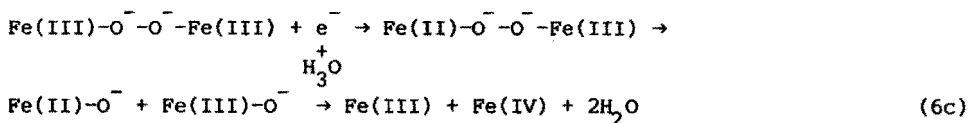
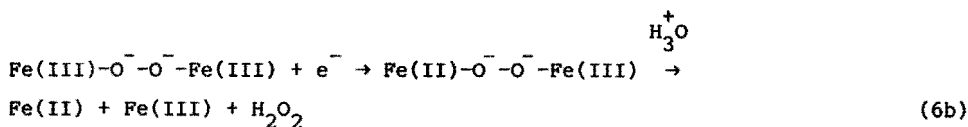
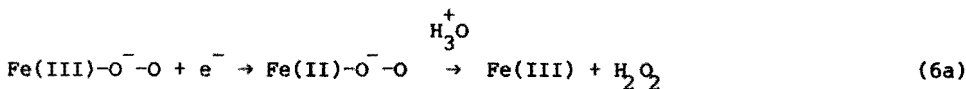
The following total picture is proposed: in the stagnant diffusion layer at the disc electrode, dioxygen reacts with Fe(II)TSPc. The following reaction scheme is proposed (TSPc is omitted in the equations):



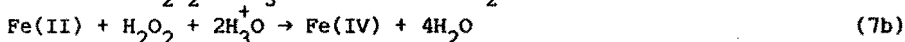
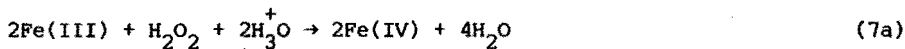
Even a μ -peroxo bridged dimer can be formed, as it has been reported that dioxygen reacts with Fe(II)TSPc in the ratio 1 to 2 [4].



At potentials below 0.6 V, probably (further) reduction of the dioxygen adducts occurs:



Also, a reaction with the produced hydrogen peroxide is possible:



For high rotation rates, the diffusion layer is so thin that the transport time for the species from the disc to the ring becomes too short for reaction (5) to (7) to occur appreciably and this explains why, at low rotation rates, the disc current is higher than at higher rotation rates. The decrease of the ring current is a logical consequence. The reaction of Fe(II)TSPc with dioxygen and the consecutive reactions (6 a,b,c) lead to a considerable reduction of the Fe(II)TSPc concentration and, therefore, the ring current decreases. The resulting Fe(III)TSPc species cannot be reduced at the applied ring potential ($E_R = 0.93$ V). To explain that the ring current becomes even negative for low rotation rates, higher oxidation states must be considered, so therefore, reactions (6c) and (7) are added to the reaction scheme.

To verify the above given reaction scheme, it was investigated whether

hydrogen peroxide was produced. For detection of this compound, the ring was platinized and a ring potential of 1.23 V was applied. At this potential, hydrogen peroxide is oxidized to dioxygen. In figure 8.10, the increase of the disc current is accompanied with also an increase in the ring current. It can be concluded that a great part of the dioxygen is reduced to hydrogen peroxide.

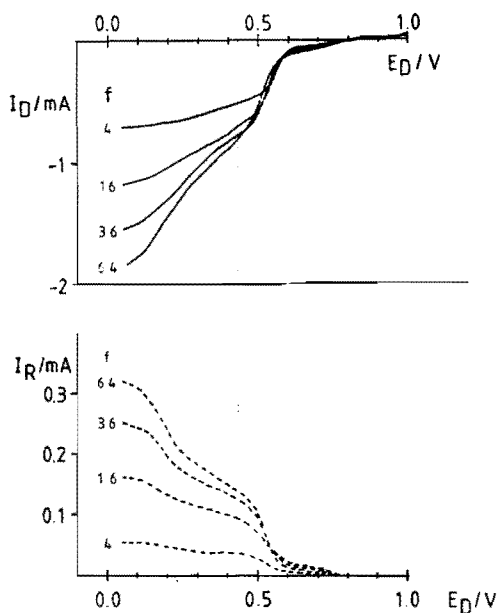


Fig. 8.10 I-E curves under the same conditions as in figure 8.8; however, the ring is now platinized and its potential is raised to 1.23 V.

Even a greater hydrogen peroxide production than could be determined from the ring current may be assumed, because in this solution (1.03×10^{-3} M FeTSPc) a rapid deactivation of the platinized ring for hydrogen peroxide oxidation is observed. Therefore, the measured ring current cannot be considered as an indication of dioxygen reduction directly to water.

To identify the species, which are reduced at the ring for low rotation rates, the potential dependence of the ring current was investigated for a constant disc potential of about 400 mV. Platinum was not used as ring electrode material because of the possibility of dioxygen reduction at a relatively high potential (about 0.9 V). Therefore, a Cg-ring/Cg-disc electrode was used with the following specifications: $A = 0.8 \text{ cm}^2$, $N = 0.374$ and $S = 0.627$. When the experiment of figure 8.8 was repeated with this electrode, it turned

out that the results were about the same as for the Pt-ring/Cp-disc electrode (see figure 8.11).

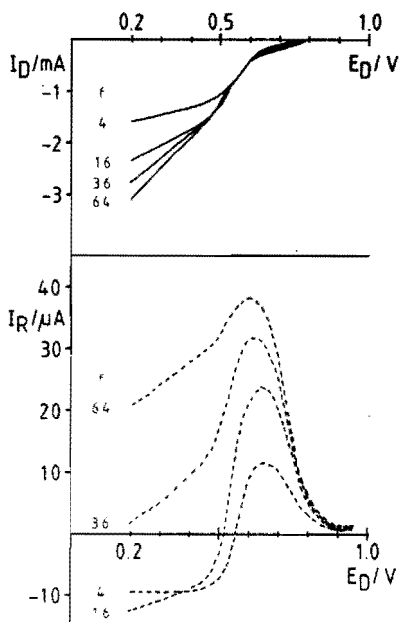


Fig. 8.11 I-E curves measured with a Cg/Cg (ring/disc) electrode in a dioxygen-saturated solution of FeTSPc (1.03×10^{-3} M) at different rotation rates (4, 16, 36 and $64 s^{-1}$). The broken lines indicate the ring current at $E_R = 0.93$ V. Electrolyte: 0.05 M H_2SO_4 . Scan rate: $10 mV s^{-1}$.

Now, the ring current is measured as a function of the ring potential for three different disc potentials (0.93, 0.63 and 0.43 V). The results are given in the figures 8.12, 8.13 and 8.14, respectively. At the disc potential of 0.93 V no reaction occurs: so, figure 8.12 can only represent the reduction and oxidation of species already present in the solution. In figure 8.13, recorded at a disc potential of 0.63 V (where only Fe(III)TSPc is reduced), we observed an increased ring oxidation current at potentials higher than 0.8 V. To obtain the right picture of the i-E curves for the new species (produced at the disc and reacting at the ring), the curves of figure 8.12 should be subtracted from those of figure 8.13. Thereby, of course, the shielding of the ring by the disc must be taken into account. The Fe(III)TSPc species, reduced

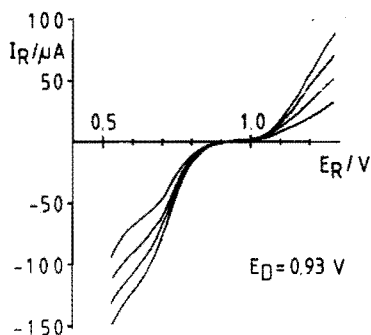


Fig. 8.12 I_R - E_R curves measured with a Cg/Cg (ring/disc) electrode for constant disc potential ($E_D = 0.93$ V) at the rotation frequency: 4, 16, 36 and 64 s^{-1} . Electrolyte: 0.05 M H_2SO_4 with 1.03×10^{-3} M FeTSPc, dioxygen-saturated. Scan rate: 2 $mV s^{-1}$.

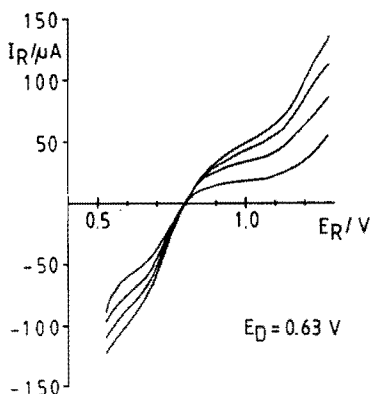


Fig. 8.13 I_R - E_R curves as in figure 8.12; however, $E_D = 0.63$ V.

at the disc ($E_D = 0.63$ V), can, of course, not be reduced at the ring too. This means that at a ring potential of 0.63 V, the cathodic ring current will be less, due to the same reaction at the disc. The shielding factor, S , of a Rotating Ring Disc Electrode is defined only for diffusion limited ring and disc currents. However, the figures (8.12, 8.13 and 8.14) clearly show that in this case no diffusion limited currents are observed. The shielding effect is, therefore, calculated by taking the ratio of the ring current at $E_R = 0.63$ V, observed for $E_D = 0.63$ V, and the ring current at the same potential, but for

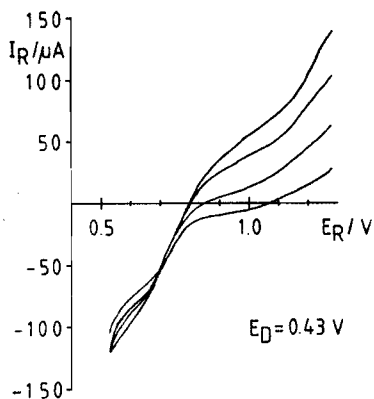


Fig. 8.14 I_R - E_R curves as in figure 8.12; however, $E_D = 0.43$ V.

$E_D = 0.93$ V. At this ring potential, the oxidation process, belonging to the reduction process at the disc for $E_D = 0.63$ V, will not give a significant contribution to the ring current. The calculated S' -value (the shielding calculated with our adapted definition is denoted as S') varies now from 0.79 for the highest to 0.86 for the lowest rotation frequency; these values were used for compensating the total cathodic part of figure 8.12. When, after this compensation procedure, the curves of figure 8.12 are subtracted from those of figure 8.13, the true i - E curves for back oxidation of the disc product(s) remain. In the resulting figure 8.15, we see that the oxidation starts at about 0.6 V with a half-wave potential of about 0.8 V. Moreover, it can be concluded that the species, reduced at the disc (half-wave potential 0.73 V), is almost reversibly oxidized back at the ring (half-wave potential 0.85 V).

Figure 8.16 is the result of the subtraction of the curves of figure 8.12 from those of figure 8.14 ($E_D = 0.43$ V). For high rotation frequencies, curves are observed, which are comparable to those of figure 8.15. For this rotation rates, the time of transport through the diffusion layer at the disc is so short that reactions (5) and (7) cannot occur to an appreciable extent. However, for low rotation frequencies a negative ring current is observed. From about 1.1 V to more negative ring potentials a small reduction wave is observed, but even at higher potentials the current is already negative. This reduction wave can be attributed to the back reduction of Fe(IV)TSPc to Fe(III)TSPc. For comparison, see also figures 8.1, 8.5 and 8.6, where the oxidation of Fe(III)TSPc to Fe(IV)TSPc is studied. The ring current at $\omega = 4$ is negative for ring potentials above 1.1 V, because the amount of FeTSPc, which

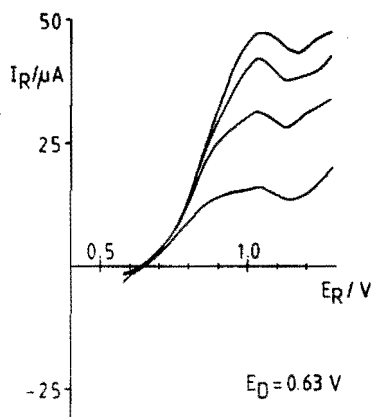


Fig. 8.15 I_R - E_R curves for $E_D = 0.63$ V, corrected for species already present in the solution; i.e. this figure is obtained by subtraction of the curves of figure 8.12 from those of figure 8.13.

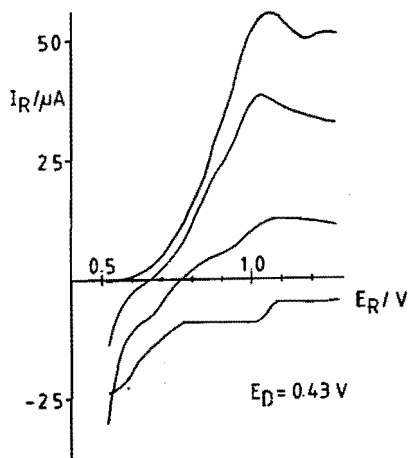


Fig. 8.16 I_R - E_R curves for $E_D = 0.43$ V, corrected for species already present in the solution; i.e. this figure is obtained by subtraction of the curves of figure 8.12 from those of figure 8.14.

is converted into Fe(IV)TSPc due to the reactions at the disc ($E_D = 0.43$ V), leads to a decrease in the ring current, observed for the oxidation of Fe(III)TSPc, at high ring potential. So, after the subtraction, a negative

ring current results also for potentials above 1.1 V. At lower potentials (E_R below 0.8 V) a reduction of Fe(III)TSPc, produced at the disc by reactions (6a, b and c) is observed (see figure 8.16).

So, from the investigations of the ring current as a function of the ring potential, it can be concluded that indeed the species Fe(III)TSPc and Fe(IV)-TSPc, as proposed products of the reactions (6a, b and c), must be present in the solution.

It is not easy to predict the relative importance of the reactions (5) to (7). One of the two reactions (5a) or (5b), and also (6a) or (6b), must occur to account for the increased hydrogen peroxide production. Reaction (5b) is given, because it is known from dioxygen uptake measurements that two Fe(II)-TSPc molecules react with one dioxygen molecule [4]. Reaction (7b) would require a relatively fast reaction of hydrogen peroxide with Fe(II)TSPc. From spectroscopic measurements, we know that acidic solutions of Fe(II)TSPc (and also Fe(III)TSPc) react with hydrogen peroxide to form Fe(IV)TSPc, however, a fast reaction is not so likely because hydrogen peroxide is not reduced to water by adsorbed Fe(II)TSPc [see chapter 2]. Also, the considerable amount of hydrogen peroxide, produced at a high overpotential for the rotation frequency of 64 s^{-1} (see figure 8.10), does not lead to a decrease of the ring current due to Fe(II)TSPc oxidation (see figure 8.8). In figure 8.9, the curve recorded in the case of FeTSPc, also dissolved in the solution, is somewhat more steep than without dissolved FeTSPc. This suggests that a different dioxygen reduction mechanism occurs on FeTSPc dissolved in solution, compared with that on adsorbed FeTSPc. Perhaps, the dimer species $(\text{Fe(III)-O}^-\text{-O}^-\text{-Fe(III)})$ of reactions (5b, 6b and 6c) results in a somewhat more reversible dioxygen reduction reaction.

8.3. Concluding remarks

Combined spectro- and electrochemical investigations show that in an acidic solution FeTSPc is mainly present in the third valence state (Fe(III)TSPc). Beside this species, a μ -oxo bridged dimer $(\text{Fe(III)-O}^{2-}\text{-Fe(III)})$ is detected (about 30%). After reduction of Fe(III)TSPc to Fe(II)TSPc a dioxygen adduct is formed. At lower potential (0.5 V), this adduct undergoes a one-electron reduction, and hydrogen peroxide together with Fe(III)TSPc is produced.

Experiments also show that the μ -oxo bridged dimer is only reduced (and dissociated) at potentials below 0.43 V. From this, it can be concluded that the formation of the μ -oxo adduct will block the dioxygen reduction. During

the reduction of dioxygen the splitting of the oxygen-oxygen bond is necessary to obtain water, as the desired reduction product. However, there is a chance that this bond splitting results in the formation of the μ -oxo adduct, which will block the catalyst site for the adsorption and reduction of a next dioxygen molecule.

Perhaps, also μ -peroxo dimers are formed from Fe(II)TSPc and dioxygen. All FeTSPc species, proposed in this chapter, are given in figure 8.17. The potential domains, in which these species could exist, are also indicated in the figure.

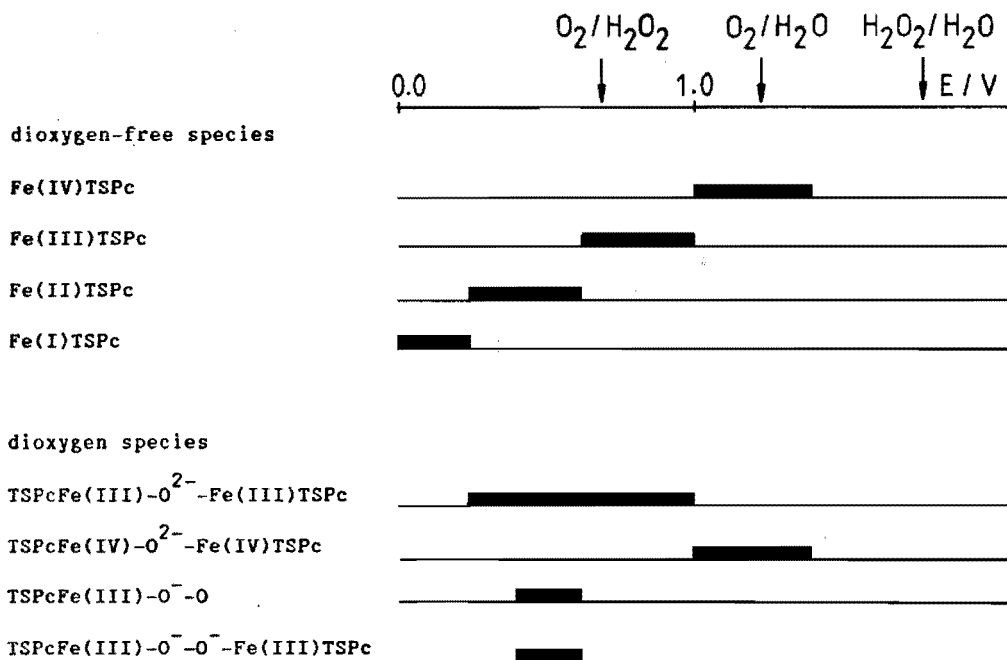


Fig. 8.17 The proposed FeTSPc species and their potential domains in 0.05 M H_2SO_4 .

The reduction current curves are, for FeTSPc also dissolved in the solution, more steep than without dissolved FeTSPc, suggesting that the μ -peroxo dimers possess a higher catalytic activity than the adsorbed FeTSPc monomers. In some of these μ -peroxo species the dioxygen bond is broken after the reduction, with as a result that water and Fe(IV)TSPc are produced.

8.4. References

1. N. Kobayashi and T. Osa, *J. Electroanal. Chem.* 157 (1983) 269.
2. P.A. Forshey and T. Kuwana, *Inorg. Chem.* 22 (1983) 699.
3. J.H. Zagal-Moya, Thesis, Case Western Reserve University, Cleveland (1978).
4. D. Vonderschmitt, K. Bernauer and S. Fallab, *Helv. Chim. Acta* 48 (1965) 951.
5. L.A. Bottomley, C. Ercolani, J-N. Gorce, G. Pennesi and G. Rossi, *Inorg. Chem.* 25 (1986) 2338.
6. C.L. Ni and F.C. Anson, *Inorg. Chem.* 24 (1985) 4754.
7. P.A. Forshey, T. Kuwana, N. Kobayashi and T. Osa, *Adv. Chem. Ser.* 201 (1982) 601.

9. Polarography of dioxygen in solutions of metal tetrasulfonato-phthalocyanines

9.1. Introduction

In this chapter, the results of a polarographic study of the catalytical behaviour of cobalt- and iron tetrasulfonato-phthalocyanine (Co- and FeTSPc), with respect to the dioxygen reduction, are described. Though mercury will never be used in a practical fuel cell system, polarography gives us an extra opportunity to the RRDE technique [used in chapter 8] to study the behaviour of these dissolved catalysts.

First, the dioxygen reduction behaviour on mercury is compared with that observed on a graphite (Cp) surface with and without Co- or FeTSPc, deposited on it. Secondly, the influence of Co- and FeTSPc, dissolved in the electrolyte (0.05 M H₂SO₄ or 0.1 M KOH), on the dioxygen reduction at mercury is studied.

9.2. Results and discussion

9.2.1. Dioxygen reduction on mercury

The polarographic equipment, as described in chapter 4, is used, with a drop time of 1 s and a scan rate of 10 mV s⁻¹. Figure 9.1 shows a typical result, obtained in a dioxygen-saturated 0.1 M KOH solution, for the dioxygen reduction on mercury. [In contrast as done in previous chapters, all figures of this chapter show the cathodic current depicted in the positive vertical direction, as usual in polarography].

Although for the measurements a Saturated Calomel Electrode (SCE) is used as a reference electrode, all potentials are quoted here vs. a Reversible Hydrogen Electrode (RHE) ($E_{\text{SCE}} = 1.020 \text{ V (RHE)}$ for 0.1 M KOH). The polarogram of figure 9.1 is recorded with 0.005% gelatin added to the electrolyte to suppress the polarographic maximum [1,2].

In figure 9.1, also the i - E curves observed for the dioxygen reduction at a Rotating pyrolytic graphite (Cp) Disc Electrode are given, with and without the adsorbed catalysts: Co- and FeTSPc. The method to obtain these results is described in chapter 6, where the catalytical activity of Cp electrodes, with and without adsorbed metal chelates, is studied. The results, given in chapter 6, are obtained in 1 M KOH, while here 0.1 M KOH is used; in principal the

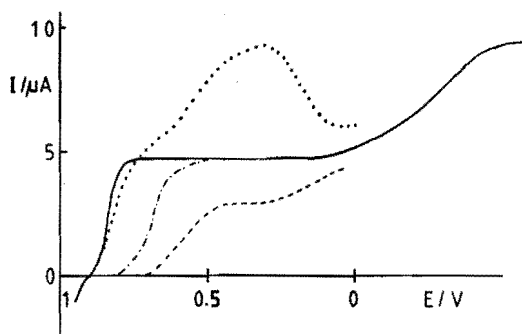


Fig. 9.1 The dioxygen reduction in 0.1 M KOH on mercury (—) and on modified graphite surfaces. The latter curves are obtained with a RDE and are normalized as described in the text. - - - - : Cp; .-. . : Cp with adsorbed CoTSPc; and : Cp with adsorbed FeTSPc.

same behaviour is found in both electrolytes. The results of figure 9.1 for Co- and FeTSPc, adsorbed on Cp, refer to a monolayer coverage (1.4×10^{-10} mol cm⁻²) of the graphite surface by the metal chelates. In order to facilitate the comparison, the disc current observed for CoTSPc, adsorbed on Cp, is normalized such that the limiting disc current is equal to the current plateau in the polarogram. This is allowed because both surfaces show a dioxygen transport limited current for the reaction of dioxygen to hydrogen peroxide [chapter 6 and ref. 3,4,5]. The *i*-*E* curves for Cp and Cp with adsorbed FeTSPc are normalized in the same way but now in relation to the normalized current for CoTSPc, adsorbed on Cp. The value of the rotation frequency is not relevant as long as only results obtained at the same rotation frequency (domain: 0-64 s⁻¹) are used for the three different surface modified RDE's. The limiting current for FeTSPc, adsorbed on Cp, is about twice that of CoTSPc because dioxygen reduction now leads to water as product [chapter 6].

The figure clearly demonstrates that bare graphite is far less active towards dioxygen reduction than mercury. Depositing a monolayer of a catalyst like CoTSPc on graphite increases its activity but the activity of mercury is not equalled. For FeTSPc, adsorbed on Cp, the onset of the *i*-*E* curve is at about the same potential as for mercury. But, contrary to mercury, the adsorbed FeTSPc gives water as reduction product for both observable waves.

For mercury, often a dioxygen reduction mechanism is proposed in which first dioxygen is reduced to a superoxide ion (O₂⁻) in an outer-Helmholtz-layer reaction. Hereafter, an irreversible formation of hydrogen peroxide

occurs [7]. The outer-Helmholtz-layer reaction is supposed to be reversible and independent of the electrode surface material [7,8] and it is, therefore, striking to see at graphite a reaction at a much higher overpotential than this outer-Helmholtz-layer reaction. This marked phenomenon was also pointed out by McIntyre et al. [9], who studied the dioxygen reduction on a special kind of graphite (the basal plane of stress annealed pyrolytic graphite, abbreviated: BP of SA-Cp) in acetonitrile. To account for this behaviour, they proposed that the superoxide ion adsorbs on the graphite surface and that it is somehow stabilized on this surface, with the result that the dioxygen reduction is deactivated. By applying a catalyst to the graphite surface, the "inhibition" is partly removed and a dioxygen reduction curve more similar to that on mercury is observed. According to Sawyer et al. [7], a search for a better catalyst would be a futile enterprise if the dioxygen reduction mechanism is such that first the superoxide ion is produced. However, this does not hold for graphite, because here it can be investigated which catalyst is most effective in the removal of the "inhibition".

In an acidic solution (0.05 M H_2SO_4) a similar behaviour is found for the different surfaces, see figure 9.2 ($E_{\text{SCE}} = 0.33 \text{ V (RHE)}$ in 0.05 M H_2SO_4). The current plateau of the polarogram is now higher than that measured in

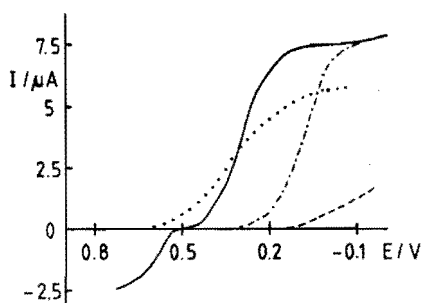


Fig. 9.2 Comparison between the dioxygen reduction in 0.05 M H_2SO_4 on mercury and on modified graphite surfaces. The same notation as in figure 9.1 is used.

alkaline solution, because of the greater diffusion coefficient of dioxygen in 0.05 M H_2SO_4 . To suppress the polarographic maximum, again gelatin was added to the electrolyte. For better comparison, the i - E curves, obtained with the RDE technique, are normalized in the same way as for the basic case. For PeTSPc, now a smaller limiting current is observed than for CoTSPc, indicating

that the selectivity of FeTSPc has decreased drastically. By using the Rotating Ring Disc Electrode (RRDE) technique, it was indeed established that hydrogen peroxide is the only product of the dioxygen reduction at FeTSPc, adsorbed on Cp, in acidic medium.

9.2.2. Dioxygen reduction on mercury in the presence of dissolved metal tetrasulfonato-phthalocyanines

A remarkable difference was observed for the polarograms in the presence of either Co- or FeTSPc. Addition of CoTSPc (10^{-3} M) has no effect on the dioxygen reduction. With FeTSPc, a different polarogram is obtained in both electrolytes (0.05 M H_2SO_4 and 0.1 M KOH). In figure 9.3, the polarogram measured in a dioxygen-saturated solution of FeTSPc (10^{-3} M in 0.1 M KOH) is given. The maximum on the polarographic wave appears not to be a polarographic

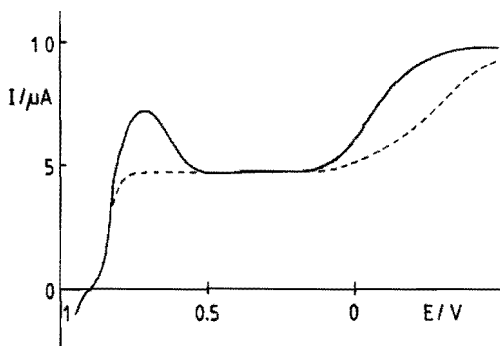


Fig. 9.3 Polarograms observed in 0.1 M KOH, with (—) and without (----) dissolved FeTSPc (10^{-3} M).

maximum of the first kind because addition of gelatin to the solution does not lead to the disappearance of the parabolically shaped maximum. Also, it was observed that the maximum is proportional to the FeTSPc concentration, which could, of course, not hold for a polarographic maximum of the first kind. It can also be considered as a polarographic maximum of the third kind, which normally occurs in the presence of organic substances [10]. Some objections against this explanation are:

- Although Co- and FeTSPc are of comparable structure, only for FeTSPc a maximum on the polarographic wave is found.
- For FeTSPc, adsorbed on graphite, also a maximum is observed on the i - E

curve measured in alkaline solution, see chapter 6. There, an explanation based on the competition in dioxygen reduction between the catalyst sites and the uncovered graphite surface parts was given for the phenomenon.

A similar explanation holds for mercury. Thus, at the beginning of the polarographic wave, dioxygen is reduced to water on FeTSPc. This results in an increase in the current as compared to the current measured in the electrolyte, free of FeTSPc, because on mercury only the reaction to hydrogen peroxide occurs in this potential domain. It is not known, whether the catalyst is adsorbed on the mercury surface or is present only in the neighbourhood of the surface, but it is most likely that in both cases the surface is not completely covered with FeTSPc. At a slightly higher overpotential, the dioxygen is reduced to hydrogen peroxide on the mercury surface before it can form an adduct with FeTSPc. At moderate overpotential, say from 0.5 V onwards to 0.2 V, the produced hydrogen peroxide is neither on mercury nor on FeTSPc further reduced, so the current has there the level observed for mercury in pure 0.1 M KOH.

The dissolved FeTSPc has also an effect on the second wave of the polarogram. This wave is the reduction of hydrogen peroxide to water. In the presence of FeTSPc the overpotential is slightly lowered and also a more steep curve results for the wave.

The above described effects of the dissolved FeTSPc on the polarogram are similar to those reported by Beyer et al. [11] for the polarogram of dissolved iron phthalocyanine in a methanol-LiOH solution (0.1 M LiOH).

The effect of FeTSPc on the dioxygen reduction at mercury in an acidic solution (0.05 M H_2SO_4) is shown in figure 9.4. The polarographic wave starts at a low overpotential and also a higher current plateau is obtained than without FeTSPc.

In this medium, contrary to alkaline solution, also a polarographic wave for FeTSPc itself is obtained (see figure 9.5). This response is measured in a solution deoxygenated by helium. The polarographic wave has an onset potential of about 0.6 V. RDE experiments with a Cp electrode show a reduction wave for FeTSPc at a slightly higher onset potential [see chapter 8]. Probably, the polarographic wave for the reduction of FeTSPc interferes with the wave for the anodic dissolution of mercury and, due to this, the i -E curve has shifted to a lower potential.

When the wave observed in the dioxygen-saturated FeTSPc solution is "corrected" for the response of FeTSPc itself, then still a higher current is

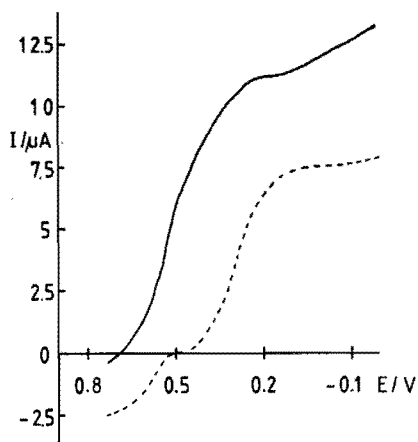


Fig. 9.4 Polarograms observed in $0.05\text{ M H}_2\text{SO}_4$, with (—) and without (----) dissolved FeTSPc (10^{-3} M).

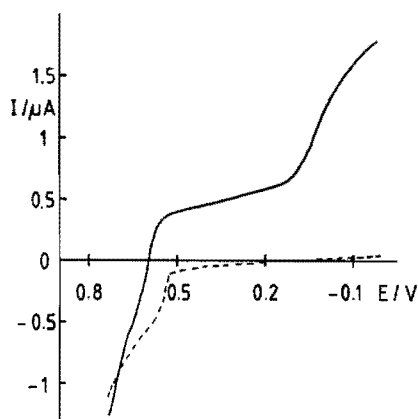


Fig. 9.5 Polarograms observed in helium-saturated $0.05\text{ M H}_2\text{SO}_4$, with (—) and without (----) dissolved FeTSPc (10^{-3} M).

obtained than for mercury without FeTSPc, dissolved in the solution. In the latter case (pure $0.05\text{ M H}_2\text{SO}_4$), the current plateau represents the diffusion limited current for the reduction of dioxygen to hydrogen peroxide. From this, the conclusion can be drawn that due to the dissolved FeTSPc, part of the dioxygen is reduced to water, as already suggested in chapter 8, where the behaviour of a dioxygen-saturated FeTSPc solution at a Cp disc electrode is

described. Spectroscopic measurements [see chapter 2 and 8] have shown that, in solutions of FeTSPc in water dioxygen bridged FeTSPc dimers are formed. Probably, these species are responsible for the increased four-electron reduction of dioxygen.

The polarographic wave observed at lower potential (see figure 9.4 as well as 9.5) can be attributed to the reduction of Fe(II)TSPc to Fe(I)TSPc, together with the reduction of μ -oxo bridged FeTSPc dimers, as proposed in chapter 8. Also, a start of the reduction of hydrogen peroxide can be the cause of the second wave in figure 9.4, but an accurate comparison of figure 9.4 and 9.5 shows that the increases in current in the potential domain of the second wave are almost equal, so that also in figure 9.4, the second wave can be ascribed to FeTSPc species.

9.3. Concluding remarks

A comparison between the results obtained for the dioxygen reduction at Cp, with and without adsorbed CoTSPc, on the one hand and the dioxygen reduction at mercury on the other hand, shows that Cp is a rather inactive material for the dioxygen reduction, and that due to the presence of CoTSPc on the graphite, only the activity of mercury can be approached. A Cp surface with adsorbed FeTSPc has in acid solution almost the same activity as a mercury surface but, in alkaline solution, due to an increased selectivity, the transport limited current in the presence of FeTSPc is twice as high.

FeTSPc, dissolved in the electrolyte, catalyzes the dioxygen reduction on mercury. In alkaline solution, the polarographic wave shows a maximum due to the reduction of dioxygen to water on FeTSPc. For the same reason, a higher transport limited current is found in acidic solution. Here again, we see that solution species of FeTSPc facilitate the 4-electron reduction of dioxygen in 0.05 M H_2SO_4 . The occurrence of dioxygen-bridged FeTSPc species suggests that these species are responsible for the increased 4-electron reduction.

9.4. References

1. A.J. Bard and L.R. Faulkner, 'Electrochemical methods. Fundamentals and Applications', J. Wiley and Sons, New York (1980).
2. J. Kůta and J. Koryta, Coll. Czech. Chem. Commun. 30 (1965) 4095.
3. C.J. van Velzen, Thesis, State University of Utrecht, Utrecht (1984).
4. J. Zagal, R.K. Sen and E. Yeager, J. Electroanal. Chem. 83 (1977) 207.

5. C.J. van Velzen, M. Sluyters-Rehbach, A.G. Remijnse, G.J. Brug and J.H. Sluyters, *J. Electroanal. Chem.* 134 (1982) 87.
6. F. van den Brink, W. Visscher and E. Barendrecht, *J. Electroanal. Chem.* 157 (1983) 305.
7. D.T. Sawyer and E.T. Seo, *Inorg. Chem.* 16 (1977) 499.
8. E. Yeager, *Electrochim. Acta* 29 (1984) 1527.
9. R. McIntyre, D. Scherson, W. Storck and H. Gerischer, *Electrochim. Acta* 32 (1987) 51.
10. J. Küta, 'Polarography' in *Comprehensive Treatise of Electrochemistry*, Vol. 8; *Experimental Methods in Electrochemistry*, edited by R.E. White, J.O'M. Bockris, B.E. Conway and E. Yeager, Plenum Press, New York (1984).
11. W. Beyer and F. v. Sturm, *Angew. Chem.* 84 (1972) 154.

10. Electroreflectance spectroscopic measurements

10.1. Introduction

In chapter 6 or in reference [1], the dioxygen reduction at Co⁻ and FeTSPc, adsorbed on pyrolytic graphite (Cp), was described. The model, proposed in that chapter for especially the dioxygen reduction at FeTSPc, requires that most of the metal chelate is adsorbed as monomers and a smaller part (about 10%) as dimers. Further independent evidence for the way of adsorption of the catalysts on the graphite surface could result from electroreflectance spectroscopic (ER) measurements [2].

The ER experiments described in this chapter were carried out in collaboration with dr. C. Hinnen at the CNRS Laboratoire d'Electrochimie Interfaciale (Meudon-Bellevue). For the experiments, the basal plane of stress annealed pyrolytic graphite (BP of SA-Cp), which has a highly reflecting surface [3], was used.

In this chapter, the ER spectra obtained for Co⁻ and FeTSPc, adsorbed on BP of SA-Cp, are compared with absorption spectra of the compounds, dissolved in acidic or alkaline solution, obtained with an Optical Transparent Thin Layer Cell (OTTLC) [reference [4], see also chapter 4 and 8]. From this comparison, some conclusions are drawn about the way of adsorption of the metal chelates on the graphite surface.

10.2. Theoretical aspects

A compound, adsorbed or deposited on a reflecting surface, can be studied with reflectance spectroscopy, if this compound absorbs light. Mostly, in catalysis or electrocatalysis, the amount of deposited molecules is small and the resulting light absorption is too weak to perform reflectance spectroscopy. By using an electron-conducting substrate, it is possible to vary the oxidation state of the deposited molecule by changing the potential of the (electrode) surface. Usually, different oxidation states also show different light absorption behaviour. By modulation of the electrode potential with a certain frequency and amplitude around the redox potential, i.e. the potential where the conversion from one oxidation state to another occurs, the intensity of the reflected light is also modulated. This intensity modulation can be detected easily by using phase-sensitive detection techniques. [See for the

experimental details chapter 4]. Due to the applied modulation technique, the obtained electroreflectance spectrum consists of the difference between the absorption spectra of both involved oxidation states [5]. Thus, this method gives an increased sensitivity, but the results are more difficult to interpret.

10.3. Results for alkaline solution

In figure 10.1, the cyclic voltammogram recorded in 0.1 M KOH for FeTSPc, adsorbed on the BP of SA-Cp, is given. An electrochemical cell was used which

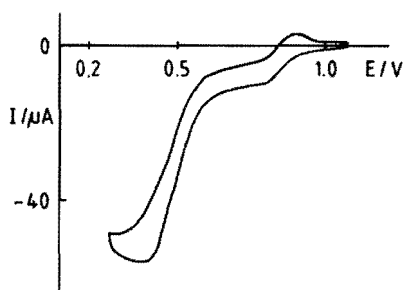


Fig. 10.1 Cyclic voltammogram recorded for FeTSPc, adsorbed on the BP of SA-Cp, in 0.1 M KOH. Electrolyte: dinitrogen-saturated (see text). Scan rate: 300 mV s^{-1} . Electrode area: 0.4 cm^2 .

was constructed in such a way that electroreflectance spectroscopy could be performed on the same electrode (see also figure 4.5). The adsorption of the compound was obtained from a concentrated solution (more than 10^{-3} M) in 0.1 M HClO_4 . Unfortunately, it was not possible to remove all traces of dioxygen from the electrolyte by bubbling dinitrogen gas through the solution. The two observed cathodic waves are, therefore, due to the reduction of dioxygen. From cyclic voltammetric measurements for FeTSPc, adsorbed on Cp, it is well known that two redox couples, which belong to the adsorbed complex, are situated, respectively, at about 0.9 V and about 0.4 V [chapter 6]. (For the measurements a Mercury Sulphate Electrode was used as reference electrode, but all potentials are given here vs. a Reversible Hydrogen Electrode (RHE)). In figure 10.1, these redox processes are not clearly visible; only the oxidation peak for the couple at 0.9 V is observed. the results of Zagal-Moya [6] on BP of SA-Cp confirm that, indeed, also for FeTSPc, adsorbed on this material, redox couples can be detected at, respectively, 0.9 V and 0.4 V.

The two redox processes are more easily observed as peaks in figure 10.2, where the capacitive behaviour of the electrode is given. This (differential) capacitive behaviour is measured by applying an ac-potential (with a 15 Hz frequency and a 10 mV amplitude) to the electrode, superimposed on a dc-potential which is raised or lowered with a slow, but constant, rate. The measured signal is an ac-current, 90° in front of the ac-potential, and converted into a differential capacity. Following the assignment of Zecevic et al. [7], the

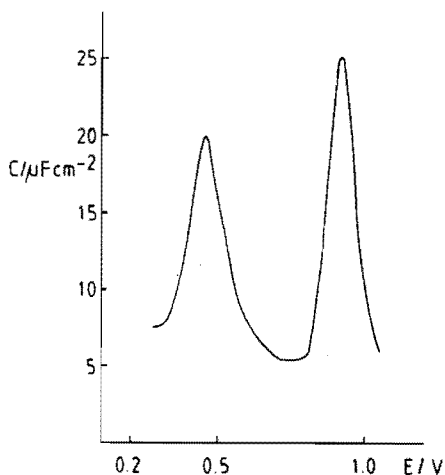


Fig. 10.2 Capacitive behaviour of FeTSPc, adsorbed on the BP of SA-Cp, in 0.1 M KOH under dinitrogen atmosphere. Modulation frequency: 15 s^{-1} and modulation amplitude: 10 mV. Scan rate: 6 mV s^{-1} .

cathodic peak at about 0.9 V can be ascribed to the conversion of Fe(III)TSPc to Fe(II)TSPc, and the 0.4 V peak to the change of Fe(II)TSPc into Fe(I)TSPc.

ER spectra are recorded in the potential domains of both redox couples. The ER spectrum, recorded at 0.90 V, shows in the UV-domain a distinct reproducible structure, although also the other part of the spectrum is completely reproducible (see figure 10.3). The lack of structure in the wavelength range of the visible light indicates that the involved oxidation states (Fe(III)TSPc and Fe(II)TSPc) of the adsorbed molecule do not differ much in their absorption behaviour. The ER spectrum at $E = 0.45 \text{ V}$ (figure 10.4) has a clear morphology.

CoTSPc, adsorbed on the BP of SA-Cp, shows at about 0.45 V also a surface redox process. The observed ER spectrum (not given here) is almost similar to that obtained for FeTSPc at the same potential.

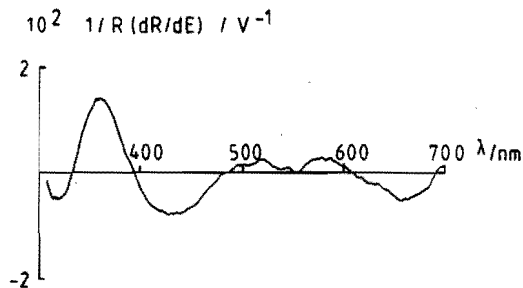


Fig. 10.3 ER spectrum of FeTSPc, adsorbed on the BP of SA-Cp, at $E = 0.90$ V. Electrolyte: 0.1 M KOH, dinitrogen-saturated. Modulation frequency: 15 s^{-1} and modulation amplitude: 100 mV.

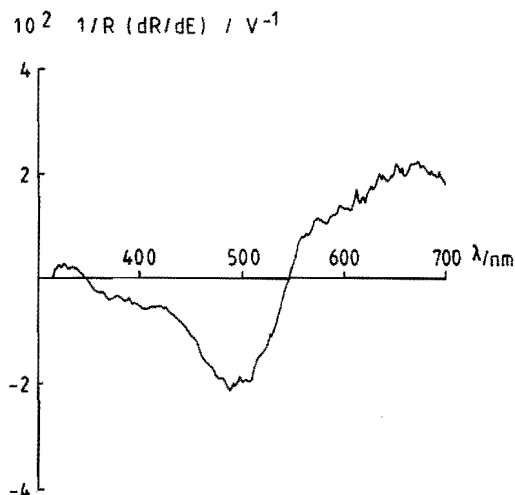


Fig. 10.4 ER spectrum of FeTSPc, adsorbed on the BP of SA-Cp, at $E = 0.45$ V. Electrolyte: 0.1 M KOH, dinitrogen-saturated. Modulation frequency: 15 s^{-1} and modulation amplitude: 100 mV.

After dioxygen saturation of the electrolyte, new peaks appear in the differential capacity curve. In figure 10.5, besides the original peak at about 0.90 V, a new one is observed at a slightly lower potential (0.80 V). In the potential domain of the other redox process also an extra peak is obtained, however, this peak lies at a slightly higher potential (at about 0.55 V) than the original one. The new peaks are probably due to the reaction of a dioxygen adduct of FeTSPc, which arises after the reduction of Fe(III)TSPc. These

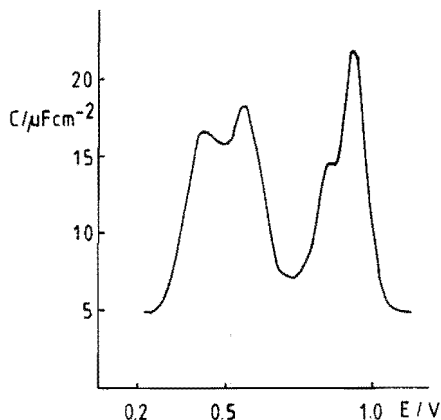


Fig. 10.5 Capacitive behaviour of FeTSPc, adsorbed on the BP of SA-Cp, in 0.1 M KOH under dioxygen atmosphere. Modulation frequency: 15 s^{-1} and modulation amplitude: 10 mV . Scan rate: 6 mV s^{-1} .

dioxygen adducts are probably more or less reversibly reduced and, therefore, these adducts contribute to the capacity of the electrode. From Rotating Ring Disc Electrode measurements [6], it is known that, at the potential of the additional peak at 0.80 V, dioxygen is (already) reduced to water. Therefore, it must be concluded that the two additional peaks, observed under dioxygen-saturated conditions, indicate the presence of two different dioxygen adducts: the first one results in dioxygen reduction at high potential, while the second one also results in dioxygen reduction, but at lower potentials. The peaks are probably associated with FeTSPc dimers and monomers, for which the existence is proposed in chapter 6.

Saturation of the solution with dioxygen has no influence on the ER spectra. The additional peaks in the capacity curve neither correspond with additional features in the ER spectra, nor result in extra ER spectra.

10.4. Results in acidic solution

The cyclic voltammogram measured in 0.1 M HClO_4 shows, like in alkaline solutions, two redox peaks in the potential region of interest for dioxygen reduction; see figure 10.6. However, contrary to the alkaline electrolyte, the reduction of traces of dioxygen, still present in the solution after dinitrogen saturation, only starts in the potential domain of the redox process at

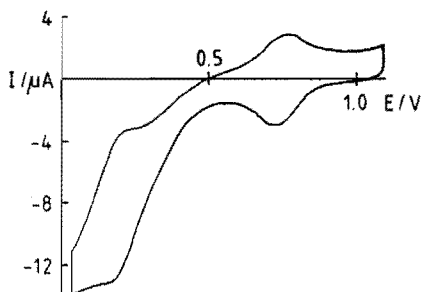


Fig. 10.6 Cyclic voltammogram recorded for FeTSPc, adsorbed on the BP of SA-Cp, in 0.1 M HClO_4 . Electrolyte: dinitrogen-saturated (see text). Scan rate: 300 mV s^{-1} . Electrode area: 0.4 cm^2 .

the lowest potential (0.2 V). From studies of the redox potential as a function of the pH [6,7,8], it can be concluded that the redox process at $E = 0.90 \text{ V}$ in alkaline solution shifts to $E = 0.70 \text{ V}$ in acidic solution. For the other couple a shift from 0.45 V to 0.20 V is observed.

For the redox peak at 0.7 V, again an ER spectrum with almost no structure is recorded (figure 10.7), differing, however, significantly from the corresponding one in alkaline medium. So, the structure of the adsorbed FeTSPc species in acidic solution differs from that in alkaline solution.

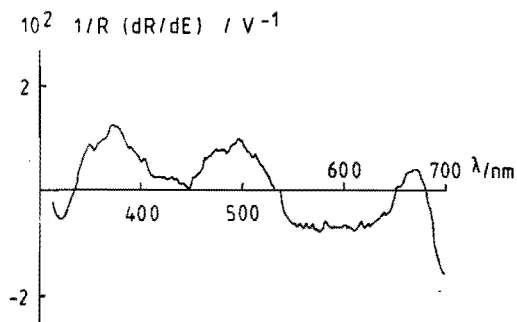


Fig. 10.7 ER spectrum of FeTSPc, adsorbed on the BP of SA-Cp, at $E = 0.70 \text{ V}$. Electrolyte: 0.1 M HClO_4 , dinitrogen-saturated. Modulation frequency: 15 s^{-1} and modulation amplitude: 50 mV.

For the 0.2 V redox process, the ER spectrum is given in figure 10.8. Comparing this figure with figure 10.4 (alkaline solution) shows that the ER spectra recorded for the redox couple Fe(II)TSPc/Fe(I)TSPc are similar.

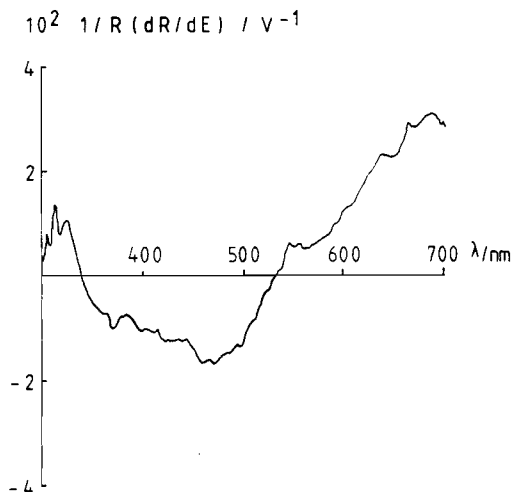


Fig. 10.8 ER spectrum of FeTSPc, adsorbed on the BP of SA-Cp, at $E = 0.21 \text{ V}$. Electrolyte: 0.1 M HClO_4 , dinitrogen-saturated. Modulation frequency: 15 s^{-1} and modulation amplitude: 50 mV .

10.5. Discussion

To obtain more information from the recorded ER spectra, a comparison is made with the absorption spectra measured for FeTSPc, dissolved in alkaline or acidic electrolytes. As described in section 10.2., an ER spectrum consists of the difference between the absorption spectra of the involved oxidation states. In the experimental part [chapter 4], a description is given of the technique to obtain absorption spectra of the several oxidation states of the metal chelate, using the OTTLC.

The two redox couples, which result in ER spectra, are Fe(I)TSPc/Fe(II)-TSPc and Fe(II)TSPc/Fe(III)TSPc, respectively. In figure 10.9 a,b, the absorption spectra recorded in alkaline electrolyte for the two components of the first couple (figure 10.9a), and for both components of the second couple (figure 10.9b) are given). It is obvious that subtraction of the absorption

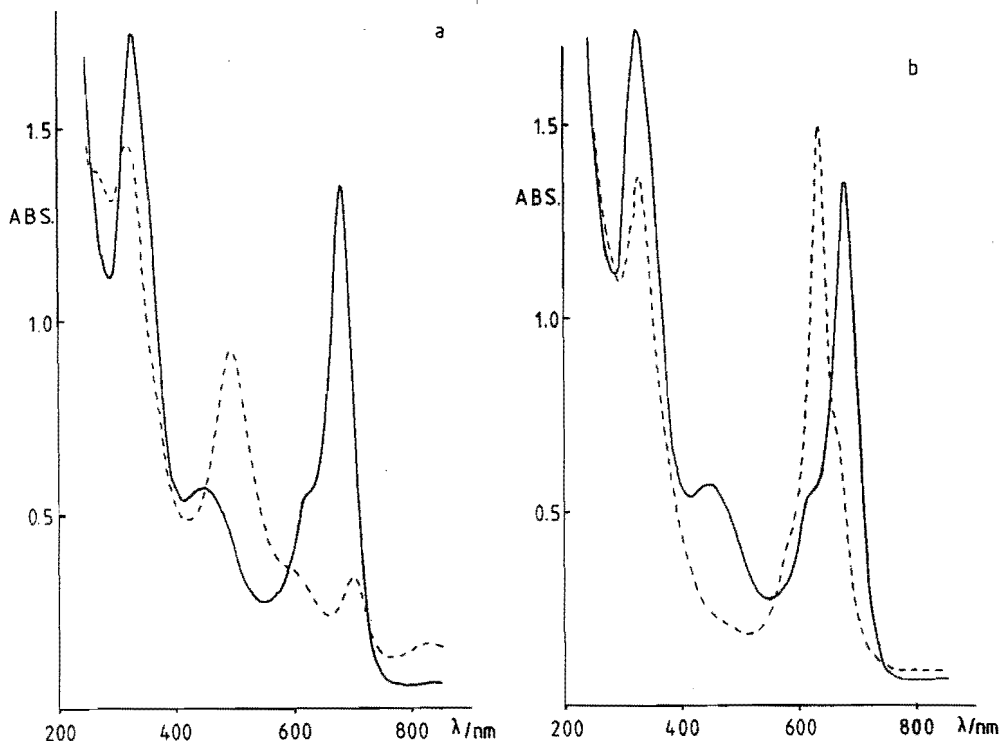


Fig. 10.9 a,b. Comparison between the absorption spectra, recorded in an OTTLC, of electrochemically prepared Fe(I)TSPc (-----) and Fe(II)-TSPc (——) (a); Fe(II)TSPc (——) and Fe(III)TSPc (-----) (b). [FeTSPc]: about 10^{-3} M. Electrolyte: 0.1 M KOH. Cell thickness: 0.4 mm.

spectrum of Fe(I)TSPc from that of Fe(II)TSPc results in a spectrum with a similar shape as the ER spectrum of figure 10.4. This indicates that the adsorption of the compound on the graphite surface has little or no influence on the optical transitions in both adsorbed Fe(I)TSPc and Fe(II)TSPc species. In the case of the other redox couple, subtraction of the spectrum of Fe(II)TSPc from that of Fe(III)TSPc (or in the other way) does not yield the shape of the ER spectrum observed for this couple (see figure 10.3). The main absorption peaks of both components of this redox couple almost coincide; therefore, small influences of the graphite surface on the optical transitions of the involved oxidation states are sufficient to yield an ER spectrum, which differs strongly from that constructed by using the absorption spectra of the dissolved redox species.

On going from alkaline to acidic solution, only small wavelength shifts are observed for the absorption bands of the dissolved redox components. Thus, the ER spectrum, recorded at the lowest redox potential, which is, as mentioned before, very similar to the corresponding one recorded in alkaline solution, can also be constructed from the absorption spectra for the pertaining redox species in acidic solution. The absorption spectra of Fe(II)TSPc and Fe(III)TSPc in acidic solution are given in figure 10.10. Like in alkaline

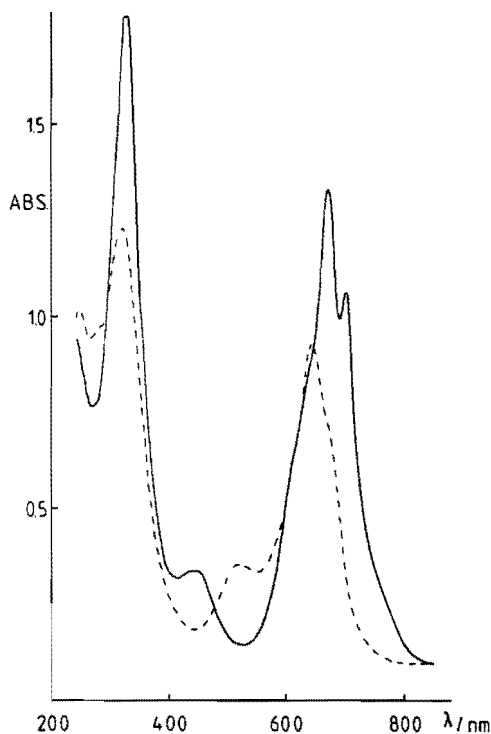


Fig. 10.10 Comparison between the absorption spectra, recorded in an OTTLC, of electrochemically prepared Fe(II)TSPc (—) and Fe(III)TSPc (----). [FeTSPc]: about 10^{-3} M. Electrolyte: 0.05 M H_2SO_4 . Cell thickness: 0.4 mm.

solution, the spectrum constructed from the difference between these two spectra does not show the same shape as the ER spectrum recorded for this couple (see figure 10.7).

From these observations, we can conclude that the adsorption of FeTSPc on the BP of SA-Cp has an effect on the chemical nature of Fe(III)TSPc or of

Fe(II)TSPc or of both. The chemical change of Fe(II)TSPc on adsorption can only be small, because by using the absorption spectrum of this oxidation state, the ER spectrum recorded at the potential of the redox couple Fe(I)-TSPc/Fe(II)TSPc can be constructed. Unfortunately, it is not known how the features of the ER spectrum can be translated into structural information about the way of adsorption of FeTSPc on the electrode. Nevertheless, a few conclusions can be drawn. First, the situation is more complicated than suggested by Nikolic et al. [3]. They reported a reflectance spectrum of adsorbed FeTSPc, which was very similar to spectra obtained for FeTSPc in solution; so, they concluded that on adsorption only minor changes occur in the metal chelate. Secondly, the absorption spectra of Fe(III)TSPc and Fe(II)-TSPc show only small differences when the solution is changed from alkaline to acidic, however, the ER spectrum changes drastically. This probably indicates that the form of adsorption in alkaline solution differs from that in acidic solution. To explain the results of electrochemical measurements, we proposed in chapter 7 another adsorption form for FeTSPc on Cp in an alkaline than in an acidic solution. It was argued that in an alkaline electrolyte part of the FeTSPc is adsorbed as dimers, while in acid almost no dimers are present on the surface.

10.6. Concluding remarks

The differential capacity curve recorded in alkaline solution for FeTSPc, adsorbed on the BP of SA-Cp, shows two peaks. After dioxygen-saturation of the electrolyte, two additional peaks appear. This indicates that two different dioxygen adducts, probably a dimeric and a monomeric species, are present. This supports the results of chapter 6, where these species are already proposed to explain the dioxygen reduction behaviour of FeTSPc, adsorbed on Cp.

In chapter 7, the low activity of FeTSPc, adsorbed on Cp, in acidic solution as compared to alkaline solution, is attributed to the absence of FeTSPc dimers on the graphite surface in the acidic electrolyte. This explanation is sustained by the results obtained with ER spectroscopy. The ER spectra recorded for the redox couple Fe(II)TSPc/Fe(III)TSPc in alkaline and acidic solution differ from each other, also suggesting a difference in the form of adsorption of the metal chelate in the two electrolytes.

More research is necessary to translate the features of the ER spectra of these redox couples, recorded in both electrolytes, into structural information about the form of adsorption of FeTSPc on the electrode.

10.7. References

1. A. Elzing, A. van der Putten, W. Visscher and E. Barendrecht, *J. Electroanal. Chem.* 233 (1987) 99.
2. J.P. Dalbera, C. Hinnen and A. Rousseau, *J. de Phys. C5*; 38 (1977) 185.
3. B.Z. Nikolic, A.R. Adzic and E.B. Yeager, *J. Electroanal. Chem.* 103 (1979) 281.
4. C.W. Anderson, H.B. Halsall and W.R. Heineman, *Anal. Biochem.* 93 (1979) 366.
5. D. van den Ham, C. Hinnen, G. Magner and M. Savy, to be published.
6. J. Zagal-Moya, Thesis, Case Western Reserve University, Cleveland (1978).
7. S. Zecevic, B. Simic-Glavaski, E. Yeager, A.B.P. Lever and P.C. Minor, *J. Electroanal. Chem.* 196 (1985) 339.
8. A. van der Putten, Thesis, Eindhoven University of Technology, Eindhoven (1986).

11. In situ light absorption spectroscopy of metal tetrasulfonato-phthalocyanine/polypyrrole layers

11.1. Introduction

In chapter 7 or reference [1], we proposed that dimers of FeTSPc play an important role in the mechanism of dioxygen reduction (in 0.05 M H_2SO_4) on FeTSPc, incorporated in polypyrrole. The aim of this chapter is to present results of in situ light absorption spectroscopy, which give some supporting evidence for the existence of MeTSPc dimers in the conducting polymer. Also, some experiments are performed to get more insight in the role of the pH in the oxygenation process of the metal complexes.

In the first section, the spectra of CoTSPc and FeTSPc, as obtained when dissolved in 0.05 M H_2SO_4 , are discussed. Also the pH-dependence of the oxygenation of CoTSPc is investigated. Hereafter, the spectra of CoTSPc, incorporated in polypyrrole, are described for several oxidation states. Finally, the spectra of the possible oxidation states of FeTSPc, incorporated in polypyrrole, are given and the features of the spectra, which possibly indicate the existence of a FeTSPc dimer, are discussed.

11.2. Co- and FeTSPc solutions

Spectra of solutions of the metal chelates are recorded in absence of dioxygen by saturation of the solution with purified helium gas [see chapter 4]. These spectra are compared with those obtained under dioxygen-saturated conditions. The spectra obtained for CoTSPc in 0.05 M H_2SO_4 are depicted in figure 11.1. Figure 11.1B shows that under dioxygen-saturated conditions a spectral change is observed compared with the dioxygen-free situation (figure 11.1A), which indicates the formation of a dioxygen adduct [see chapter 3 for the assignment of the absorption peaks]. Our observations are in agreement with those of Simic-Glavaski et al. [2], who also concluded that in acid solution dioxygen adduct formation is possible. Contrary to this, Wagnerova et al. [3] and Gruen et al. [4] claimed that only in alkaline solutions a dioxygen adduct can be observed, because of the promoting effect of the OH^- ion [for comparison, see also the chapters 2 and 6 where the corresponding spectra for alkaline solutions are given in the figures 2.2, 2.3 and 6.3]. To come to a decision on this "contradiction", the pH-dependence of the dioxygen

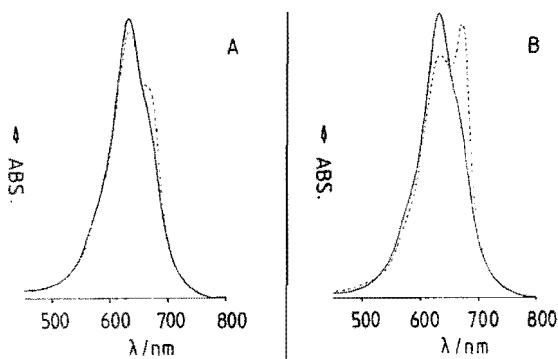


Fig. 11.1 UV-Vis. spectra for CoTSPc (10^{-5} M)

- A) ——— recorded immediately after addition of CoTSPc to 0.05 M H_2SO_4 (dioxygen-free).
 ----- after 2 hours of helium saturation.
- B) ——— same as A (———).
 ----- after 2 hours of dioxygen saturation.

adduct formation rate of CoTSPc was investigated over the whole pH-range from 1 to 13.

In figure 11.2, the absorbance at the absorption wavelengths of the dioxygen adduct (668 nm) and the dioxygen-free dimer (628 nm) are given as a function of the pH. The method to obtain the data of the figure was as follows: after bubbling of dioxygen through the solution for a period of 5 hours the solution was stored over night under dioxygen-saturated conditions and hereafter the absorbance at the above mentioned wavelengths was measured. Solutions with different pH but with the same anions were prepared by mixing NaOH and H_2SO_4 solutions, until the desired pH-value was obtained, though we know that the buffer capacity of such mixtures is rather low.

Both for low and high pH, the peak which corresponds to the dioxygen adduct increases at the expense of the dimer peak. The ionic strength of the solution has no effect on the dioxygen adduct formation rate, as was found by addition of a salt, like $LiClO_4$ or Na_2SO_4 , to a neutral CoTSPc solution up to a concentration of 1 M.

A possible explanation for the observed pH-dependence is that not only OH^- but also H^+ promotes the formation of an adduct. As was shown in chapter 3, fundamental calculations predict a charge transfer from the cobalt ions to the dioxygen molecule in the adduct. This adduct is probably stabilized by proto-

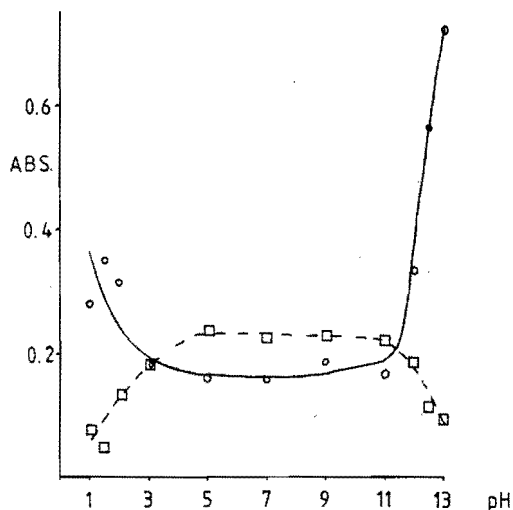


Fig. 11.2 The dioxygen adduct formation of CoTSPc as a function of the pH. [CoTSPc]: 10^{-5} M. o o : absorbance at 668 nm (dioxygen adduct), -□-□-: absorbance at 628 nm (dioxygen-free dimer).

nation of one of the negatively charged oxygen atoms. In alkaline solutions OH^- probably stabilizes in a similar way the positive charge on the cobalt atom.

Dioxygen adducts of FeTSPc are observed for all pH-values. In figure 11.3A, the spectrum under helium conditions is given, while in 11.3B, the changes occurring under a dioxygen atmosphere are shown. Both spectra are recorded in 0.05 M H_2SO_4 [see again chapter 2 for the assignment of the peaks]. In alkaline solutions, a more or less reversible oxygenation is observed. By helium saturation, it is possible, when the temperature is raised to 70°C , to remove in alkaline solution the dioxygen from the dioxygen bridged dimer [see chapter 6]. As is obvious from figure 11.3, the oxygenation is not reversible in 0.05 M H_2SO_4 . The spectrum taken immediately after addition of FeTSPc to the dioxygen-free 0.05 M H_2SO_4 solution, shows that, like in alkaline solutions, a considerable part of the FeTSPc is already present as a dioxygen adduct in the solid form.

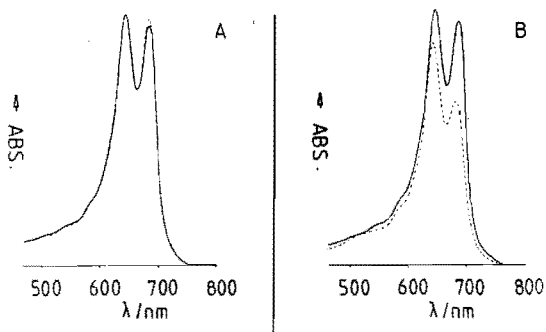


Fig. 11.3 UV-Vis. spectra for FeTSPc (10^{-5} M).

- A) ——— recorded immediately after addition of FeTSPc to 0.05 M H_2SO_4 (dioxygen-free).
 ----- after 2 hours of helium saturation.
- B) ——— same as A (———).
 ----- after 2 hours of dioxygen saturation.

11.3. Co- and FeTSPc in polypyrrole

11.3.1. General considerations

When Co- or FeTSPc are incorporated in the electron-conducting polymer polypyrrole, which is attached to an Au-electrode, it is possible to control the oxidation state of the complex by varying the potential of the electrode. [The preparation of the polypyrrole/MeTSPc layer, is given in the experimental section of chapter 5]. During the preparation of the polypyrrole layer, the electrode has a potential high enough to oxidize pyrrole. At this electrode potential (above 1.2 V (RHE)), however, also CoTSPc and FeTSPc are oxidized to their third oxidation state: Co(III)TSPc and Fe(III)TSPc, respectively. To make a comparison possible between the spectra of the incorporated molecules and the spectra of the molecules free in solution, the potential of the electrode should be set at a value where Co(III)TSPc and Fe(III)TSPc are reduced to the divalent oxidation state.

In figures 11.4 and 11.5, the cyclic voltammograms in 0.05 M H_2SO_4 of, respectively, a polypyrrole/CoTSPc and a polypyrrole/FeTSPc layer are shown. [Figure 11.4 is the same as figure 5.3B and figure 11.5 is identical with figure 7.3A]. When we use the same assignment as Zecevic et al. [5] for the redox peaks of CoTSPc species adsorbed on graphite, then the peak at about 800

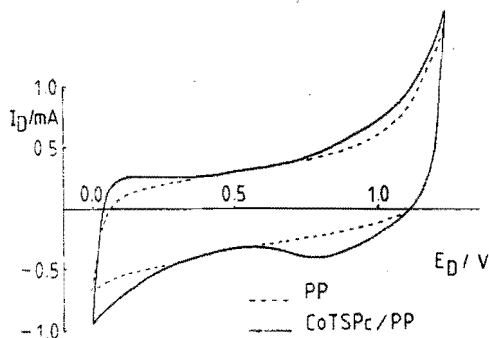


Fig. 11.4 Cyclic voltammogram of a 30 mC CoTSPc/polypyrrole layer. Electrolyte: 0.05 M H_2SO_4 , dioxygen-free; scan rate: 100 mV s^{-1} .

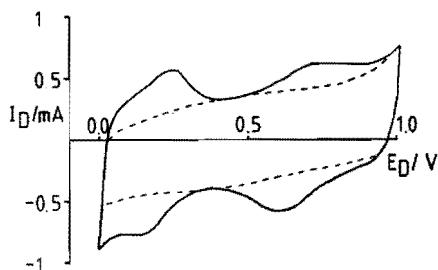


Fig. 11.5 Cyclic voltammogram of a 30 mC FeTSPc/polypyrrole layer. Electrolyte: 0.05 M H_2SO_4 , dioxygen-free; scan rate: 100 mV s^{-1} .

mV for CoTSPc can be ascribed to the transition of Co(III)TSPc to Co(II)TSPc. Below zero volt, according to Zecevic et al., a transition of the ligand occurs (or Co(II)TSPc is converted to Co(I)TSPc). Both redox peaks are more or less smoothed out in figure 11.4 because they are both lying close to the upper and lower potential limits, respectively, of the polypyrrole layer. At high positive potential, the polypyrrole layer is slowly and irreversibly oxidized and below zero volt, hydrogen evolution interferes with CoTSPc reduction.

For FeTSPc, incorporated in polypyrrole, the clearly visible redox peak at about 650 mV can be ascribed to reduction of Fe(III)TSPc to Fe(II)TSPc, again according to Zecevic et al. [5], while at about 150 mV, Fe(II)TSPc is converted into Fe(I)TSPc.

The spectra of the MeTSPc's, incorporated in polypyrrole, are recorded

by using the cell and the transparent gold electrode described in chapter 4. Another gold film electrode on glass was placed in the reference beam. To establish the absorption of the polypyrrole layer itself, a polypyrrole layer was prepared without catalysts (instead of MeTSPc, ClO_4^- was incorporated in the film). In figure 11.6, the spectra recorded in $0.05 \text{ M H}_2\text{SO}_4$ for a polypyrrole layer with a thickness of 20 mC (electrode area: 1.5 cm^2) at three different electrode potentials are depicted. The absorption spectrum of this

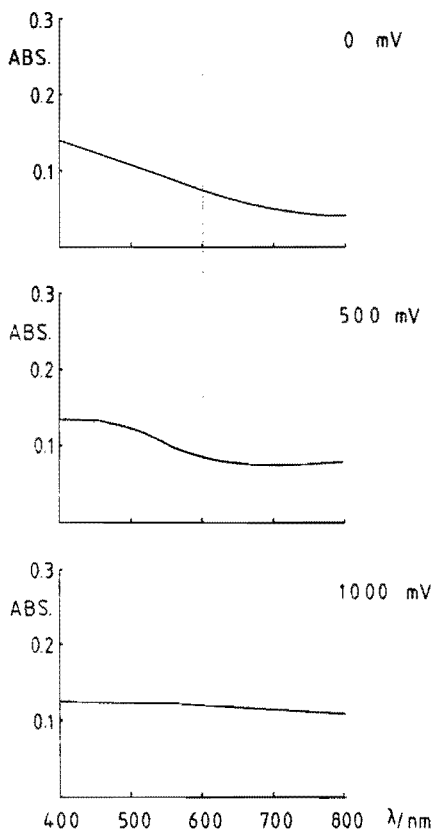


Fig. 11.6 UV-Vis. spectra for a 20 mC polypyrrole layer at three different potentials. Electrolyte: $0.05 \text{ M H}_2\text{SO}_4$, dioxygen-free.

polypyrrole layer shows nearly a continuous absorption over the entire wavelength range of the visible light, with only a small wavelength- and potential dependency. To determine the true absorption spectrum of Co- (or Fe-)TSPc, incorporated in the polymer, the absorption measured for the polymer layer

with only ClO_4^- incorporated in it, is subtracted from the absorption measured for the polypyrrole/catalyst layer.

11.3.2. Spectra of CoTSPc, incorporated in polypyrrole

In figure 11.7, the spectra measured for a polypyrrole/CoTSPc layer at three different potentials are shown. These spectra were recorded in a dini-

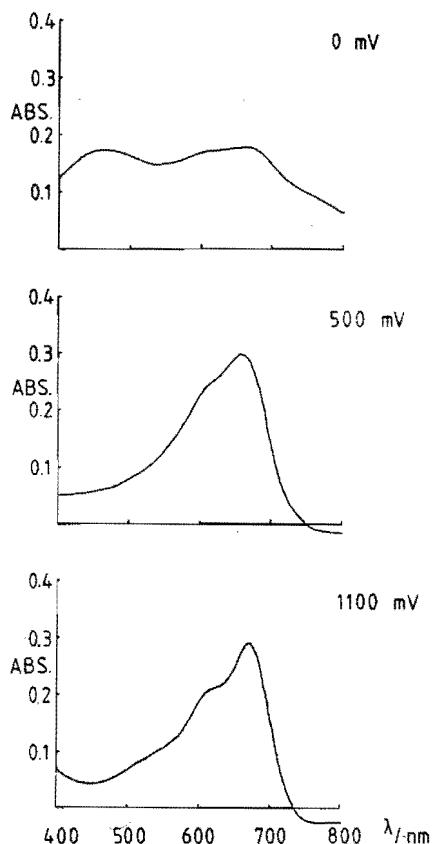


Fig. 11.7 UV-Vis. spectra for a 20 mC polypyrrole/CoTSPc layer at three different potentials. Electrolyte: 0.05 M H_2SO_4 , dioxygen-free.

trogen-saturated solution after one complete cyclic potential sweep in the potential range between 0 and 1 V (RHE). Under these conditions the possible dioxygen adducts are removed by the reduction of the dioxygen. [See also

chapter 8, where the results obtained with an optical transparent thin layer cell are discussed].

The spectra show broad peaks, indicating that in the polypyrrole layer the catalyst molecules occupy a broad distribution of environments [6]. The spectrum at 1100 mV, with a main absorption peak at 675 nm, resembles the spectrum of chemically prepared Co(III)TSPc, recorded in THF [7]. By lowering the potential to 500 mV the absorption peak shifts to about 662 nm, i.e. the absorption wavelength of a monomer Co(II)TSPc molecule. The shoulder at about 620 nm can be ascribed to a dimer Co(II)TSPc species [3,4]. In both spectra at 1100 mV and 500 mV, part of the spectrum lies a little below zero, most probably due to the applied subtraction method. Nevertheless, it can be concluded that the majority of Co(II)TSPc molecules exists as monomers in the polypyrrole matrix: the shoulder at 620 nm indicates, however, that even in polypyrrole dimers of Co(II)TSPc are possible.

At lower potential (0 mV) a new peak appears at 462 nm, which corresponds very well with the absorption wavelength, observed by Kobayashi et al. [8], for Co(I)TCPC, cobalt tetracarboxy-phthalocyanine. [See also chapter 2 of this thesis].

It is difficult to determine the CoTSPc redox potentials from the cyclic voltammogram of figure 11.4. An alternative method was pointed out by Ikeda et al. [9]. They showed that the changes in absorption behaviour as caused by varying the electrode potential could be used to measure the formal potential of the redox couples. Therefore, the spectroscopic method is applied here. Figure 11.8 gives the absorption data for $\lambda = 660$ nm during a potential scan from 500 mV to -200 mV, with a scan rate of 5 mV s^{-1} . The half-wave potential of the obtained curve yields the formal potential of the redox couple [9].

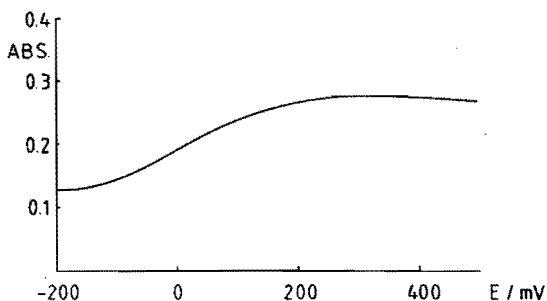


Fig. 11.8 The absorption at 660 nm as a function of the potential for a 20 mC polypyrrole/CoTSPc layer. Electrolyte: 0.05 M H_2SO_4 , dioxygen-free; scan rate: 5 mV s^{-1} .

For the Co(I)TSPc/Co(II)TSPc couple a formal potential of 30 mV was determined. The advantage of this method is, moreover, that the hydrogen evolution current does not disturb the measurement as was the case for the voltammetric method. For the determination of the redox couple Co(II)TSPc/Co(III)TSPc, the spectroscopic method appeared to be unsuccessful, because the spectra of the involved oxidation states are not different enough (c.f. figure 11,7, the spectra at 500 and 1100 mV).

11.3.3. Spectra of FeTSPc, incorporated in polypyrrole

In figure 11.9, the spectra recorded for a 20 mC polypyrrole/FeTSPc layer at three different electrode potentials, are shown. The recording

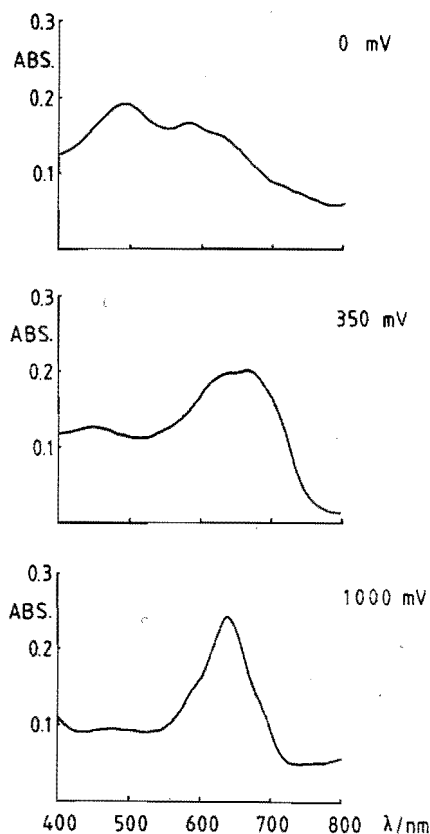


Fig. 11.9 UV-vis. spectra for a 20 mC polypyrrole/FeTSPc layer at three different potentials. Electrolyte: 0.05 M H_2SO_4 , dioxygen-free.

conditions were the same as for incorporated CoTSPc. The spectrum measured at a potential of 1000 mV shows a main absorption peak at 642 nm, which is very close to the value of 635 nm reported for Fe(III)TSPc free in solution [10]. It corresponds also very well with the absorption wavelength of Fe(III)TCPC (Fe tetracarboxy-phthalocyanine) (640 nm) [8].

The spectrum at 350 mV shows a very broad absorption band. At this potential the FeTSPc molecule should be present in its second oxidation state, see section 11.3.1. According to Vonderschmitt et al. [10], a monomer Fe(II)TSPc species absorbs light with a wavelength of 668 nm. Thus, we can conclude that part of the broad absorption band is due to the absorption of monomer Fe(II)TSPc species. However, because the absorption peak is too broad to be attributed only to the absorption of monomer Fe(II)TSPc species, probably a second FeTSPc species exists with an absorption wavelength of about 630 nm, being the same wavelength as for the absorption maximum of Fe(III)TSPc; but at the applied potential this species should be reduced to Fe(II)TSPc. The assignment of the absorption to a dioxygen bridged FeTSPc dimer can also be rejected, because under the measuring conditions (a dinitrogen-saturated solution and an applied potential where dioxygen can be reduced), the presence of dioxygen adsorbed on FeTSPc is very unlikely. Moreover, before recording the spectrum at 350 mV a complete potential sweep between 0 and 1000 mV was made and it is to be expected that traces of dioxygen are fully reduced during this scan. Saturation of the solution with dioxygen results in a dioxygen reduction current at this potential (350 mV), but without change in the spectrum. This can be explained by an immediate reduction of dioxygen after its adsorption on FeTSPc. An alternative explanation for the peak at 630 nm points to the existence of FeTSPc dimers without a dioxygen (or oxygen) bridge. However, for Fe(II)TSPc solutions no dimer species are observed [10], so an easy comparison, from which can be concluded whether the peak can be ascribed to a Fe(II)TSPc dimer or not, is not possible. On the other hand, the FeTSPc dimer should, if existing in the incorporated state, absorb - analogous to CoTSPc - at a shorter wavelength than the monomer species. The absorption wavelength proposed for the dimer satisfies this requirement. Through the interaction with polypyrrole, changes probably occur in the Fe(II)TSPc molecule such that it is now energetically favourable to form a considerable amount of dimer species.

By lowering the electrode potential, the Fe(II)TSPc is further reduced to Fe(I)TSPc. The spectrum recorded at 0 mV has a main absorption at 490 nm (see figure 11.9). The difference in the spectra of Fe(I)TSPc and Fe(II)TSPc

is sufficient enough to allow a determination of the redox potential by the spectroscopic method, in the same way as for CoTSPc. In figure 11.10, the potential dependence of the absorption at 490 nm is given. From this figure a redox potential of 175 mV follows for the Fe(I)TSPc/Fe(II)TSPc couple.

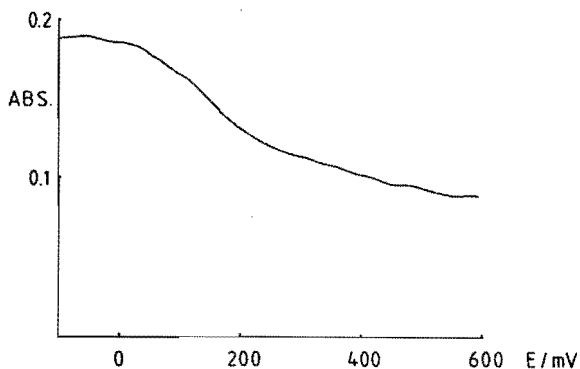


Fig. 11.10 The absorption at 490 nm as a function of the potential for a 20 mC polypyrrole/FeTSPc layer. Electrolyte: 0.05 M H_2SO_4 , dioxygen-free; scan rate: 5 mV s^{-1} .

11.4. Concluding remarks

The spectra of CoTSPc and FeTSPc, incorporated in polypyrrole, show broad peaks. This indicates that the chelate molecules occupy a broad distribution of environments in the polypyrrole matrix.

Changes of oxidation state of the metal chelate, which can be detected in a cyclic voltammogram, are accompanied by changes in the spectrum. The spectrum of Co(II)TSPc, incorporated in polypyrrole, can be ascribed to monomer species, but a shoulder, which corresponds to dimer species, should also be noted. The spectrum of Fe(II)TSPc in polypyrrole is thought to be build up of monomer and dioxygen-free dimer absorption bands. The introduction of this dimer species for Fe(II)TSPc is based upon analogy with Co(II)TSPc, because other assignment methods, as comparing with spectra of Fe(II)TSPc in solution, are not possible due to the fact that in Fe(II)TSPc solution no dioxygen-free dimer is present. These observations are in agreement with the proposal done in chapter 7 that a polypyrrole/FeTSPc layer possesses FeTSPc dimers and that they play an important role in the dioxygen reduction mechanism.

11.5. References

1. A. Elzing, A. van der Putten, W. Visscher and E. Barendrecht, *J. Electroanal. Chem.* 233 (1987) 113.
2. B. Simic-Glavaski, S. Zecevic and E. Yeager, *J. Electroanal. Chem.* 150 (1983) 469.
3. D.M. Wagnerova, E. Schwertnerova and J. Veprek-Siska, *Coll. Czech. Chem. Commun.* 39 (1974) 1980.
4. L.C. Gruen and R.J. Blagrove, *Aust. J. Chem.* 26 (1973) 319.
5. S. Zecevic, B. Simic-Glavaski, E. Yeager, A.B.P. Lever and P.C. Minor, *J. Electroanal. Chem.* 196 (1985) 339.
6. C.A. Linkous, H. Teoh and M.V. Rosenthal, *The Electrochem. Soc., 169th Meeting, Boston, Ext. Abstr., Abstr. no. 283* (1986) 412.
7. J. Zwart, *Thesis, Eindhoven University of Technology, Eindhoven* (1978).
8. N. Kobayashi and Y. Nishiyama, *J. Phys. Chem.* 89 (1985) 1167.
9. O. Ikeda, K. Okabayashi, N. Yoshida and H. Tamura, *J. Electroanal. Chem.* 191 (1985) 157.
10. D. Vonderschmitt, K. Bernauer and S. Fallab, *Helv. Chim. Acta* 48 (1965) 951.

12. Concluding remarks

In this thesis, it is demonstrated [especially in chapter 5] that not only the choice of the catalyst is important but also that the deposition method of the catalyst onto the electrode determines for a great part the dioxygen reduction activity observed for the electrode. The deposition method determines the number of active catalyst sites, otherwise stated: differences in activity between electrodes, prepared using different methods, are often due to differences in the number of catalytically active sites. To study the "intrinsic" catalytic activity of a catalyst, an electrode system must be used for which the number of active sites can be determined, as for instance can be done for irreversible adsorption on pyrolytic graphite (Cp).

Careful analysis, including correction for the number of active catalyst molecules [chapters 7, 8 and 9], suggests that in special cases the preparation method or the environment influences the "intrinsic" catalytic activity of the catalyst, for instance, incorporation of FeTSPc in polypyrrole or dissolution of it in 0.05 M H_2SO_4 results in an increased activity which cannot be accounted for only by an increased number of active catalyst molecules. The proposed FeTSPc dimers, which are held responsible for the increased activity, are induced by the environment. The dioxygen reduction mechanism via FeTSPc dimers has some fundamental importance too, because it seems that the most favourable pathway for dioxygen reduction starts with a dioxygen molecule simultaneously interacting with two metal atoms (or two other active centres). For materials, such as platinum and silver, which both show a high dioxygen reduction activity, often bridged adsorption of dioxygen is assumed [1,2]. In the cofacial dicobalt porphyrins a high activity and selectivity is combined, so the assumption that this is caused by bridge adsorption of dioxygen is rather straightforward [3]. The reaction rate depends on the free enthalpy or Gibbs energy of the activated complex, viz. the enthalpy and the entropy of the activated complex [4]. For the monomer reduction pathway, the activation enthalpy is probably so high, that it is not completely cancelled by the favourably high activation entropy; so, a free enthalpy results which is higher than for the dimer pathway, despite the unfavourably low entropy of the activated dimer complex.

To prove more rigorously the role of FeTSPc dimers in the reduction mechanism, more research is necessary about the form of adsorption of FeTSPc or FePc on Cp (or on BP of SA-Cp). For the Cp surface, it was argued

[chapter 6] that two different species (monomer and dimer) are present. Despite the sophisticated spectroscopic techniques applied to reveal the form of adsorption [5], it is still a matter of debate whether the metal chelates are adsorbed with the molecular plane parallel or perpendicular to the surface. Also a structure in which dimers are adsorbed perpendicular to the surface has been proposed [6]. The differences in adsorption behaviour between CoTSPc and FeTSPc [chapter 6] suggest that the metal ions are involved in the binding to the surface and, therefore, the complexes must be adsorbed parallel to the surface. In chapter 10, it is demonstrated that the adsorption of the MeTSPc's influences the optical properties of the compounds. This gives us an indication for parallel adsorption, because only in this configuration a strong interaction can be expected between the surface and the adsorbed molecule. However, more studies must be performed to enable translation of this optical information into structural information about the adsorbed metal chelate.

For cobalt chelates, with exception of the cofacial dicobalt porphyrins, always a reduction of dioxygen to hydrogen peroxide is observed, while the iron compounds often result in a 4-electron reduction of dioxygen to water. In most of the models for the adsorption of dioxygen on metal chelates, [chapter 3], the charge of the dioxygen ligand bonded to the cobalt ion, is negative; thus a charge transfer occurs between a cobalt(II) ion and the dioxygen ligand ($\text{Co}^{3+}-\text{O}_2^-$) upon adsorption. For iron, most of the models consist of a neutral dioxygen ligand ($\text{Fe}^{2+}-\text{O}_2$). Probably the charge on the dioxygen ligand in the case of cobalt results in a reduction of the ligand to hydrogen peroxide before splitting of the dioxygen bond can occur. The uncharged dioxygen ligand for the iron compounds is expected to facilitate the splitting of the dioxygen bond before or during the reduction of the ligand.

Unfortunately, it is not possible to predict the redox potentials of the compounds and of the dioxygen adducts from the models for the metal chelates and the dioxygen adducts of these, as presented in chapter 3. Perhaps, these data are more important in determining the selectivity of the reduction process than the form of adsorption of dioxygen. For compounds with a redox potential in the potential domain of the formal potential of the dioxygen reduction to hydrogen peroxide, often a 4-electron reduction of dioxygen is observed. With respect to this, it is noteworthy that the cofacial dicobalt porphyrin offers, besides a centre for bridge adsorption, also a redox potential of about 0.6 V (RHE) for the conversion of one of the Co(III) centres

into Co(II). This redox potential is much lower than the one (0.8 V) observed for the monomeric cobalt porphyrin, due to the interaction between the two porphyrin rings [3.7].

For practical application of the metal phthalocyanines in a fuel cell, a higher stability is required, especially in acidic media. The activity in acidic media is, for reasons outlined in chapter 2, also too low. In chapter 7, we observed a rapid deactivation of the electrode modified by a polypyrrole/FeTSPc layer, although for a RDE, due to the forced convection, the turn-over number, compared with a practical gas diffusion electrode system, is high. In situ UV-Vis. spectroscopy, performed as described in chapter 8, has demonstrated that FeTSPc is especially unstable in high oxidation states: Fe(III)TSPc and Fe(IV)TSPc (or Fe(III)TSPc⁺). In this chapter, it is also established that these high oxidation states originate from the dioxygen reduction at FeTSPc if dissolved in acidic solution. For adsorbed FeTSPc, these species will be, depending on the applied electrode potential, directly converted back to the more stable Fe(II)TSPc state but, in the short time before the reduction, decomposition can occur. An interesting alternative could be the search for metal chelates with the same redox behaviour as FeTSPc, however, with a higher stability in the higher oxidation states in acidic media.

As to the often reported μ -oxo bridged FeTSPc (or FePc) species [8], we remark that it can only be produced in a side-reaction, because this species is reduced (and only hereafter, it dissociates rapidly) at much higher overpotential than where usually dioxygen reduction is observed at FeTSPc [see chapter 8]. The formation of this adduct results in a temporarily deactivation of the electrode, because it blocks the involved sites for the adsorption and the reduction of a next dioxygen molecule.

Incorporation of the catalysts in electron-conducting polypyrrole has no practical significance, because of the instability of the polymer layer. However, for research applications, it is very convenient because it represents an easy method to obtain a high coverage of the electrode with active catalyst material. Due to this high coverage, the electrode processes can be easily studied by applying in situ absorption spectroscopy, as is demonstrated in chapter 11.

References

1. P. Fischer and J. Heitbaum, *J. Electroanal. Chem.* 112 (1980) 231.
2. V. Jalan and E.J. Taylor, *J. Electrochem. Soc.* 130 (1983) 2299.
3. J.P. Collman, P. Denisevich, Y. Konai, M. Marocco, C. Koval and F.C. Anson, *J. Am. Chem. Soc.* 102 (1980) 6027.
4. W.J. Moore, 'Physical Chemistry' (fifth edition), Longman, London (1974).
5. B. Simic-Glavaski, S. Zecevic and E. Yeager, *J. Phys. Chem.* 87 (1983) 4555.
6. B.Z. Nikolic, R.R. Adzic and E.B. Yeager, *J. Electroanal. Chem.* 103 (1979) 281.
7. R.R. Durand and F.C. Anson, *J. Electroanal. Chem.* 134 (1982) 273.
8. B.J. Kennedy, K.S. Murray, P.R. Zwack, H. Homborg and W. Kalz, *Inorg. Chem.* 24 (1985) 3302.

Abbreviations

Compounds

Bp of SA-Cp	basal plane of stress annealed pyrolytic graphite
Cg	glassy carbon
Cp	pyrolytic graphite
Me	metal
P	porphyrin
Pc	phthalocyanine
PP	polypyrrole
TCPc	tetracarboxy-phthalocyanine
THF	tetrahydrofuran
TSPc	tetrasulfonato-phthalocyanine

Electrodes (E)

CE	counter electrode
NHE	normal hydrogen electrode
RE	reference electrode
RHE	reversible hydrogen electrode
SCE	saturated calomel electrode
WE	working electrode

Techniques

ER spectroscopy	electroreflectance spectroscopy
ESR spectroscopy	electron spin resonance spectroscopy
OTTLC	optical transparent thin layer cell
OTTLE	optical transparent thin layer electrode
R(R)DE	rotating (ring) disc electrode
UV-Vis. spectroscopy	Ultraviolet-Visible light spectroscopy

Quantum mechanics

CNDO-CI	complete neglect of differential overlap-configuration interaction
INDO-CI	intermediate neglect of differential overlap-configuration interaction
M.O.	molecular orbital
SCC-EH	self consistent charge-extended Hückel approximation

<u>Symbols</u>		
A(ABS)	absorbance	absorbance unit
A	surface area	cm ²
a	distance	nm
B ^j	crystal field parameter	
C _m ⁱ (θ, φ)	spherical harmonic	
c	concentration	mol cm ⁻³
D	diffusion coefficient	cm ² s ⁻¹
d	cell thickness	cm
E	potential	V
e	unit charge	1.6 x 10 ⁻¹⁹ C
F	Faraday	96495 C mol ⁻¹
f	frequency	s ⁻¹
g	electron g-factor	
I	current	mA
i	current density	mA cm ⁻²
J	L + S	
k	1st order rate constant	cm s ⁻¹
L(l)	angular momentum quantum number	
n	number of electrons	
q	transferred charge	C
R	place or coordinate of ligand	
R	gas constant	J K ⁻¹ mol ⁻¹
S(s)	spin quantum number	
T	temperature	K
t	surface diffusion time	s
<x ² >	mean square displacement	cm ²
Z	charge of ligand in e	
α	transfer coefficient	
δ	diffusion layer thickness	cm
»	molar absorption coefficient	mol ⁻¹ cm ²
η	overpotential (E-E _{eq})	V
λ	wavelength	nm
ν	kinematic viscosity	cm ² s ⁻¹
τ	diffusion time	s
ω	rotation frequency	rad s ⁻¹
(r, θ, φ)	pole coordinates	
[]	concentration	M or mol l ⁻¹

Superscripts

a	from 2px- and 2pz-orbitals
b	from 2py- orbital.
s	bulk
σ	surface

Subscripts

D	disc
d	diffusion
eq	equilibrium
g	gerade
i	species i
L	diffusion limited
N	Nernst
R	ring
s	surface
u	ungerade
o	standard conditions
1/2	half-wave

Summary

The dioxygen reduction is an important reaction for the energy conversion. In a fuel cell, the chemical energy of the fuel is directly converted into electric energy. In this cell, dioxygen is reduced at the cathode. Although this reaction is thermodynamically favourable, it is a kinetically slow process. Metal phthalocyanines, among which those of cobalt and iron (CoPc and FePc), catalyze the dioxygen reduction [chapter 1].

In this thesis, the interaction between dioxygen and these metal complexes is described. A literature survey shows that the dioxygen reduction, catalyzed by CoPc, leads to hydrogen peroxide, while at FePc in alkaline solution mainly water is formed as the endproduct [chapter 2]. In this chapter also the light absorption spectra of cobalt- and iron tetrasulfonato-phthalocyanine (Co- and FeTSPc) are discussed.

Theoretical models for the description of the adsorption of dioxygen on metal chelates are treated in chapter 3. For CoPc mostly "end-on" (bent) bonding of the dioxygen molecule to the metal atom is concluded. It appears that after adsorption a shift in the electronic structure from cobalt to dioxygen occurred, so that the latter is partly negatively charged. For FePc, "side-on" bonding is also theoretically possible, although considerations concerning the dioxygen bonding to other iron chelates indicate "end-on" (bent) bonding as the most favourable one. Often, it is assumed that the charge separation in the dioxygen adduct of FePc is smaller than for the adduct of CoPc.

Hereafter, the applied experimental methods, such as the Rotating Ring Disc Electrode (RRDE) technique and the in situ light absorption spectroscopy are treated [chapter 4].

From a comparison of the results of different electrode preparation methods, such as: vacuum deposition, irreversible adsorption, incorporation in a conducting polymer, evaporation of the (catalyst containing) solvent, and impregnation of porous carbon, it appears that the number of active, i.e. available sites can deviate strongly from the number of present catalyst molecules. Also, a relation is derived between the half-wave potential observed for the dioxygen reduction and the number of active sites [chapter 5].

The dioxygen reduction on an irreversibly adsorbed layer of Co- and FeTSPc on graphite is investigated as a function of the coverage. For small coverage a kinetic limitation is observed, which can be attributed to a slow

chemical step as well as to a slow diffusion of dioxygen across the electrode surface to an active site. This last model leads for FeTSPc to the conclusion that high active (dimeric) and less active (monomeric) sites are present on the electrode surface [chapter 6].

FeTSPc, incorporated in polypyrrole, shows in acidic media ($0.05 \text{ M H}_2\text{SO}_4$) a higher activity than if adsorbed on graphite. The increased activity is ascribed to the presence of FeTSPc dimers in polypyrrole [chapter 7].

Spectro-electrochemical measurements indicate that in a FeTSPc solution ($0.05 \text{ M H}_2\text{SO}_4$) Fe(III)TSPc and μ -oxo FeTSPc dimers are present. After the electrochemical reduction to Fe(II)TSPc, dioxygen adsorption occurs, and the formed adduct is reduced at a slightly more cathodic potential than the redox potential for the original Fe(III)TSPc species. From RRDE measurements, it is concluded that hydrogen peroxide is the predominant product of the reduction, with also Fe(IV)TSPc (or Fe(III)TSPc⁺) formed. These valence states can originate from the reaction of Fe(II)TSPc (or Fe(III)TSPc) with hydrogen peroxide, but also a reaction of a dioxygen molecule with two Fe(II)TSPc molecules is possible, leading to the fourth oxidation state of the FeTSPc molecule, with simultaneously some direct reduction of dioxygen to water. The μ -oxo FeTSPc dimers dissociate only appreciably at potentials more cathodic than for the reduction to Fe(I)TSPc [chapter 8].

In chapter 9, a comparison is made between the polarographic behaviour, and the voltammetric behaviour of a RDE with a graphite disc, both recorded in a dioxygen-saturated solution. In comparison with mercury, the graphite surface shows an "inhibition" of the dioxygen reduction. The adsorption of a catalyst like CoTSPc cancels the "inhibition", while adsorption of FeTSPc also increases the selectivity (the ratio between water and hydrogen peroxide formed). Dissolving FeTSPc into the electrolyte changes the polarographic behaviour such that more water is produced.

Electroreflectance spectroscopy, performed on FeTSPc, adsorbed at the basal plane of stress annealed pyrolytic graphite, is described in chapter 10. The spectrum obtained for the redox couple Fe(I)TSPc/Fe(II)TSPc is similar to the spectrum composed from the absorption spectra of both components. The other electroreflectance spectrum (Fe(II)TSPc/Fe(III)TSPc) cannot be constructed from the absorption spectra of the components, indicating that the adsorption of FeTSPc on graphite changes the optical properties of the complex.

In situ light absorption measurements at FeTSPc/polypyrrole layers result in spectra, which make the presence of FeTSPc dimers, proposed in chapter 7, more acceptable [chapter 11].

This thesis ends with some concluding remarks about the research of the electrocatalysis of the dioxygen reduction. This also includes the discussion of the dimeric reduction mechanism, as proposed for FeTSPc, in a more general way.

The difference in selectivity between CoPc and FePc could be explained by the fact that the dioxygen adduct of FePc has, contrary to the adduct of CoPc, a neutral character. But, it is pointed out that also the redox potential of the complex has an influence on the selectivity.

The stability of FePc (or FeTSPc) under dioxygen reducing conditions is too small for practical application. Probably, this is due to the instability of FeTSPc (FePc) in the higher valence states (Fe(III)TSPc and Fe(IV)TSPc) [chapter 12].

Samenvatting

De reductie van zuurstof is voor de energieconversie een belangrijke reactie. In een brandstofcel wordt de chemische energie van de brandstof rechtstreeks omgezet in elektrische energie. In deze cel wordt aan de kathode de zuurstof gereduceerd. Hoewel deze reactie thermodynamisch gunstig ligt, verloopt hij traag. Metaal-ftalocyaninen, waaronder die van cobalt en ijzer (CoPc en FePc), kunnen de zuurstofreductie katalyseren [hoofdstuk 1].

In dit proefschrift wordt de interactie tussen zuurstof en deze metaal-complexen beschreven. Een literatuuroverzicht laat zien dat de zuurstofreductie, gekatalyseerd door CoPc, leidt tot waterstofperoxyde, terwijl aan FePc (in loog) hoofdzakelijk water als eindprodukt ontstaat [hoofdstuk 2]. In dit hoofdstuk worden ook lichtabsorptiespectra van cobalt- en ijzer-tetrasulfonato-ftalocyanine (Co- en FeTSPc) besproken.

In hoofdstuk 3 worden theoretische modellen behandeld voor de beschrijving van de adsorptie van zuurstof aan metaal-chelaten. Voor CoPc besluit men meestal tot een zogenaamde "end-on" (bent) binding van het zuurstofmolekuul aan het metaal-atoom. In de elektronenstructuur blijkt na adsorptie een verschuiving te zijn opgetreden van cobalt naar zuurstof, zodat deze laatste gedeeltelijk negatief geladen is. Voor FePc blijkt een "side-on" binding theoretisch ook mogelijk te zijn, hoewel beschouwingen die gewijd zijn aan zuurstofbinding aan andere ijzer-chelaten "end-on" (bent) aangeven als de meest gunstige configuratie. Vaak wordt aangenomen dat de ladings-scheiding in het zuurstofaddukt van FePc kleiner is dan in het geval van CoPc.

Hierna worden de gebruikte meetmethoden, zoals de roterende ring-schijf-elektrode techniek en de in situ lichtabsorptiespectroscopie, behandeld [hoofdstuk 4].

Uit een vergelijking van de resultaten van verschillende elektrode-bereidingswijzen, zoals: vacuümdepositie, irreversibele adsorptie, inbouwen in een geleidend polymeer, verdamping van het oplosmiddel en impregnatie van poreuze kool, blijkt dat het aantal beschikbare actieve sites sterk kan afwijken van de hoeveelheid aanwezige katalysatormolekulen. Tevens is er een relatie afgeleid tussen de halfwaardepotentiaal voor de zuurstofreductie en het aantal actieve sites [hoofdstuk 5].

De zuurstofreductie aan een irreversibel geadsorbeerde laag van Co- en FeTSPc aan grafiet is onderzocht als een functie van de bedekking. Bij een kleine bedekking wordt een kinetische limitering waargenomen, die zowel met

een langzame chemische stap als met een trage diffusie van zuurstof over het elektrode-oppervlak naar een actieve plaats beschreven kan worden. Dit laatste model leidt voor FeTSPc tot de conclusie dat er zeer actieve (dimere) en minder actieve (monomere) sites op het elektrode-oppervlak aanwezig zijn [hoofdstuk 6].

FeTSPc, geïncorporeerd in polypyrrool, vertoont in zuur milieu (0,05 M H_2SO_4) een hogere activiteit dan wanneer het geadsorbeerd is aan grafiet. De aktiviteits-toename wordt toegeschreven aan de aanwezigheid van FeTSPc-dimeren in polypyrrool [hoofdstuk 7].

Spectro-elektrochemische metingen tonen aan dat in een FeTSPc-oplossing (0,05 M H_2SO_4) Fe(III)TSPc en μ -oxo FeTSPc-dimeren voorkomen. Na de elektrochemische reductie tot Fe(II)TSPc treedt er zuurstofadsorptie op, waarna het gevormde addukt bij een iets kathodischer potentiaal dan de redoxpotentiaal, behorende bij het oorspronkelijke Fe(III)TSPc, gereduceerd wordt. Uit roterende ring-schijf-elektrode metingen kan geconcludeerd worden dat het reductieproduct voornamelijk waterstofperoxyde is. Ook blijkt dat er Fe(IV)TSPc (of Fe(III)TSPc⁺) gevormd wordt. Deze valentietoestanden kunnen ontstaan uit de reactie van Fe(II)TSPc (of eventueel Fe(III)TSPc) met waterstofperoxyde, maar ook is een reactie van een zuurstofmolekuul met twee Fe(II)TSPc-molekulen mogelijk, waarbij de vierwaardige oxydatietoestand van het FeTSPc-molekuul ontstaat, terwijl tegelijkertijd enige direkte reductie van zuurstof naar water optreedt. De μ -oxo FeTSPc-dimeren ontleden alleen merkbaar bij potentialen die meer kathodisch zijn dan die voor de reductie naar Fe(I)TSPc [hoofdstuk 8].

In hoofdstuk 9 wordt een vergelijking gemaakt tussen het polarografische gedrag, en het voltammetrische gedrag van een roterende grafiet-elektrode, beide gemeten in een zuurstofverzadigde oplossing. Opvallend hierbij is dat grafiet, in vergelijking met kwik, een inhibitie van de zuurstofreductie te zien geeft. De adsorptie van een katalysator als CoTSPc heft deze inhibitie op, terwijl de adsorptie van FeTSPc ook de selektiviteit (de verhouding tussen de hoeveelheid geproduceerd water en de hoeveelheid gevormd waterstofperoxyde) verhoogt. Door het oplossen van FeTSPc in het elektrolyt verandert het polarografische gedrag zodanig dat er meer water wordt geproduceerd.

De elektroreflektie-spectroscopie, uitgevoerd aan FeTSPc geadsorbeerd op het "basal plane of stress annealed pyrolytic graphite", wordt beschreven in hoofdstuk 10. Het gemeten spectrum voor het redoxkoppel Fe(I)TSPc/Fe(II)TSPc is identiek aan het spectrum dat kan worden samengesteld uit de absorptie-

spectra van de componenten. Het andere elektroreflectie-spectrum (Fe(II)TSPc/Fe(III)TSPc) kan niet geconstrueerd worden uit de absorptiespectra van de componenten, wat erop duidt dat de adsorptie van FeTSPc aan grafiet de optische grootheden van het complex verandert.

In situ lichtabsorptiemetingen aan FeTSPc/polypyrrroollagen resulteren in spectra, die de in hoofdstuk 7 veronderstelde aanwezigheid van dimeren nog meer aannemelijk maken [hoofdstuk 11].

Dit proefschrift eindigt met enige slotopmerkingen over het onderzoek naar de elektrokatalyse van de zuurstofreduktie. Dit houdt ook in de bespreking van het dimere zuurstofreduktiemechanisme, zoals voorgesteld voor FeTSPc, op een meer algemene manier. Het verschil in selektiviteit tussen CoPc en FePc kan verklaard worden uit het feit dat het zuurstofaddukt van FePc, in tegenstelling tot het addukt van CoPc, een neutraal karakter heeft. Maar ook wordt gewezen op de mogelijke invloed van de redoxpotentiaal van de complexen op de selektiviteit.

De stabiliteit van FePc of FeTSPc onder zuurstofreducerende omstandigheden is te gering voor praktisch gebruik. Waarschijnlijk is dit het gevolg van de instabiliteit van FeTSPc (FePc) in hogere valentietoestanden (Fe(III)TSPc en Fe(IV)TSPc) [hoofdstuk 12].

Curriculum vitae

De schrijver van dit proefschrift is geboren op 21 februari 1958 te Sleen. Na het behalen van het diploma V.W.O. aan de Christelijke Scholengemeenschap voor Z.O. Drenthe te Emmen begon hij in september 1976 met de studie Scheikunde aan de Rijksuniversiteit te Groningen. Hij specialiseerde zich in de Fysische Chemie en op 10 februari 1983 legde hij het doctoraal examen af. Op 1 september van hetzelfde jaar startte hij, bij de vakgroep Elektrochemie van de Technische Universiteit te Eindhoven, met het promotieonderzoek, waarvan dit proefschrift het resultaat is.

Op 11 mei 1984 trad hij in het huwelijk met Lizette Platzer.

Dankwoord

Aan de totstandkoming van dit proefschrift heeft een groot aantal personen bijgedragen. Al dezen, ook als ze hieronder niet met name genoemd worden, wil ik hartelijk danken.

In de eerste plaats wil ik noemen mijn ex-collega, André van der Putten. Beste André, zonder de vele boeiende en leerzame discussies met jou zou de kwaliteit van dit proefschrift veel geringer zijn geweest.

Mijn le promotor, Prof. E. Barendrecht, wil ik danken voor het ruimte geven aan de fundamentele richting waarin het onderzoek zich ontwikkelde. Zijn vertrouwen in het uiteindelijke succes van de brandstofcel en de hieruit voortvloeiende enthousiaste begeleiding zijn voor mij een grote stimulans geweest gedurende het onderzoek.

Aan dr. W. Visscher, mijn copromotor, ben ik veel dank verschuldigd voor haar opbouwende kritiek, haar inlevingsvermogen in de van tijd tot tijd gerezen problemen en het nauwkeurig nakijken van het concept-proefschrift.

Prof.dr. R. van Santen bedank ik voor de bereidheid om als 2e promotor op te treden en het geven van konstruktieve opmerkingen.

Ad Wonders voor de nauwgezette wijze, waarop hij het complexe spectroscopische gedrag van metaal-ftalocyanine-oplossingen ontrafelde.

Netty Rijpkema-Hölscher voor het zorgvuldig uittypen en zelfs tegelijkertijd corrigeren van mijn, niet-altijd-even-goed-leesbare, manuscript.

Bert Boeringa en de medewerkers van de glasblazerij voor het omzetten van mijn ruwe schetsen in ongeëvenaarde elektroden en cellen.

I want to thank Mohammed Elmorsi for his collaboration during my attempt to build in a very short time a setup for reflectance spectroscopy.

De studenten Albert Pouwels, Carry Emons, Gerrit Groenenboom, Rob Diks en Ruud Brunschot voor hun bijdrage aan het in dit proefschrift beschreven onderzoek.

Je veux remercier Mme.dr. C. Hinnen et ses collègues du Laboratoire d'Electrochimie Interfaciale (Meudon-Bellevue) pour la collaboration aux mesurages, décrits dans le chapitre 10, et pour leur hospitalité.

Riek Bossong voor het schoonhouden van mijn bureau.

De (ex-)kamerogenoten en de overige leden van de vakgroep voor de prettige werksfeer.

Tenslotte wil ik Lizette bedanken voor het zorgvuldig op schrijffouten nakijken van het manuscript en voor het opgebrachte begrip gedurende die tijden, dat ik geen onderhoudend gezelschap was, omdat mijn gedachten nog op de TU waren.

STELLINGEN

1. Beschouwingen over de mogelijke elektrokatalytische activiteit van een polypyrroolfilm dienen vergezeld te gaan van gegevens over de dikte en de porositeit van de film.
 - *K. Okabayashi, O. Ikeda and H. Tamura, J. Chem. Soc. Chem. Comm. (1983) 684.*
 - *R.C.M. Jakobs, Proefschrift: "The polymer modified electrode, characterization and electrocatalytical possibilities of polypyrrole", Technische Universiteit Eindhoven, Eindhoven (1984).*
 - *Hoofdstuk 7 van dit proefschrift.*
2. Bij de analyse van het zuurstofreductieproces aan cobalt-tetraazaannuleen gaat Wiesener ten onrechte uit van "side-on" adsorptie van het zuurstofmolekuul op het cobalt-ion.
 - *K. Wiesener, Sov. Electrochem. 18 (1982) 672.*
 - *Hoofdstuk 3 van dit proefschrift.*
3. Zowel zuurstofadditie aan cobalt-tetrasulfonato-ftalocyanine als dimerisatie van het cobalt-chelaat zelf, beïnvloeden het lichtabsorptiespectrum. Daar deze effecten door Simic-Glavaski et al. niet van elkaar worden gescheiden, vormt hun bespreking van de spectra een duister geheel.
 - *B. Simic-Glavaski, S. Zecevic and E. Yeager, J. Electroanal. Chem. 150 (1983) 467.*
4. Vanwege het mogelijk-zijn van oppervlakreorganisatie en eventueel het oplossen van zelfs edelmetalen bij potentialen lager dan hun redoxpotentiaal, geven voorbehandelingsprogramma's, waarbij een potentiaalbelasting van de elektrode wordt toegepast, geen reproduceerbaar metaaloppervlak.
 - *R.M. Cervino, W.E. Triaca and A.J. Arvia, J. Electroanal. Chem. 182 (1985) 51.*
5. Degrez et al. houden ten onrechte geen rekening met het feit dat de kinetiek van de elektrochemische depositie van koper uit een zuur koperbad

bij hoge stroomdichtheid sterk wordt beïnvloed door de vorming van geadsorbeerde waterstofatomen en/of moleculaire waterstof.

- *M. Degrez and R. Winand, Electrochim. Acta 29 (1984) 365.*

6. Wanneer in een bemonsteringsexperiment (het toelaten van een gasmonster met een atmosferische druk door een kleine opening in een vacuümkamer van een massaspectrometer) geen rekening gehouden is met de supersonische uitstroming, dienen de resultaten zeer kritisch te worden geëvalueerd.
 - *J. Skalny and R.S. Sigmond, Proc. Int. Conf. Phys. Ion. Gas. (1983) 554.*
 - *B. Gravendeel, Proefschrift: "Negative Corona Discharges, a fundamental study", Technische Universiteit Eindhoven, Eindhoven (1987).*

7. Titels als "Dat boek leest erg vlot", welke frequent voorkomen in taalkunde-tijdschriften, zijn wel boeiend maar niet informatief voor een aankomend neerlandicus.
 - *P.C. Paardekooper, De nieuwe taalgids 76-3 (1983) 193.*

8. Vakbonden beijveren zich alleen voor de huidige generatie werknemers, getuige het feit dat de afspraak "geen gedwongen ontslagen maar inkrimping door natuurlijk verloop" door hen als een overwinning wordt beschouwd.

9. Het door de (gemeentelijke) overheid niet meer registreren van de kerkelijke gezindte van de burger leidt niet tot een verhoging van zijn privacy, omdat kerkelijke genootschappen als reactie hierop een centraal registratiesysteem opzetten dan wel hun bestaand registratiesysteem perfectioneren.

10. Veel wetenschappers kunnen geen weerstand bieden aan de verleiding om supergeleiding te onderzoeken.

Eindhoven, 11 december 1987

Bert Elzing